Feasibility Studies on the Design and Usage of Steel Pile Piles for ALDOT Bridges

by

Rosy Sharma

A thesis submitted to the Graduate Faculty of
Auburn University
in partial fulfillment of the
requirements for the Degree of
Master of Science

Auburn, Alabama
August 05, 2023

Keywords: steel pipe pile, reinforced-concrete bent cap, bridge-load demands, connection-failure, design methodologies

Approved by

Kadir C. Sener, Ph.D., P.E., Assistant Professor of Civil Engineering
Robert W. Barnes, Ph.D., P.E., Associate Professor of Civil Engineering
James Davidson, Ph.D., Professor of Civil Engineering

ABSTRACT

Large diameter steel pipe piles provide an efficient and cost-effective alternative to conventional reinforced concrete bridge piles (drilled shafts) and steel piles (HP-piles). The steel pipe columns offer increased strength and stiffness, enabling swift construction. Several US states have embraced the use of steel pipe piles in bridge structures, and Alabama Department of Transportation (ALDOT) is currently contemplating their utilization as replacements for regular drilled shafts and HP-piles.

This study aims to compare steel pipe piles with existing pile types, with a particular focus on developing steel pipe pile-to-cap beam connections while incorporating best practices and addressing associated challenges. To accomplish this, a comprehensive literature review was conducted, specifically focusing on studies related to steel pipe piles and their connections with reinforced concrete bent caps. Additionally, a survey was administered to state departments of transportation to ascertain the current state of practice regarding the usage of steel pipe piles. The primary objective was to gain insights into the utilization and experiences with such piles, as well as to explore the design methodologies for connections.

From both qualitative and quantitative perspectives, steel pipe piles demonstrate their suitability as replacements for traditional piles. Robust and reliable connections can be established between the piles and reinforced concrete bent caps using three distinct anchorages: i) non-contact lap splice with straight rebars, 90^0, and 180^0 hooked rebars; ii) annular ring; and iii) shear studs. These connections are established to effectively withstand force and moment demands exerted on them from design loads while considering various failure limit states.

ACKNOWLEDGEMENTS

I would like to express my heartfelt gratitude to Dr. Kadir Sener for his exceptional guidance and support throughout my graduate studies at Auburn University. Dr. Sener's expertise, encouragement, and unwavering dedication to my research have played a crucial role in shaping my academic journey. His insightful feedback, valuable suggestions, and constant motivation have been instrumental in the successful completion of my research.

I would also like to extend my sincere appreciation to my esteemed committee members, Dr. Robert Barnes and Dr. James Davidson. Their expertise, constructive criticism, and valuable insights have greatly contributed to the improvement and refinement of my research. Their thoughtful feedback and rigorous evaluation have been invaluable in shaping the quality and depth of my work.

Furthermore, I am immensely grateful to my family members for their unwavering love, encouragement, and support throughout my academic pursuits. Their constant belief in my abilities, sacrifices, and understanding have been instrumental in my achievements. Their unwavering presence and belief in me have provided me with the strength and motivation to overcome challenges and reach new heights.

I am truly fortunate to have had such incredible individuals in my life who have shaped my academic and personal growth. Their guidance, support, and belief in my abilities have been truly invaluable, and I am deeply thankful to each and every one of them.

Table of Contents

List of Figures

List of Tables

Chapter 1 INTRODUCTION

1.1 Overview

One of the most prevalent bridge configurations employed in the United States involves multi-span bridges featuring precast, prestressed concrete girders and pile bents. These pile bents comprise a cast-in-place, reinforced concrete (RC) bent cap, along with either RC drilled shafts or driven steel HP piles, as depicted in Figure 1.1(a) and Figure 1.1(b) respectively. Despite the extensive use of these pile types in bridge construction, they suffer from certain limitations in terms of construction practices and cost-effectiveness. To overcome these challenges, alternative members such as steel pipe piles have emerged as a viable solution. With their potential to deliver superior force and moment capacities, large-diameter steel pipe piles (Figure 1.1(c)) offer a promising alternative to the existing options.

Figure 1.1. (a) RC drilled shaft Steel [1]; (b) HP piles [2]; (c) Large diameter steel piles [3]

Large pipe piles with diameters ranging from 3 to 4 ft. hold significant potential as a viable alternative to existing piers in various scenarios. Steel pipe piles are extensively utilized in bridge

construction due to their numerous advantages. These advantages include: i) Enhanced vertical bearing strength and lateral load resistance, enabling the possibility of accommodating larger bridge superstructures, ii) Elimination of the need for battered members or inclined braces, iii) Offering a practical and cost-effective solution for reaching the bearing strata when deep beneath soft soil, iv) Suitable for deployment in areas with hard ground or lacking distinct bearing layers, v) Demonstrating excellent environmental performance by requiring minimal earth removal, vi) Facilitating accelerated bridge construction compared to alternative options, vii) Availability in various lengths, diameters, and thicknesses, enabling customization to suit specific bridge requirements in an economical manner, viii) Easy production of longer piles through welding joint connections, and ix) Lightweight and high toughness, facilitating easy handling and transportation.

1.2 Problem Statement

Similar to many other states, ALDOT commonly employs drilled shafts and H-piles as the primary pile types for bridge construction. These piles serve as bearing elements for deep foundations and extend into the bridge cap to function as piers. They are typically used to support structures with significant axial and lateral loads. However, discussions with ALDOT engineers have revealed that the department is exploring alternatives to RC drilled shafts and HP-piers due to a range of issues, which will be detailed in the respective sections below.

1.2.1 Driven Piles

H-piles are a commonly utilized pile type in bridge construction, specifically designed for deep foundations. These piles are extensively employed as substructures for small to mid-size bridges constructed on soft soils. The typical approach involves utilizing cast-in-place reinforced

concrete bent caps supported by driven steel HP shapes. Unlike other piling systems that face challenges in penetration, H-piles can be driven deep into the ground to reach the necessary soil properties required for supporting buildings and bridges.

ALDOT-funded previous research studies (Marshall et. al., 2017) have shown that in such bridge configurations, a combination of simply supported precast, prestressed concrete girders and pile bents is adopted. These pile bents consist of a cast-in-place reinforced concrete bent cap and driven steel HP piles. Typically, the two outermost HP piles are inclined at a slope of 1.5:12 to provide lateral resistance against overturning moments induced by winds, waves, and other lateral loads, as illustrated in Figure 1.2. Moreover, additional bracing is necessary to ensure sufficient lateral stiffness and strength against these lateral loads.

Figure 1.2. Multi-span bridge with cast-in-place reinforced concrete bents supported on H-piles [4]

In cases where the bridge bent is positioned within a flow channel, additional measures are taken to protect H-piles. This involves either providing encasement for the H-piles or applying galvanization for section protection. The extension of HP piles into the bent cap by approximately 12 in. can disrupt the arrangement of bottom longitudinal reinforcement in the bent cap. Due to the relatively small size of H-piles, each HP pile system directly supports a single girder located

directly above it. This member layout results in minimal transfer of shear force or bending moment into the bent cap, as the force is directly transmitted between the girders and corresponding H-piles. Consequently, smaller bent caps can be employed.

Figure 1.3 showcases a representative ALDOT bridge bent with HP-piles. The bent cap measures 38 ft. 6 in. in length and has a trapezoidal shape, with a smaller base of 2 ft. and a larger base of 3 ft. The bridge substructure comprises six girders positioned on top of six HP-piles of size 14 x 73. In cases where the clear height of the pile exceeds 14 ft., lateral bracing is provided using struts measuring 4 in. x 3 ½ in. When the bent is located within the flow channel, the steel piles are encased in concrete, extending 3 ft. above the mudline. Typically, the pile encasements extend at least 5 ft. below the projected ground elevation.

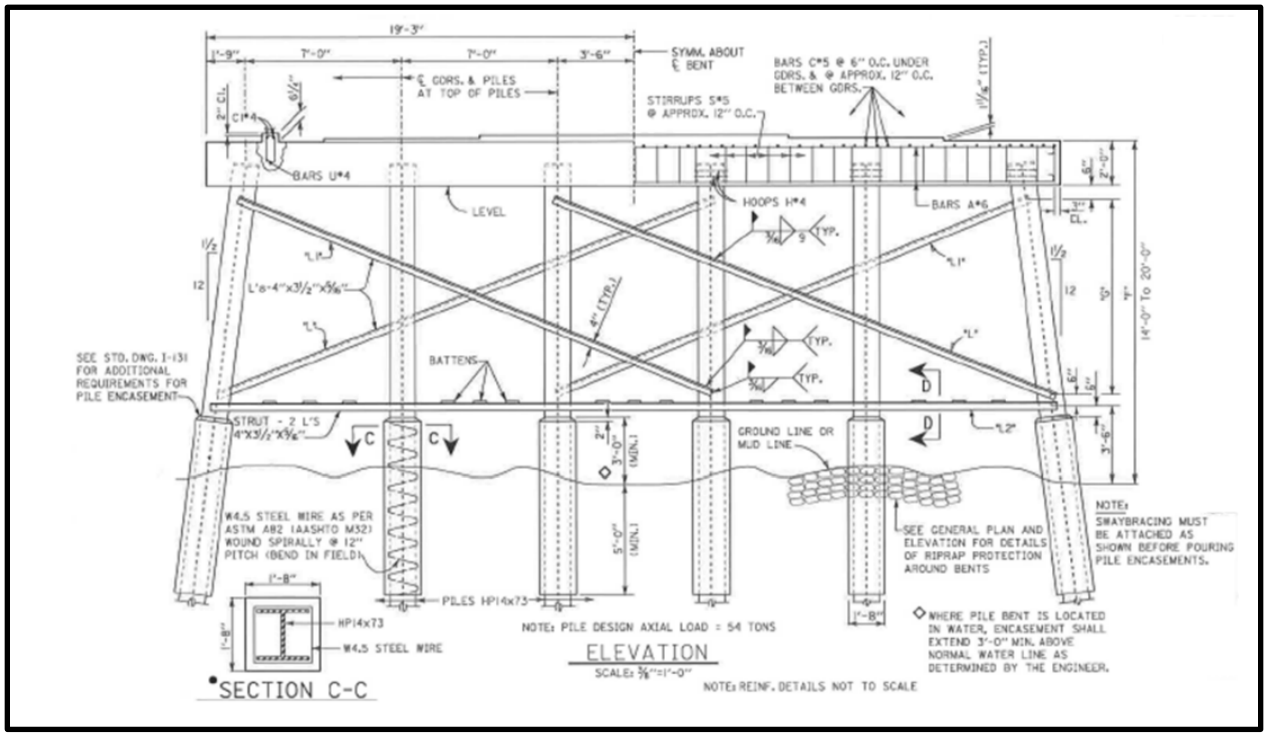

Figure 1.3. Typical multi-span bridge supported on H-piles on flow channel [5]

Despite the widespread use of H-piles in bridge construction, numerous issues have arisen based on field inspections, particularly concerning cracking and damage in the bent cap,

specifically near the exterior battered piles. These observations have been supported by previous studies (Marshall et. al., 2017). Consequently, the construction of bridges using such piles entails a laborious design process, a complex construction procedure, and ultimately results in long-term performance problems.

1.2.2 Drilled shafts

Reinforced concrete (RC) piles, commonly known as drilled shafts, are frequently employed to provide deep foundations capable of supporting substantial axial and lateral loads. This involves excavating cylindrical shafts into the ground, inserting reinforcement cages into the shafts, filling them with concrete, removing the permanent casing, and ultimately forming a reinforced concrete pile, as depicted in Figure 1.4.

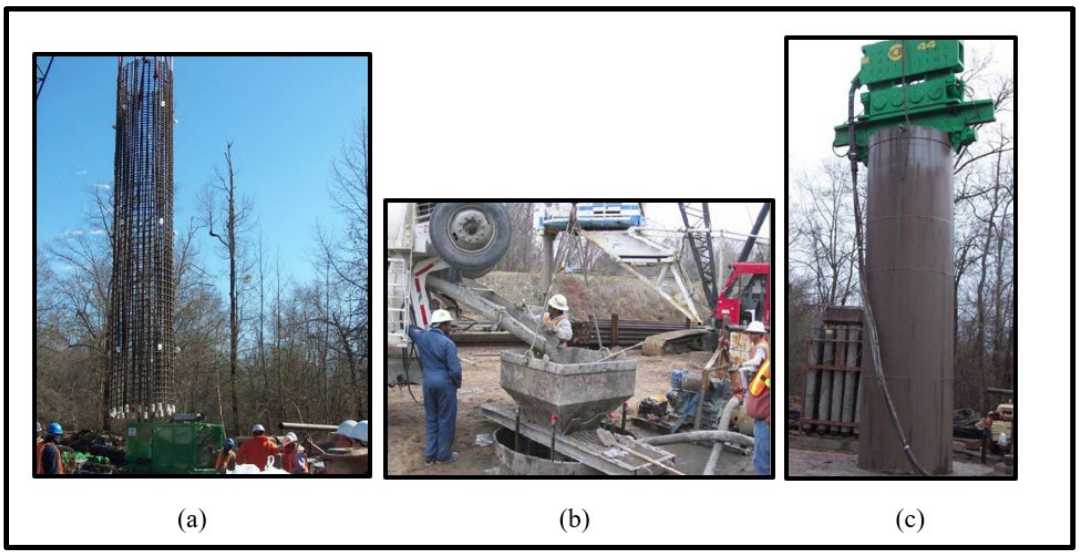

Figure 1.4. Construction process of drilled shaft; (a) Drilling and reinforcement casing; (b) Concrete pouring; (c) Removal of permanent casing [6]

RC drilled shafts are commonly utilized for longer spans or wider bridges due to their ability to withstand higher load demands associated with such structures. In the case of a multi-

lane bridge featuring a 40 ft. long bent cap with six longitudinal girders, generally, only two large diameter drilled shafts are required. Unlike H-pile bridges, this beam and pier configuration necessitates designing the bent caps to accommodate high moment and shear forces resulting from having fewer piers than girders. As a result, the bent cap beams must be designed to withstand these forces, leading to the utilization of deeper bent caps, such as the 4 ft. 6 in. x 4 ft. bent cap illustrated in Figure 1.5.

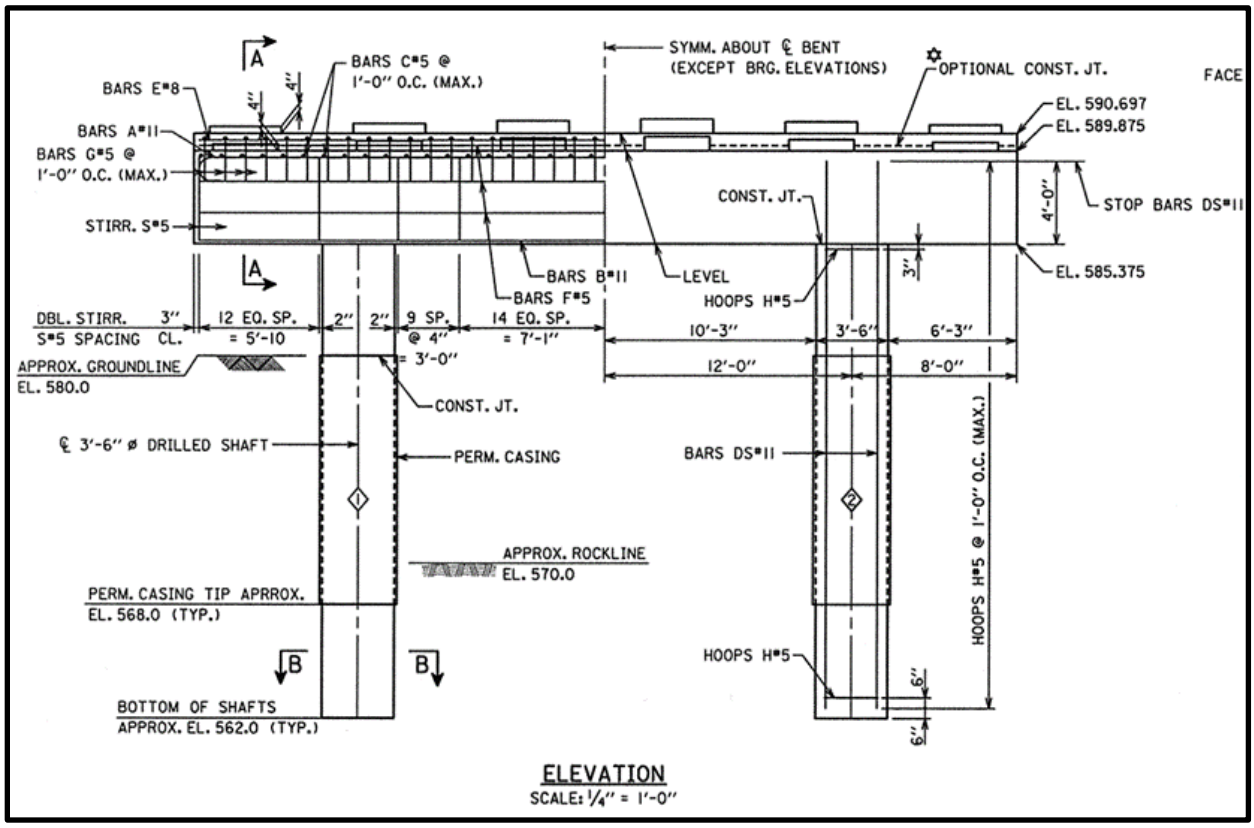

Figure 1.5. RC Drilled shaft use in SR-3 over Cedar Creek in Morgan County, AL

While considered structurally robust and well-established, one of the significant drawbacks of RC drilled shafts lies in their laborious and expensive construction process. This can be attributed to the challenges encountered during drilling, installation, and casting operations.

1.3 Objectives

The main objectives of this research study is to examine the feasibility of utilizing steel pipe pile bridges as an alternative to the current pile bents in Alabama. Additionally, the study aims to propose robust connection details and design methodologies for various steel pipe pile to bent cap connections for generic ALDOT bridges, ensuring compliance with the current LRFD specifications and relevant ALDOT construction practices. The research findings will emphasize the advantages of steel pipe piles and serve as preliminary work for future studies, potentially leading to their adoption by ALDOT. The adoption of steel pipe piles has the potential to offer an efficient and effective substructure construction method for bridges of various sizes, resulting in reduced construction costs and improved utilization of taxpayer resources. The tasks involved in achieving these primary objectives include: i) Conducting a comparative design study to assess the benefits of steel pipe piles over existing piles, ii) Investigating the current state of practice regarding steel pipe and bent cap connections among state DOTs, iii) Examining the strength of potential connections and evaluating design methodologies proposed by researchers, and iv) Proposing the necessary anchorages for the connection between steel pipe piles and reinforced concrete bent caps, as well as establishing design methodologies for the proposed connections.

1.4 Scope

The scope of work to accomplish the research objective includes collecting and reviewing previous studies on steel pipe pile to bent cap connections, as well as obtaining other state DOT approaches to designing and detailing these connections. Based on the literature findings, a comparative study against steel pipe piles and existing alternatives was conducted to highlight the potential advantages. Lastly, studies was also conducted for developing connection details to

evaluate several alternative approaches for connecting pipe piles to bent caps, and developing design methodologies for the calculation of strength of proposed connections based on the design code provisions and literature review.

1.5 Bridge Design Manual Provisions for Steel Pipe Pile Bridge Bent

A bent cap is a flexural substructure element that is supported by columns or piles and is responsible for receiving loads from the superstructure and transferring them to the piles. The combination of the bent cap and the connected piles is collectively referred to as a bridge bent. In the United States, the AASHTO LRFD Bridge Design Manual (AASHTO, 2020) is the standard reference for the design and construction of bridge structures. The AASHTO manual provides guidelines for various types of pile bents, including reinforced concrete bent caps with both vertical and battered H-piles, composite steel piles (concrete-filled steel pipes), and concrete columns. However, it does not specifically address the specific design considerations and construction practices related to hollow large diameter steel pipe piles.

Based on a study sponsored by the National Cooperative Highway Research Program (NCHRP, 2015) regarding large diameter open-end piles (LDOEP), the current design methodology for piling, as well as the testing and quality assurance procedures employed in practice, are incorporated in the AASHTO code. However, it should be noted that this code was not specifically developed for hollow large diameter piles, and many transportation agencies lack extensive experience with such piles. Despite this, several state Departments of Transportation (DOTs) widely utilize steel pipe piles in bridge construction, including agencies such as the Mississippi DOT, Minnesota DOT, California DOT, and Florida DOT. These steel pipe piles are commonly chosen for bridges that require deep foundations, high force resistance, and resilience against harsh marine environments, based on the individual state's provisions. However, there is

limited guidance available regarding the utilization of steel pipe piles, especially in terms of the specific connection configurations to concrete bent caps. Each state DOT tends to employ its unique type of connection, without a standardized and rigorously engineered connection configuration established across all DOTs.

In accordance with the AASHTO LRFD Bridge Design Manual (AASHTO, 2020), specific guidelines are provided for the design of connections between bent caps and piles. These guidelines aim to ensure the robustness and integrity of the connection to prevent failure. The manual states that the top of driven piles should extend a minimum of 12 inches into the pile cap, considering the removal of any damaged material caused by hammering. If the pile is attached to the cap using embedded bars or strands, the pile should still extend no less than 6 inches into the cap. In the case where a reinforced concrete beam is cast-in-place and utilized as a bent cap with support from piles, the concrete cover on the sides of the piles should be at least 6 inches, with an additional allowance for permissible pile misalignment. Furthermore, the center-to-center spacing between piles should not be less than 30 inches or 2.5 times the diameter of the pile. To ensure structural integrity, the distance from the side of any pile to the nearest edge of the pile cap should be no less than 9 inches. These specific details provided by the AASHTO manual play a crucial role in designing a robust connection between the bent cap and piles, minimizing the risk of failure.

ALDOT follows the guidelines and regulations outlined in the Structural Design Manual (SDM, 2023), which has been approved by the ALDOT Bridge Bureau. This manual serves as the reference for designing bridges and other transportation structures for ALDOT, ensuring compliance with the ALDOT bridge design manual. The primary objective of the manual is to provide interpretation and promote consistency in the application of the AASHTO LRFD Bridge Design Specification. It aims to foster uniformity in the preparation of plans and specifications for

bridge projects. Currently, the prevailing design approach employed by ALDOT bridge engineers for multi-span bridges with spans exceeding 50 ft. involves the use of concrete bents. Historically, these bridges have been constructed using various types of piles, such as H-piles, square prestressed concrete piles, or spun-cast cylindrical concrete piles driven into cast-in-place reinforced concrete bent caps. However, in addition to these conventional options, large-diameter steel pipe piles present a promising alternative due to their potential to withstand higher force and moment capacities. It should be noted that the use of steel pipe piles must be preapproved by state bridge engineers before proceeding with the design process. Moreover, there is limited guidance available regarding the connection of steel pipe piles to concrete bent caps, further emphasizing the need for investigation and research in this area.

1.6 Large diameter steel pipe piles

Steel pipe piles offer numerous advantages, including their large vertical bearing and bending strength, excellent environmental performance, ability to be customized for each structure, ease of joining with other structures, and convenient handling. These piles come in various dimensions, production methods, strengths, and applications, which are summarized below.

1.6.1 Types of steel pipe piles

Various types of steel pipes are manufactured by steel companies, including electric resistance welded (ERW) pipes, spiral welded pipes, rolled and welded pipes, and micropiles. The product catalog of Nucor Pipes [7], one of the largest steel producers in the US, provides

information on the available geometries of steel pipes, which are presented in Table 1.1. The lengths and geometries of the pipes can be customized to suit specific applications and uses.

Table 1.1. Dimension of different types of pipes

Types of pipes	Diameter (in.)	Thickness (in.)	Length (ft.)
ERW	$2^{3}/_{8}$-24	0.179- 5/8	Up to 80
Spiral welded	16-120	0.188-1	Up to 130
Rolled and Welded	24-204	0.25-$2^{1}/_{4}$	Up to 120
Micropile	7-16	0.472-0.5	-

Among the listed pipe piles, all except for spirally welded ones are straight. For straight pipes, the manufacturing process involves rolling up and welding steel plates, which requires larger plates. This process generally increases manufacturing difficulties, and the sizes of straight pipes do not vary significantly. In contrast, spiral welded steel pipe piles are preferred over other types because they experience less stress on the seam, enabling them to withstand greater pressure. Spiral welding also offers advantages such as crush resistance and better control over diameter tolerance. The direction of rolling the skelp is neither perpendicular nor parallel to the longitudinal axis of the pipe, enhancing its crack resistance. Additionally, spirally welded pipes are more flexible and customizable, allowing for larger diameters and longer lengths compared to other types of pipe piles.

1.6.2 Manufacturing process of spiral welded pipe

The production process of steel pipes offers flexibility in manufacturing a wide range of pipe diameters and wall thicknesses. This flexibility is essential due to the diverse applications of

steel pipes in both structural and non-structural construction projects. Manufacturers can tailor the production to meet the specific requirements of different construction works.

Steel pipes are manufactured using steel coils and a helical double submerged arc weld (DSAW) process. The manufacturing process involves several steps, as depicted in Figure 1.6. The process begins with a steel coil placed on a horizontal uncoiler mandrel and fed into a straightener. The strip is then passed through a flattener to remove the coil set. As the coil moves through the straightener, the leading and trailing edges of the strip are trimmed in preparation for butt welding. Carbide teeth are used to trim the edges of the coil for welding. The strip enters a three-roll apparatus consisting of lead, buttress, and mandrel roll sets, where it starts to take on a spiral shape, eventually forming a pipe. The welding system performs the welding process, starting from the inside diameter and continuing to the outside diameter using a submerged arc welding technique. After welding, the pipe undergoes visual testing by Quality Control (QC), and if necessary, Ultrasonic (UT) testing is conducted to ensure the absence of defects in the weld. Finally, the pipes are cut to the desired length using a cut-off machine, and specific end properties such as bevel or square cuts can be produced for easier splicing on-site.

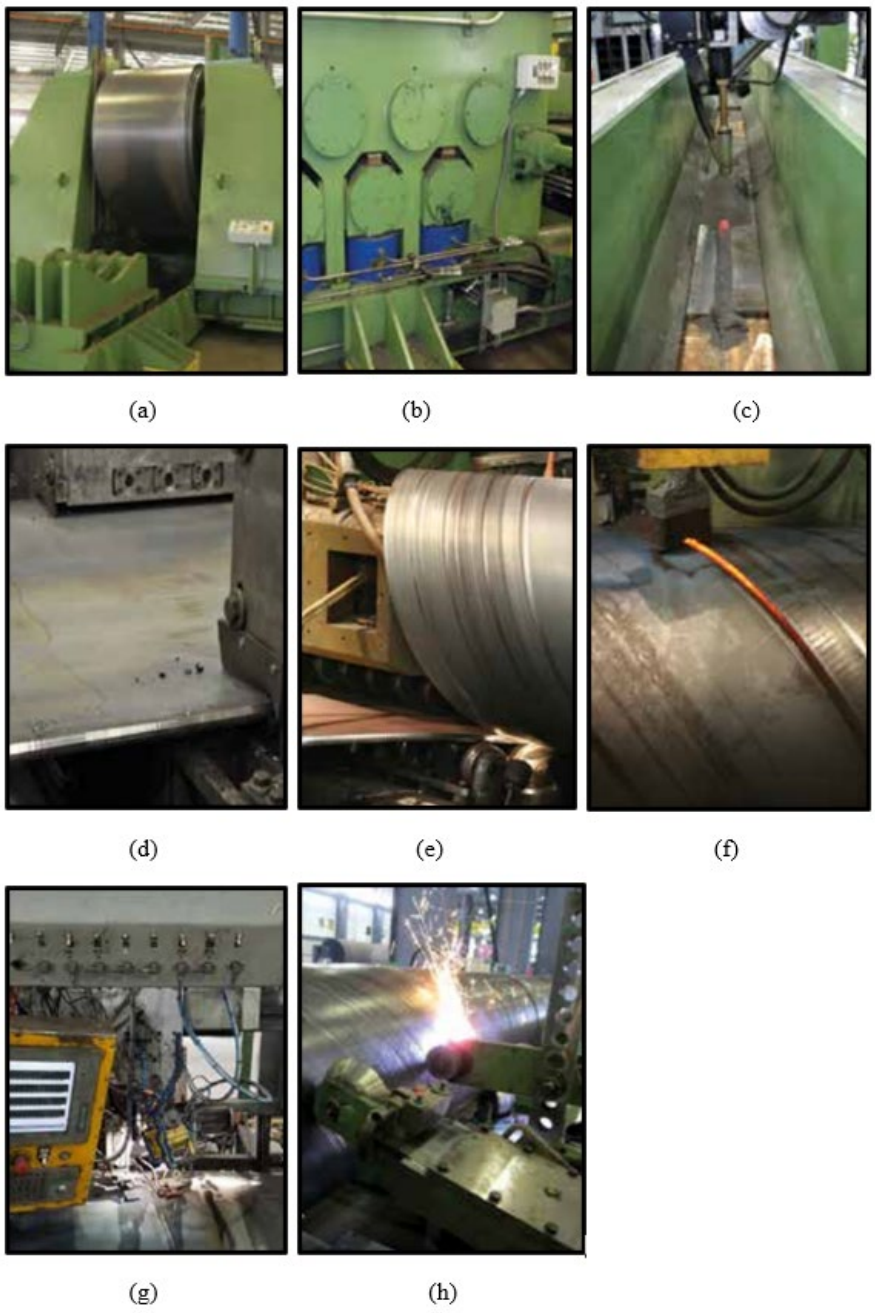

Figure 1.6. Manufacturing process of spiral weld pipe; (a) Uncoiling; (b) Flattening; (c) Joining of the coil ends; (d) Edge milling; (e) Pipe spiraling; (f) Pipe welding; (g) QC; and (h) Pipe cut-off [7]

1.6.3 Pipe Specifications

Steel pipe piles are manufactured according to the pipe specifications expressed in Table 1.2 which provides guidance on manufacturing processes, dimensional requirements, and tolerances. Among all these ASTM 252 Grade 3 having a yield strength of 50 ksi is the most commonly used and readily available steel pipe. Based on the product catalog of Nucor pipes [7] , this specification especially covers steel pipe piles of average wall thickness. It applies to pipe piles in which the steel cylinder acts as a permanent load-carrying member, or as a shell to form cast-in-place concrete piles. The piles should be made by the seamless, electric resistance welded, flash welded, or fusion welded process whereas, the seams of welded pipe piles should be longitudinal, helical-butt, or helical-lap.

Table 1.2. Steel Pipe Grades

ASTM	Yield Strength (ksi)	Manufacture process		
		Spiralweld	ERW	Rolled and Welded
A 139 Grade A	30	✓	✓	✓
A 139 Grade B	35	✓	✓	✓
A 139 Grade C	42	✓	✓	✓
A 139 Grade D	46	✓	✓	✓
A 139 Grade E	52	✓	✓	✓
A 252 Grade 1	30	✓	✓	✓
A 252 Grade 2	35	✓	✓	✓
A 252 Grade 3	45	✓	✓	✓
A 252 Grade 3	50	✓	✓	✓
A 252 Grade 3	60-80	✓	✓	✓
A 500 Grade B	42		✓	
A 500 Grade C	50		✓	
A 1085	50-70		✓	

1.6.4 Application of steel piles

As mentioned earlier, steel pipes possess mechanical and physical properties that make them highly versatile in construction. They provide strength, cost-effectiveness, and ease of

installation. Due to the flexibility afforded by the production process and stringent quality control measures, steel pipe piles find applications across a wide range of construction projects. They are commonly utilized in foundation works for marine structures, civil structures, bridge footings, abutments, and even as casings for concrete piles. The following are some examples of the uses of steel pipe piles:

1. Bearing piles

   Circular steel pile (Figure 1.7 (a)) offers several advantages over other types of driven piles, making them an efficient choice for load-bearing structures. The circular geometry of the pipe eliminates any weak axes, ensuring uniform load distribution. Additionally, the interior of the pile can be driven into the ground to remove obstructions, further enhancing their effectiveness. To further enhance the strength of these piles, they can be reinforced with concrete.

2. Drilled shaft casing

   Steel piles can also serve as casings for drilled shafts, as depicted in Figure 1.7 (b). These casings encompass a reinforcement cage and concrete. By using casings, the flow of concrete is controlled, preventing the formation of voids within the structure caused by soil or water intrusion. Furthermore, the casings help mitigate the deterioration of the shafts.

3. Combination walls

   Large diameter steel pipes exhibit high bending strengths, making them ideal for constructing walls. A highly efficient system can be achieved by combining pipe piles and steel sheet piles, as shown in Figure 1.7 (c). In this system, the pipe piles bear the majority of the loads, while the steel sheet piles transfer the loads to the surrounding soil. This combination results in a robust and effective structural solution.

4. Structural sections

The geometry of steel pipes offers uniform bending strength in all directions, making it an excellent material for resisting buckling and ensuring structural stability. This characteristic makes steel pipes well-suited for use in structural sections, as exhibited in Figure 1.7 (d).

5. Sign poles, Towers, and Transmission lines

Sign poles and towers, as depicted in Figure 1.7 (e), are specifically designed to withstand significant bending loads at their bases. The extensive availability of large diameter pipes, coupled with a wide range of thicknesses and lengths, offers designers the flexibility to select the precise size required for their specific project. Additionally, the use of reduction collars enables efficient splicing of different pipe diameters, further enhancing the overall design efficiency.

6. Mining

Air shafts are crucial for mining operations conducted in hazardous underground environments. Steel pipe piles, illustrated in Figure 1.7 (f), offer a versatile solution for constructing shafts of various diameters, thicknesses, and lengths, tailored to specific project requirements.

7. Jacked and Bored

Jacked and bored pipes, depicted in Figure 1.7 (g), are employed for the installation of underground utilities. This process involves several steps. Initially, sections of piles are pushed into the ground using hydraulic jacks, and subsequent pipes are spliced onto the first section to continue the jacking process. Once jacking is completed, the pipe serves as a conduit for utility installation, eliminating the need for extensive excavation.

8. Line pipe

Spirally welded pipes, illustrated in Figure 1.7 (h), serve as excellent construction materials for transporting liquids, air, and gas. These pipes exhibit exceptional strength compared to other options and are specifically designed to withstand internal and external pressures in various applications.

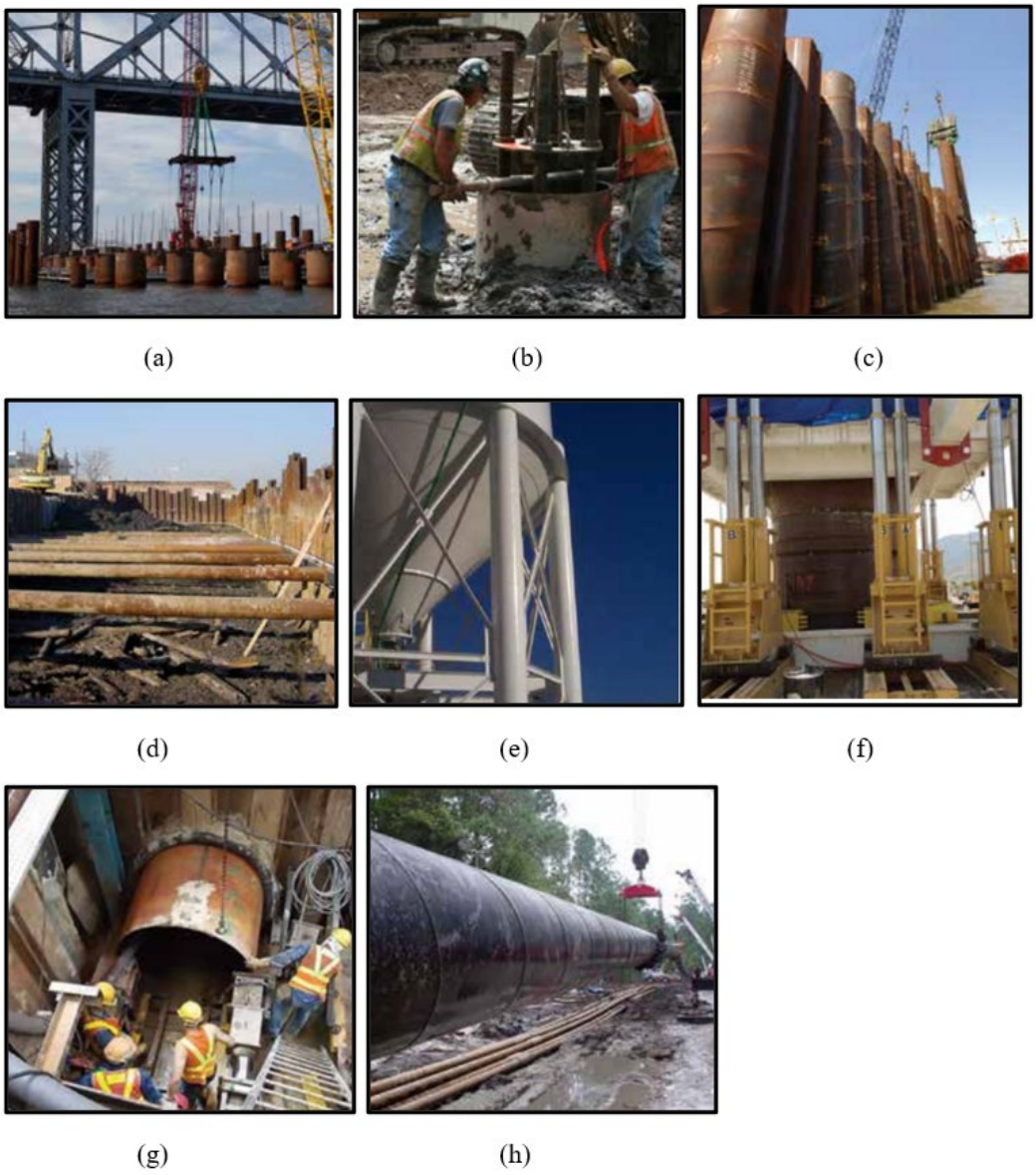

Figure 1.7. Uses of steel pipe; (a) Bearing piles; (b) Drilled shaft casing; (c) Combination walls; (d) Structural sections; (e) Sign poles, Towers & Transmission line; (f) Mining; (g) Jacked and Bored; and (h) Line pipe [7]

1.6.5 Limitations of steel pipe piles

Steel pipe piles have numerous advantages for foundation applications; however, they also come with certain drawbacks. One significant disadvantage is their susceptibility to corrosion, particularly in marine environments or areas with high moisture content. The corrosive effects can gradually erode the structural integrity of the piles, leading to potential issues over time and necessitating expensive maintenance or even replacement. Based on the Nucor Skyline catalogue [7], various corrosion rates have been provided for steel pipes. These rates are compiled and presented in Table 1.3, providing valuable information about the expected corrosion tendencies of steel pipes under different conditions and environments. This data can help in making decisions regarding the selection and application of steel pipe piles, considering the specific corrosion challenges they may face.

Another drawback is the installation process. While HP-piles are more numerous, their smaller size makes installation easier. However, when dealing with large-diameter steel pipe piles, the installation process can become challenging due to the large size of the structures involved. The size difference affects various aspects, including the logistics involved in handling and transporting the piles, the specific equipment required for installation, and the overall complexity of the installation procedure.

These drawbacks related to steel pipe piles should be considered during the design and construction of bridge structures.

Table 1.3. Corrosion rate of steel pipe in various locations

Location of piles	5 years	25 years	50 years	75 years	100 years
	(in)				
Undisturbed natural soils	0	0.012	0.024	0.035	0.047
Polluted natural soils	0.006	0.03	0.059	0.089	0.118
Aggressive natural soils	0.008	0.039	0.069	0.098	0.128
Non-compacted and non-aggressive fills	0.007	0.028	0.047	0.067	0.087
Non-compacted and aggressive fills	0.02	0.079	0.128	0.177	0.226
Common fresh water	0.006	0.022	0.035	0.045	0.055
Very polluted fresh water	0.012	0.051	0.091	0.13	0.169
Sea water	0.022	0.074	0.148	0.22	0.295

1.7 Organization of thesis

Chapter 2 provides a comprehensive literature review on the connections between piles and foundation/bent cap. Numerous research studies have investigated various types of connections and developed calculation procedures to determine connection strengths. This section emphasizes different design methodologies and examines the effects of various parameters associated with these connections.

Chapter 3 offers an in-depth examination of the current state of practice regarding the utilization of steel pipe piles in bridge structures. The emphasis is placed on the specifications set by various state Departments of Transportation (DOTs), their allowance for the use of steel piles, and the benefits and challenges encountered during their implementation. The main focus is directed toward the investigation of drawings, details, and design methodologies about the connection between pipe piles and reinforced concrete bent caps, as employed by diverse state DOTs in their bridge structures.

Chapter 4 delves deeper into the design methodologies established in the studies reviewed in the previous section. It conducts a comparative analysis of various design methods used to calculate the strength of connections by implementing these methods on tested specimens. Additionally, this chapter provides a comprehensive summary of the provisions concerning connections as outlined in different design codes.

Chapter 5 presents a comprehensive summary of the comparative study conducted on various types of pile bents and examines the reasons why steel pipe piles are considered favorable replacements for existing piles.

Chapter 6 presents the proposed connection details for steel pipe piles and provides a thorough analysis of their strength calculations. The chapter outlines the design methodology employed for determining the connection and their connection strength and showcases the recommended connection configurations for optimal performance.

Chapter 7 concludes the thesis by presenting a comprehensive discussion on the connection details between steel pipe piles and bent caps. The study findings are summarized, highlighting the anticipated advantages of using steel pipe piles, as well as identifying potential challenges associated with specific connection details. Additionally, the chapter offers recommendations for future research in this field, aiming to further enhance the understanding and implementation of steel pipe pile connections for improved structural performance.

Chapter 2 LITERARURE REVIEW

This chapter provides an overview of the research programs conducted on the connection between steel pipe piles and bent caps/foundations. The review begins by examining the use of concrete-filled steel tubes (CFST) embedded within reinforced concrete bent caps/foundations. It then explores various types of anchorage methods utilized in these connections, along with the corresponding strength calculation methodologies.

2.1 General Studies

2.1.1 Comparison of Steel Pipe piles (M. N. Baig et.al., 2006)

This study primarily focuses on Concrete-Filled Steel Tubes (CFSTs), which are widely recognized as popular structural elements in buildings and bridges. CFSTs exhibit excellent structural performance characteristics, such as high strength, stiffness, and ductility. They offer several advantages over other composite members. Firstly, the steel tube acts as formwork for the concrete, ensuring efficient construction. Additionally, the concrete filling enhances the resistance to local buckling of the steel tube wall. The steel tube also serves as a protective barrier, preventing excessive spalling of the concrete. Moreover, the incorporation of CFST columns significantly increases the stiffness of a structural frame compared to conventional steel frame construction.

The purpose of this research was to evaluate the strength of steel tubular columns, considering different shapes and levels of confinement. The experimental program involved a total of 24 specimens, which were subjected to axial compressive loads until failure. The study utilized identical circular steel columns, half of which were filled with concrete while the other half remained hollow (6 specimens with concrete fill and 6 without). A similar approach was followed for square columns as well. The tests were conducted on 30 in. short steel columns made of grade

36 steel, with a thickness of 0.1 in. The concrete used in the specimens had a compressive strength of 4 ksi. Detailed information about the specimens used in the experiments is provided in Table 2.1.

Table 2.1. Detail of specimens

Type of column	Size (in.)	Thickness (in.)	Nomenclature of specimens	Number of specimens
Circular hollow	4.5	0.1	4CH	3
	6	0.1	6CH	3
Circular filled	4.5	0.1	4CF	3
	6	0.1	6CF	3
Square hollow	3.5	0.1	4SH	3
	5	0.1	6SH	3
Square filled	3.5	0.1	4SF	3
	5	0.1	6SF	3

Figure 2.1 illustrates the results of the experimental programs that were conducted. These experiments demonstrated that the compressive strength increased significantly in circular columns compared to square columns, primarily due to increased confinement. The addition of concrete in circular columns played a crucial role in enhancing compressive strength, leading to an increase of nearly 60% in most cases. Furthermore, the presence of concrete reduced the occurrence of local buckling in circular columns, whereas square columns exhibited prominent local buckling in both scenarios. While a confining effect could be anticipated in circular CFST columns, square columns displayed only a marginal increase in axial strength due to triaxial effects, even when the wall thickness was substantial. Conversely, the cross-sectional shape had a remarkable influence on the axial load-deformation behavior of the columns. Circular columns demonstrated strain-hardening or elastic perfectly plastic behavior after yielding, as observed in the load vs. deformation relationship. In contrast, square columns exhibited a degrading load-deformation curve.

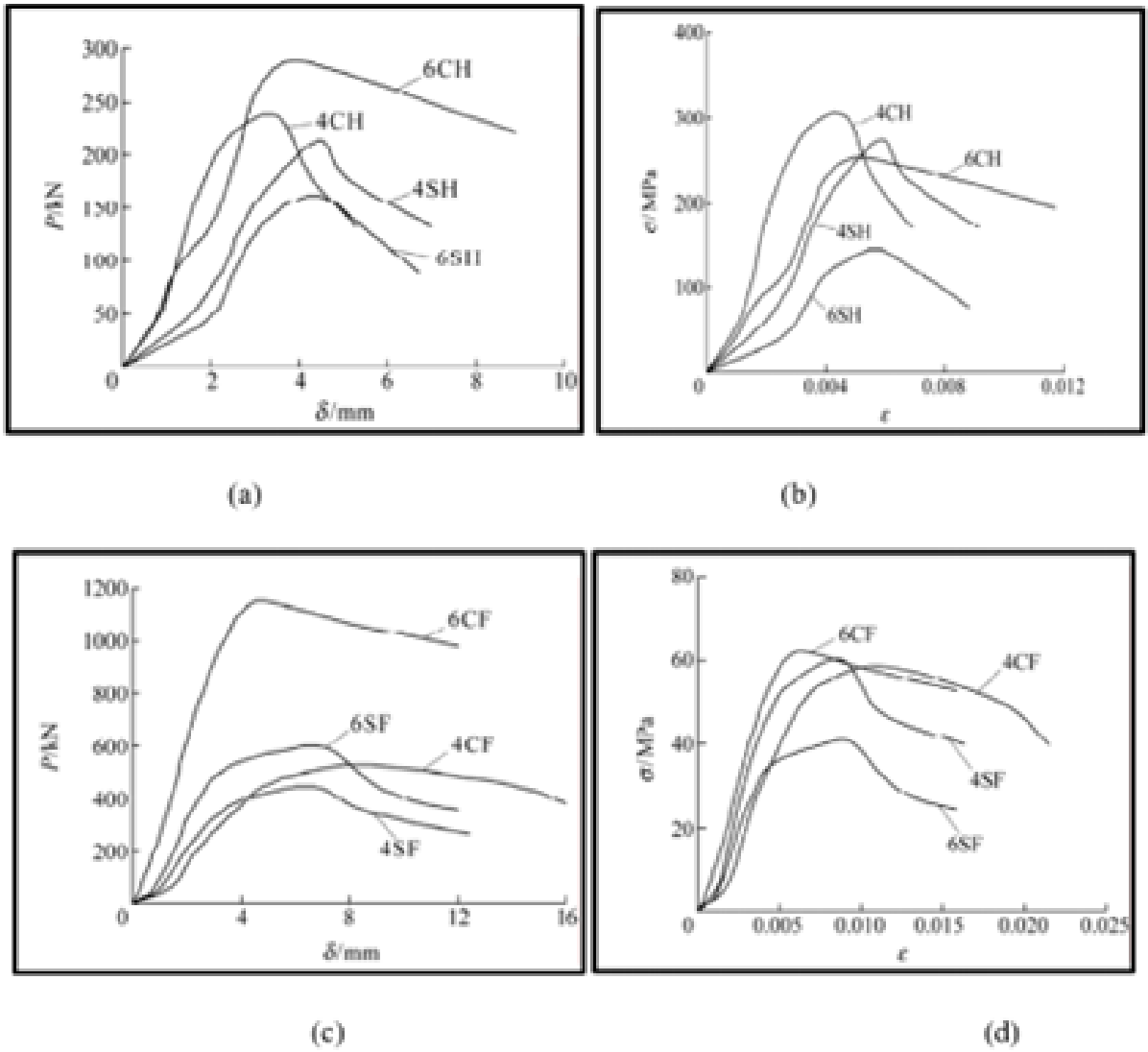

Figure 2.1. (a) Load-displacement; (b) Stress-Strain for hollow columns; (c) Load-displacement; (d) Stress-Strain for filled columns [8]

2.1.2 Connection between concrete and embedded steel (Marcakis et. al., 1979)

Marcakis and Mitchell conducted a series of 21 experiments focusing on precast connections that involved steel members embedded within reinforced concrete sections. The steel members varied, ranging from welded or embedded H piles and concrete-filled or unfilled pipe piles to standard steel plates. The strength of these connections depended on factors such as the width of the embedded steel, embedment depth, concrete strength, and eccentricity of loading. The

primary goal of the study was to develop an analytical model capable of capturing the behavior of these connections, which could serve as the foundation for a design procedure.

The design methodologies commonly used for such connections were presented in the Design Handbook of the Prestressed Concrete Institute (PCI). Figure 2.2 illustrates the simplified assumptions applied in the calculations for lateral load. For the ultimate compressive stress block on the front face, it was assumed that the block's width, represented as "b," matched the width of the embedded steel member, while its depth equaled one-third of the embedment length, denoted as "l_e." The stress block was assumed to have a uniform stress of $0.85f'_c$, and the compressive strain at the front face was assumed to be 0.003. By assuming equilibrium between the forward compressive force, C_f, and the backward compressive force, C_b, the strength of the connection was determined using Eq. (2.1).

$$V_c = \frac{0.85f'_c b l_e}{3.67 + 4\frac{a}{l_e}} \quad \textbf{(2.1)}$$

where, V_c is nominal capacity of connection, f'_c is compressive strength of connection, l_e is embedment depth, a is distance between lateral load and face of column.

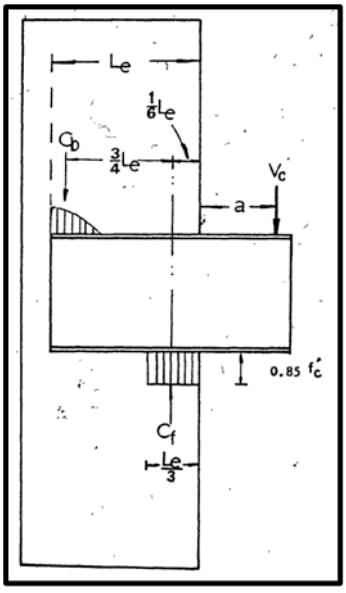

Figure 2.2. PCI stress distribution for steel members [9]

This series of experiments yielded several key findings regarding such connections. Firstly, it was observed that thin-walled hollow sections tended to fail due to local buckling, which was effectively mitigated by the presence of a concrete plug. The study concluded that the strength of the steel increased when the connection region was filled with concrete. Furthermore, the width of the embedded steel was found to be a critical factor influencing the strength of the connection. The wider the steel width, the greater the strength observed. In their work, Marcakis and Mitchell proposed Eq. (2.2) as a means to calculate the ultimate shear force (V_u) carried by a pile-pile cap connection. This equation was based on a strut-and-tie approach and utilized uniform stress distributions along the embedment zone to determine the required embedment length (l_e). To determine the moment capacity of a connection, the shear capacity as expressed in Eq. (2.2), was multiplied by the eccentricity (e) measured from the point of zero moment to the center of the effective embedment (embedment length minus the cover depth, c).

$$V_u = \frac{0.85 f'_c b' (l_e - c)}{1 + 3.6 \frac{e}{(l_e - c)}} \quad \textbf{(2.2)}$$

The experimental results revealed that the actual strength observed was greater than the strength calculated using the effective width (b') assumed to be equal to the width of the embedded steel. This observation was attributed to the load being distributed over a wider area due to the confinement provided by the surrounding concrete. To determine the effective width (b'), it was assumed to be either equal to the width of the pile cap or a maximum of 2.5 times the width of the steel section (w).

The study concluded that several factors significantly influenced the strength of the connection between the embedded steel and reinforced concrete sections. These factors included the width of the steel section, embedment depth, concrete strength, and the eccentricity of loading.

2.1.3 Steel pile embedded into concrete cap (R. S. Eastman et. al., 2011)

In a typical moment resisting connection, reinforcement is commonly employed. However, the purpose of this study was to investigate pile-to-cap connections without the use of reinforcement. Three pile-to-cap specimens were tested, each having a different pile embedment depth and featuring a cover plate at the end. Lateral loading was applied to these specimens until failure occurred. The general specimen configuration is depicted in Figure 2.3. Specimens 1, 2, and 3 had embedment depths of 18 in., 6 in., and 5 in., respectively. The lateral loading was performed at a distance of 60 in. from the end of the bent cap.

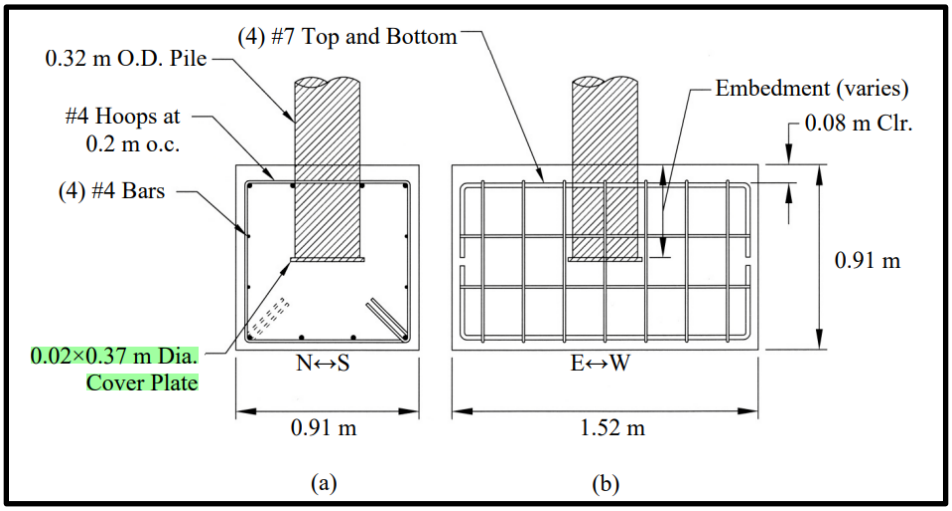

Figure 2.3. Typical specimen (a) End view; (b) side view [10]

By utilizing the properties of the pile, the yield moment and plastic moment were calculated to be 207 kips-ft and 275 kips-ft, respectively. The experimental results revealed the ultimate moment capacities of the connections for specimens 1, 2, and 3 to be calculated as 288 kips-ft, 75.5 kips-ft, and 39.5 kips-ft, respectively. The results indicated that the connection in specimen 1 had sufficient capacity to withstand the yielding of the pile, whereas the other two specimens lacked adequate capacity. This highlights the importance of providing sufficient embedment depth within the cap for a strong connection.

The calculation of the connection strength for specimen 1, based on Eq. (2.2) using the effective width equal to the width of the pile, yielded a reasonable maximum shear force. However, this approach did not perform well for specimens 2 and 3, which had shallow embedment depths. The test results confirmed that pile-to-cap connections with shallow pile embedment depths exhibited significant stiffness and higher strength compared to what was calculated using the Marcakis and Mitchell equation. To address this, an improved model was developed to estimate the elastic and ultimate capacities of embedded connections. In addition to the embedment mechanism considered by Marcakis and Mitchell, this model incorporated a bearing mechanism with a limit on friction at the end of the pile. For pile-to-cap connections where the ratio of pile bearing area to pile embedment depth was large, the bearing mechanism provided greater strength than the embedment mechanism. Conversely, for pile-to-cap connections with a small ratio of pile bearing area to pile embedment depth, the bearing mechanism made little contribution to the connection's strength.

2.1.4 Steel column embedded into flat slab (Y. Wang et. al., 2017)

A flat slab is a type of reinforced concrete slab that is directly supported by concrete columns, eliminating the need for beams. In such slabs, reinforced columns are typically employed. This paper presents experimental research on an innovative and straightforward connection between a steel tubular column and a flat slab, utilizing shear studs, as presented in Figure 2.4. The experimental studies aimed to investigate the effects of various design variables on the punching shear behavior and resistance of the proposed shear connection system. These variables included the depth of concrete above the shear stud, concrete grade, and dimensions of the shear studs (length and diameter).

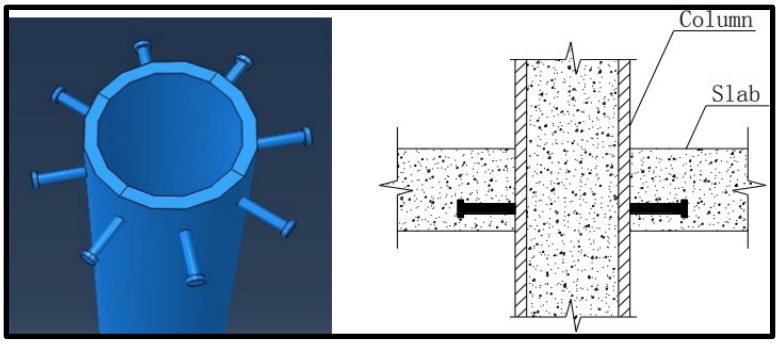

Figure 2.4. Arrangement of shear studs in steel tube to flat slab shear connection system [11]

Push-out tests were conducted to gain a better understanding of the shear behavior of the proposed connection and to analyze the effects of various factors involved in the tests. Seven different specimens were prepared to investigate the influence of concrete above the shear studs, concrete grade, and shear stud dimensions. The key details of the specimens are provided in Table 2.2. In each specimen, two shear studs were securely welded to the outer perimeter of the steel tube, as shown in Figure 2.5.

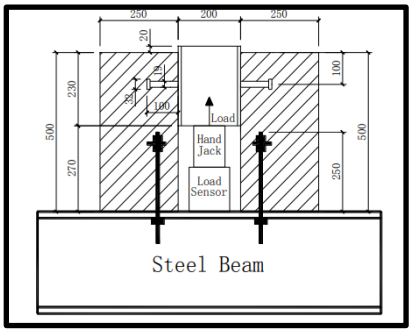

Figure 2.5. Arrangement and dimensions of push out test [11]

Table 2.2. Main parameters of the experiment program

Specimen	Concrete Grade	Concrete depth above shear stud (in.)	Stud size (in.)	Remarks
1	C40	3.94	0.75x3.94	Reference model
2	C20	3.94	0.75x3.94	Concrete grade
3	C60	3.94	0.75x3.94	
4	C40	2.95	0.75x3.94	Concrete depth above shear stud
5	C40	1.58	0.75x3.94	
6	C40	3.94	0.75x5.9	Stud length
7	C40	3.94	0.98x3.94	Stud diameter

During the push-out test, an initial load of up to 40% of the anticipated failure load was applied. In subsequent steps, the load increment was reduced to 5% of the expected failure load. The testing process was halted once the applied load had decreased to 50% of the peak load.

All the specimens exhibited a similar failure pattern. A crack formed at an approximate angle of 35° relative to the top edge, originating from the center of the shear studs and extending towards the edge of the concrete block. Subsequently, the crack width rapidly expanded as the applied load reached its peak value. As the load decreased, the crack width continued to widen. The cracking behavior of the concrete block is portrayed in Figure 2.6.

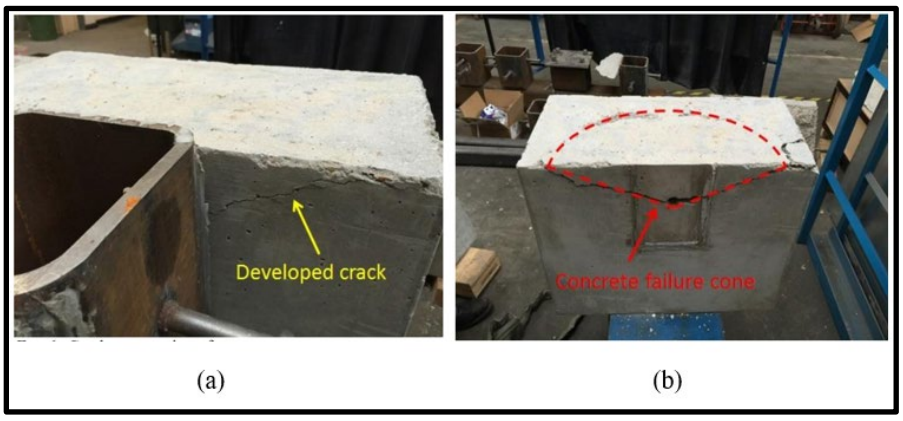

Figure 2.6. (a) Crack propagation of concrete; (b) Failure pattern of concrete [11]

The graphs in Figure 2.7 present comparative studies among the specimens with varying concrete depths above the shear studs, shear stud dimensions, and concrete grade.

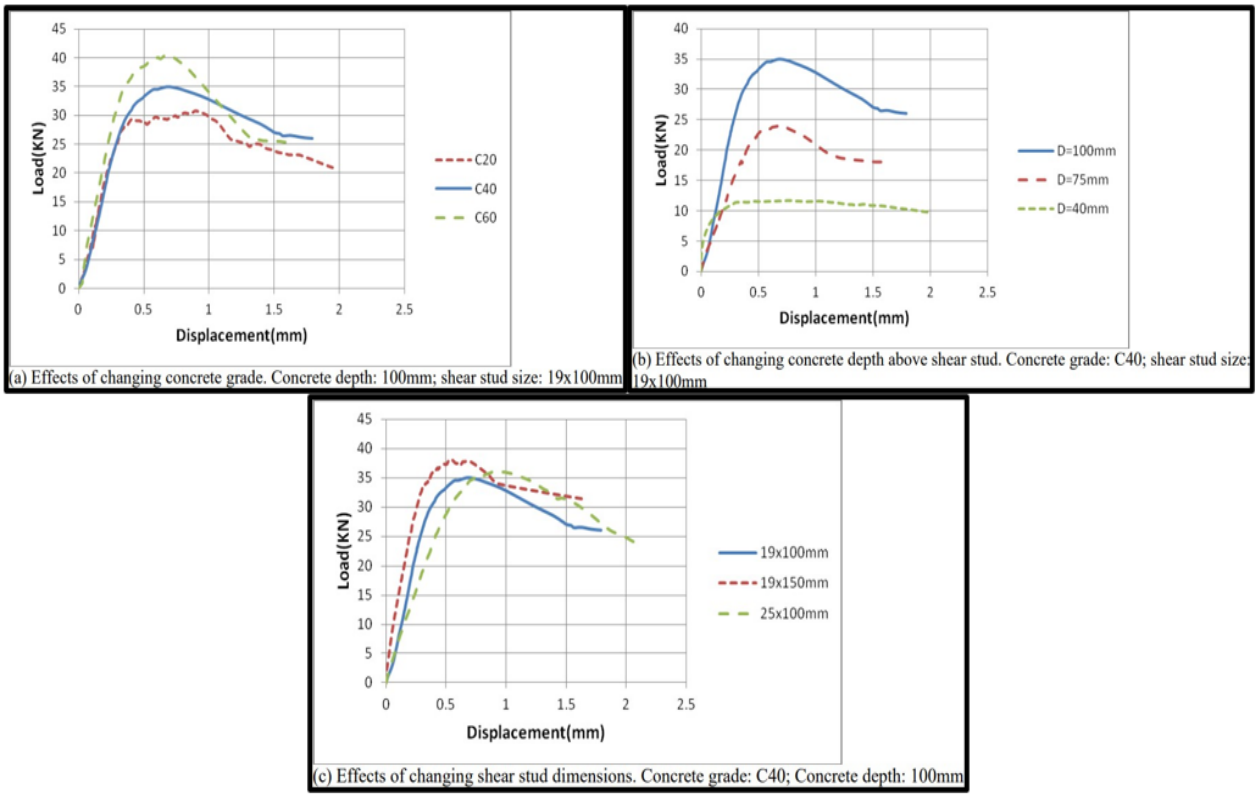

Figure 2.7. Load-displacement curve with varying factors [11]

(1 in.=25.4 mm and 1 KN=0.225 kips)

The experimental results demonstrated the effectiveness of the proposed connection utilizing shear studs in providing the required punching shear resistance between the flat slab and the steel column. The study concluded that the punching resistance was directly related to the tensile strength of the concrete and could be enhanced by welding shear studs to the bottom surface of the flat slab whenever feasible. The dimension of the shear studs had a moderate influence on the punching resistance.

2.2 Studies based on connection between foundation and steel pile

2.2.1 Connection between concrete filled steel pipe pile and reinforced concrete foundation (D. E. Lehman et. al., 2012)

The research programs conducted by Washington University focused on embedded ring connections between reinforced concrete foundations and concrete-filled steel tubes (CFSTs) without any additional reinforcements. These connections were designed to achieve the full moment capacity of CFST columns. A flanged annular ring was welded to the tip of the pile, which was embedded into the foundation. The ring provided an anchorage, transferring axial and shear stresses, as well as moments, to the surrounding reinforcement and concrete, as illustrated in Figure 2.8.

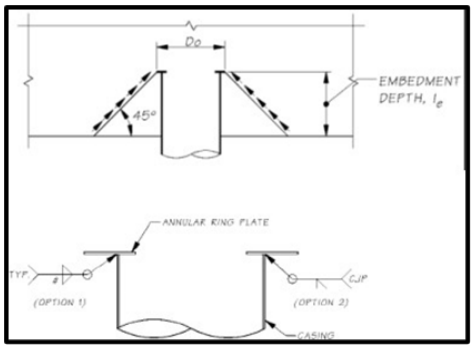

Figure 2.8. Annular ring [12]

As mentioned previously, an annular ring was welded at the end of the pile, with an external projection 16 times the thickness of the steel tube and an internal projection 8 times the thickness. The purpose of this configuration was to provide anchorage and ensure efficient transfer of shear and moment to the surrounding concrete and reinforcement, as illustrated in Figure 2.9. For the experimental programs, two variations were considered for the embedment technique: I) the monolithic option and II) the grouted option, as depicted in Figure 2.10(a) and Figure 2.10(b)

respectively. In the monolithic connection, the foundation and column were cast simultaneously, while in the grouted option, the column and ring were placed after the foundation had been cast.

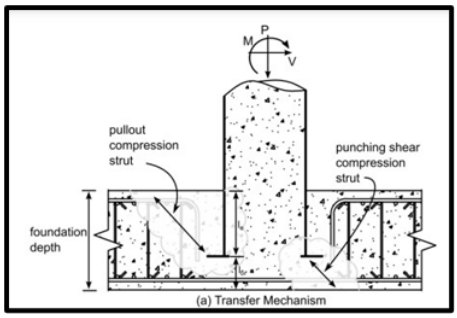

Figure 2.9. Working mechanism of annular ring [12]

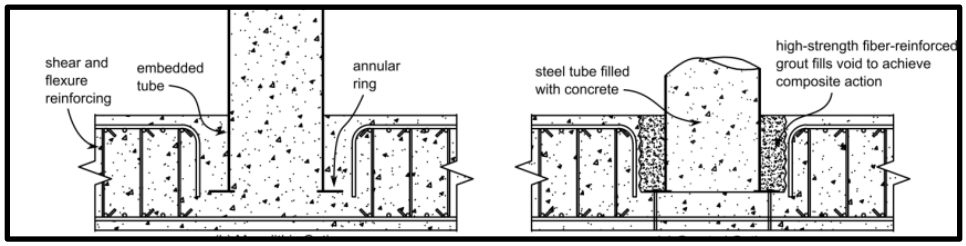

Figure 2.10. Connection options; (a) Monolithic; and (b) Grouted [12]

The experimental programs conducted to assess the CFST column-to-foundation connections comprised a series of 19 specimens. The primary objectives of the program were to: i) analyze the behavior of different types of embedment under axial compression and cyclic lateral load, ii) examine the impact of yield strength, geometry, and embedment depth of the connection (l_e), iii) evaluate the effect of varying loads on the connection, and iv) develop design procedures for the connection. Figure 2.11 illustrates the details and geometry of a typical specimen. In the majority of the specimens, the steel tube had a diameter of 20 in. and a thickness of 0.25 in., resulting in a diameter-to-thickness ratio (D/t) of 80. The dimensions and primary flexure reinforcement of the footing were selected to withstand the plastic moment capacity of the column.

Most of the specimens were tested under an applied load approximately equal to 10% of the gross compressive load capacity of the CFST column. However, various additional axial load

ratios were also examined. The details of the specimens, along with the nominal material strengths, are summarized in Table 2.3.

Table 2.4 presents a summary of the results obtained from the experimental programs conducted on various specimens. Due to the extensive nature of the testing program, this discussion focuses on the hysteretic performances of selected specimens to emphasize the impact of different parameters on the connection's performance. These parameters include the type of connection, tube embedment depth, axial load ratio, and column diameter.

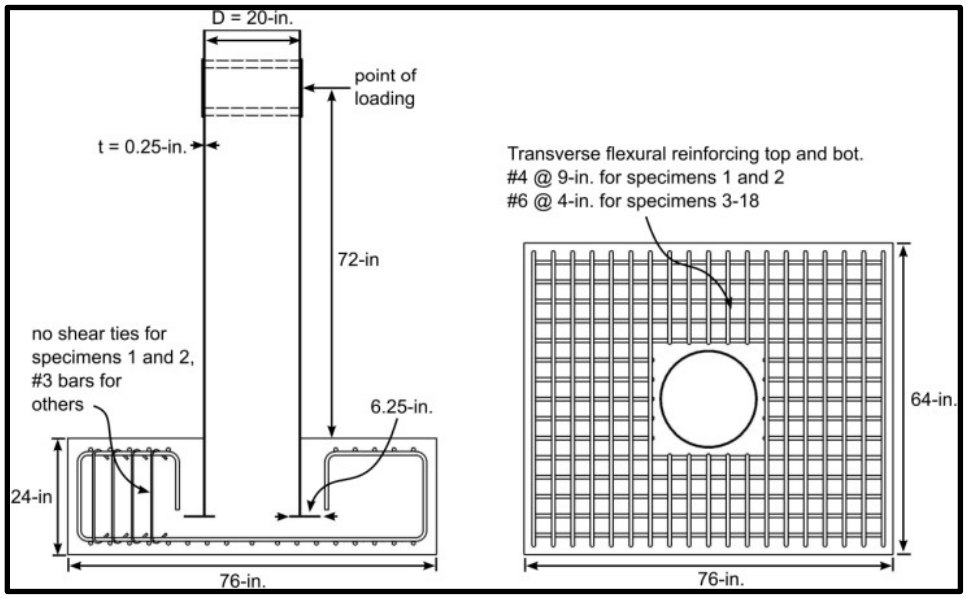

Figure 2.11. Typical specimen of experiments [12]

Table 2.3. Experimental Parameters and Material Properties from Prior Research

Specimen	D (in.)	t (in.)	L_e/D	Connection type	Study parameter
1	20	0.25	0.6	Monolithic	No vertical reinforcement
2	20	0.25	0.6	Monolithic	Vertical reinforcement
3	20	0.25	0.9	Monolithic	Embedment depth
11	20	0.25	0.9	Recessed	0.15 axial load
12	20	0.25	0.9	Recessed	0.2 axial load
13	20	0.25	0.8	Monolithic	Straight seam tube
14	20	0.25	0.775	Recessed	Straight seam tube
19	30	0.25	0.62	Recessed	Larger diameter, 0.05 axial load

The experimental results obtained from Specimens 1 and 2 revealed that the shear strength of the concrete did not increase with the inclusion of vertical footing reinforcement. However, it did enhance the deformability of the connection. Therefore, the test results indicated that the vertical shear reinforcement influenced the deformability of the system rather than its strength.

Specimens 1 and 3 exhibited both ductility and strength, with the failure mode being dependent on the embedment of the column. The test results clearly demonstrated that a sufficient embedment of the pile inside the foundation is necessary for the connection to possess strength.

Specimens 13 and 14 exemplified the strength and ductility of the monolithic and grouted connection types, respectively. As depicted by the hysteretic curves in Figure 2.12, the use of a grouted connection did not impact the performance of the embedded connection.

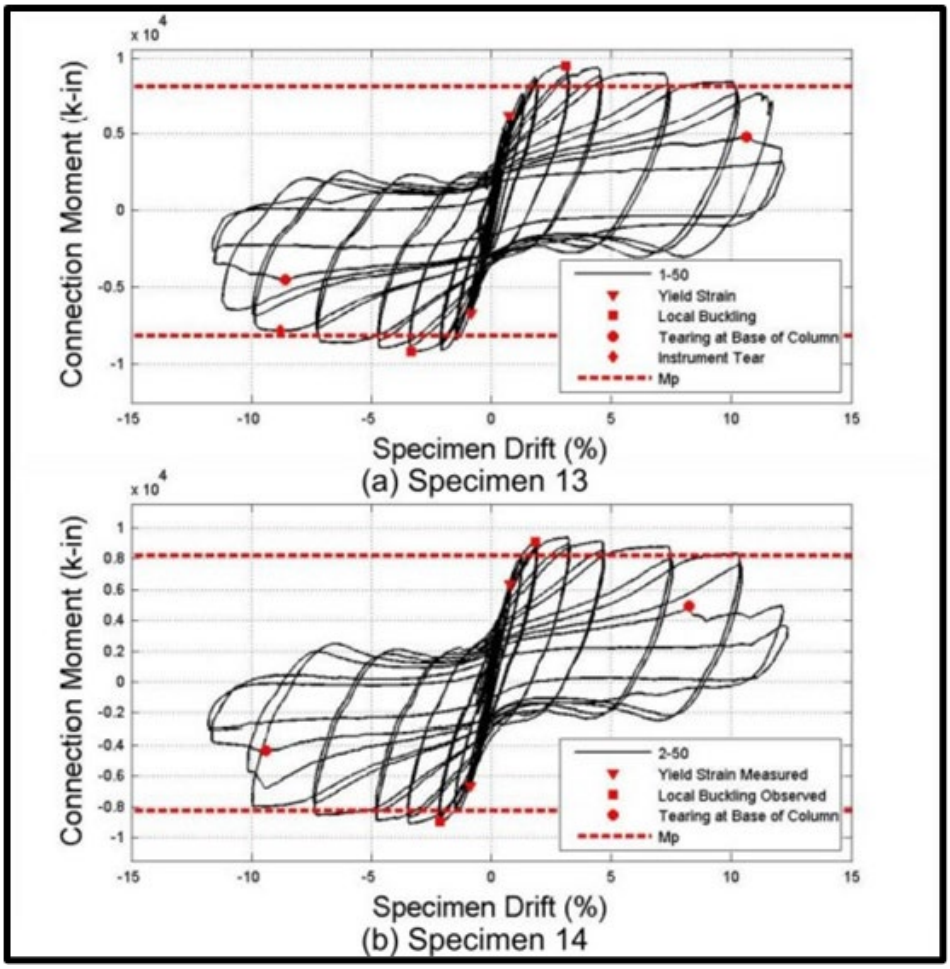

Figure 2.12. Typical Moment-Drift Response From Monolithic and Grouted Connection Types [12]

Specimens 11, 12, and 19 were examined to assess the impact of axial load ratio on the behavior of the embedded connections. These specimens were subjected to constant axial load ratios of 15%, 20%, and 5% respectively, and were subsequently subjected to increased cyclic lateral loading.

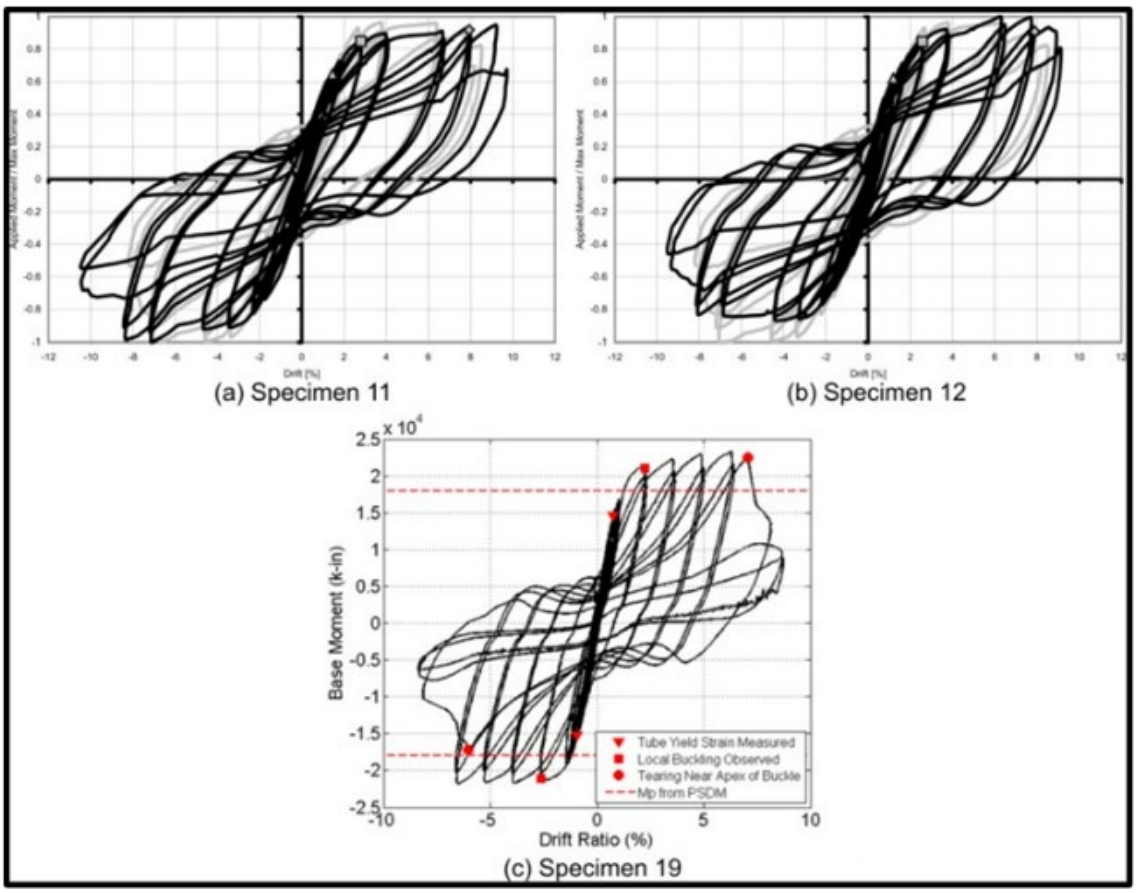

Figure 2.13. Typical Moment-Drift Response for Embedded Connection Specimens Subjected to Axial Load Ratios of (a) 15%; (b) 20%; and (c) 5% [12]

The behavior of the embedded connection was minimally affected by the axial load ratio, as demonstrated by the hysteretic curves presented in Figure 2.13. Furthermore, the hysteretic curves indicated that the embedded connection had the capability to reach the full plastic capacity of the CFST for relatively large connection diameters. Notably, Specimen 19, with a diameter of 30 inches, was the largest CFST ever tested.

Table 2.4. Experimental results

Specimen	Lateral Load (kips)	$M_{peak}/M_{P, PSDM}$	Failure mode
1	130.73	0.88	Cone pullout
2	134.78	0.92	Cone pullout
3	165.38	1.13	Ductile tearing
11	167.18	1.14	Ductile tearing
12	177.3	1.23	Ductile tearing
13	121.05	1.17	Ductile tearing
14	119.25	1.17	Ductile tearing
19	87.01	1.3	Ductile tearing w/ cracking

The experimental results were utilized to establish design methodologies for the following aspects: i) determining the appropriate size of weld and annular ring, ii) deriving equations to calculate the necessary embedded length to prevent pullout failure, and iii) formulating equations to determine the required footing thickness to prevent punching failure. The design methodologies pertaining to this study, which complete the design approach for the proposed connection, are presented in Section 4.2.1.

2.2.2 CFSTs embedded inside the foundation for punching resistance (S. Tan et. al., 2022)

In this paper, the punching shear behavior of an embedded concrete-filled steel tube with shear studs welded to its outer surface and an end plate on top of the tube was studied experimentally.

Six specimens were prepared, each with its own replica for result comparison. The typical details of the specimens are illustrated in Figure 2.14. The tests were divided into two groups, as explained in Table 2.5. All specimens had a 5.52 in. column with a thickness of 0.18 in. The first group, BS, aimed to determine the bond strength between the outer surface of CFSTs and the surrounding concrete. These specimens did not have welded shear studs. Similarly, the second group, P, focused on studying the punching shear behavior of such connections. In the first specimen, P-900/P-500, which had different spacing between end supports, no shear studs were provided. However, the other specimens were equipped with welded shear studs. Specimens P-SD-10-3-50 and P-SD-10-3-100 had three rows of twelve shear studs with a diameter of Φ0.39 and varying stud lengths. Specimen P-SD-10-5-50 had five rows of twenty shear studs with a diameter of Φ0.39, while specimen P-SD-16-3-100 had three rows of twelve shear studs with a diameter of Φ0.63. These different specimens were used to study the effect of stud dimensions and the number of studs.

Table 2.5. Basic details of the specimens

Specimen	Type of test	*D* (in.)	*t* (in.)	Shear stud	*D* (in.)	*r*	*S* (in.)	No. of studs
BS-I/II	Push-out	5.52	0.18	without	-	-	-	-
P-900/P-500-I/II	Punching	5.52	0.18	without	-	-	-	-
P-SD-10-3-50-I/II	Punching	5.52	0.18	with	0.39	3	1.97	12
P-SD-10-3-100-I/II	Punching	5.52	0.18	with	0.39	3	3.94	12
P-SD-10-5-50-I/II	Punching	5.52	0.18	with	0.39	5	1.97	20
P-SD-16-3-100-I/II	Punching	5.52	0.18	with	0.63	3	3.94	12

where *D* is the diameter of tube, *t* is the thickness of pipe, *d* is the diameter of shear studs, *r* is the number of rows of studs, and *s* is the spacing between the rows of studs.

After the completion of the pushout test, the average bond stress, which was taken as the bond strength, was calculated to be 160 psi. The critical loads, namely the cracking load (P_o), the first diagonal crack load (P_1), and the peak load (P_u) were recorded and compared in Figure 2.15. The results showed that the shear studs had a significant contribution to the punching resistance of the connection. They increased the load carrying capacity of the connection by approximately two times.

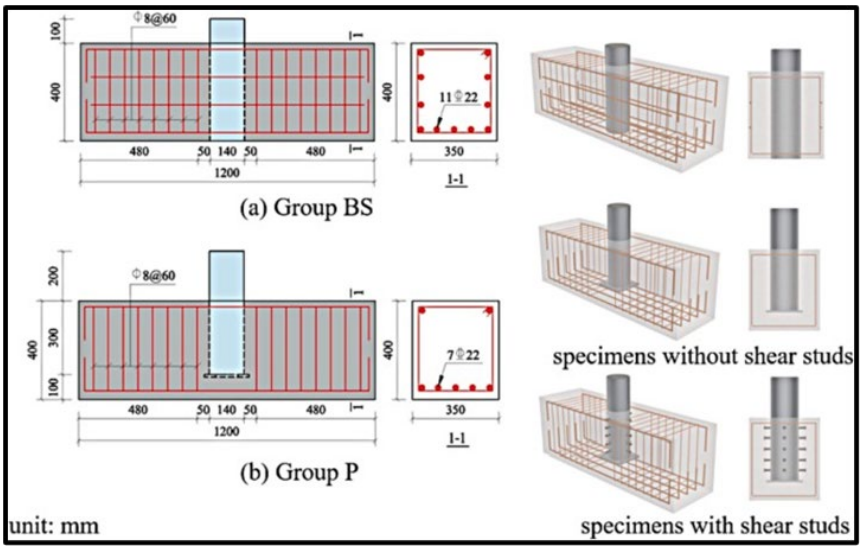

Figure 2.14. Configuration of specimens in different groups [13]

(1in.=25.4mm)

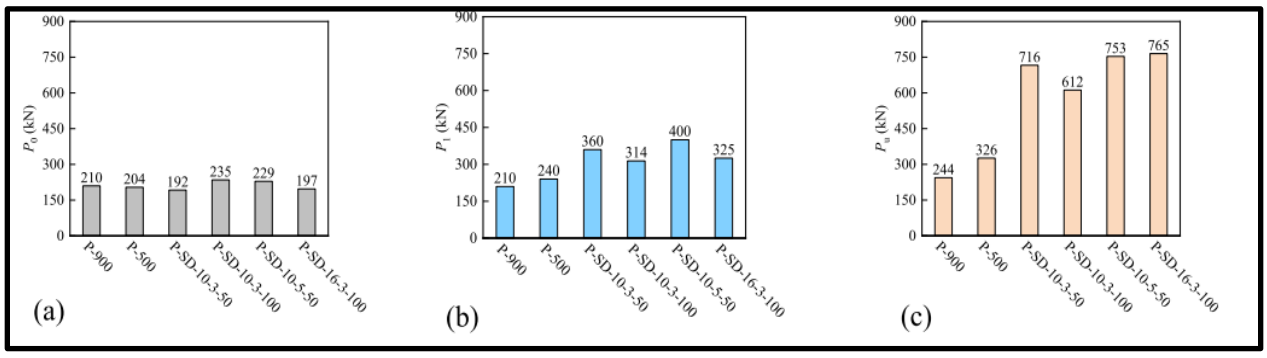

Figure 2.15. Critical loads in Specimen P [13]

(1 KN= 0.225 kips)

The process involved calculating the strength using various design codes, which are discussed in Section 4.2.2. To assess the adequacy of existing codes, the calculated values were compared with the test results. The comparison between the test results and the punching resistance calculated based on design codes is shown in Figure 2.16 and Table 4.1. It can be observed that the predicted values were around 200 kN, significantly lower than the test results, which were approximately 700 kips. The prediction errors were primarily attributed to the neglect of the contribution of bond strength and shear studs.

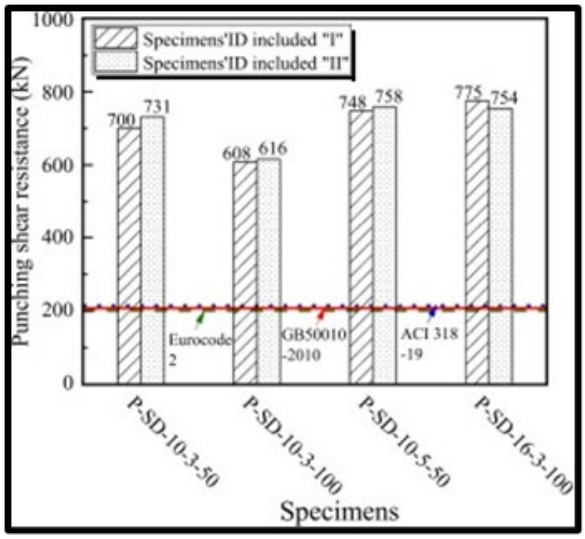

Figure 2.16. Comparison of test results with codes [13]

(1KN= 0.225 kips)

Subsequently, new empirical formulas were developed, as discussed in Section 4.2.2, which incorporated the contributions from the reinforced concrete cap, bond strength, and shear studs. Figure 2.17 and Table 4.1 provide a summary of the comparison between the test results and the predicted results based on the developed formulas. It can be observed that the predicted results were within a 15% margin of the test results, indicating that the empirical formulas performed well.

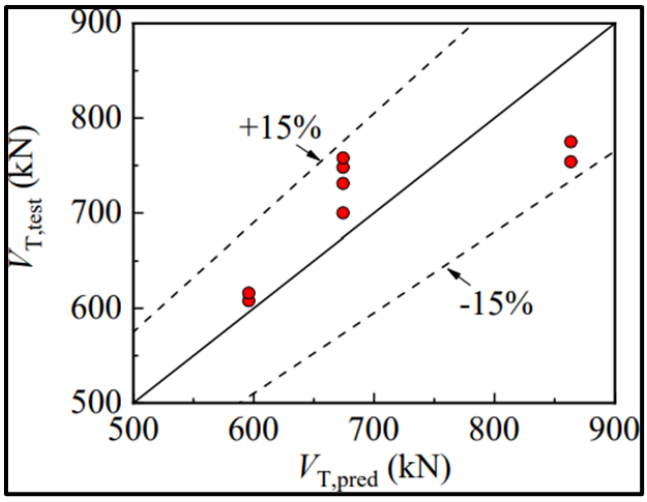

Figure 2.17. Comparison of the predicted and experimental results [13]

(1 KN=0.225 kips)

The study concluded that the bond strength between the steel pile and surrounding concrete played a crucial role in punching resistance, and a larger diameter and a smaller distance between studs improved the punching shear strength. A modified formula was developed to estimate the punching resistance, considering the bonding strength, shear resistance of the shear studs, and shear resistance of the reinforced concrete foundation.

2.3 Studies based on connection between bent cap and steel pile

2.3.1 Connection between concrete filled steel pipe pile and reinforced concrete bent cap (D. E. Lehman et. al., 2015)

This research was based on experimental programs aimed at developing a design methodology for the connection between CFST columns and cap beams. It was an extension of the study conducted at Washington University, as discussed in Section 2.2.1. In this study, an annular ring was welded to the top of the pile embedded within the bent cap to create a fully restrained moment connection.

Four large-scale specimens were subjected to constant axial and reversed cyclic lateral loading to assess the performance of the proposed connections. Two specimens with diameters of 20 in. and 24 in. were chosen to evaluate the performance of the connections under transverse loading conditions. Additionally, two CFSTs with diameters of 25.75 in. and 24 in. were selected to assess performance under longitudinal loading. Due to limitations of the available testing apparatus, the specimens were tested in an inverted configuration. The typical longitudinal and transverse geometries of the specimens are depicted in Figure 2.18 and Table 2.6.

Specimen ER80T was designed to assess the performance of the connection and cap beam by utilizing a reduced outer diameter of the annular ring (D+16t) and a narrower cap beam width. ER96T shared similar characteristics to ER80T but with an increased column geometry. ER96L, on the other hand, evaluated the effects of loads and deformations in the longitudinal axis of the bridge instead of the transverse direction, while maintaining similarities to ER96T. Lastly, specimen ER103L was subjected to loading and deformations in the longitudinal direction, akin to ER96L, but utilized a lower grade of steel compared to ER96L.

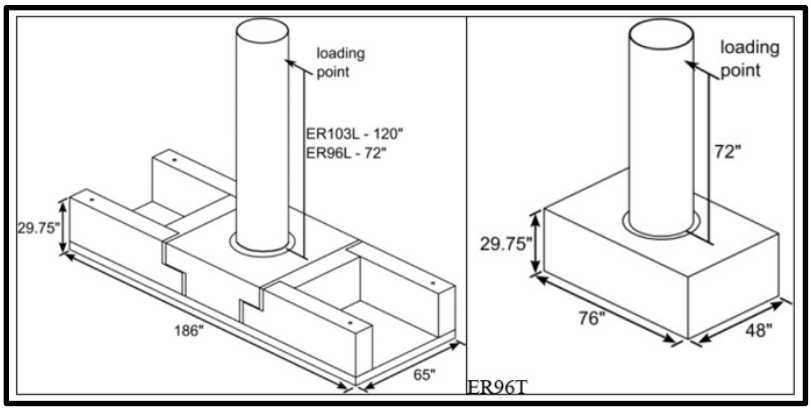

Figure 2.18. Overview of longitudinal and transverse specimen geometry [14]

Table 2.6. Connection Experiment Test Matrix

Specimen	Loading direction	D (in.)	t (in.)	L_e (in.)	L_{pc} (in.)	Axial load ratio (%)
ER80T	Trans.	20	0.25	18	7	10
ER96T	Trans.	24	0.25	20	9.75	5
ER103L	Long.	25.75	0.25	20.25	9.5	10
ER96L	Long.	24	0.25	20	9.75	5

A summary of the test results, including the hysteretic response, was provided for each specimen. The moment-drift behaviors were normalized using the theoretical plastic moment capacity of the CFT component, calculated using the PSDM. The experimental results for all specimens are presented in Table 2.7, and the response of each specimen is illustrated in Figure 2.19.

The performance of each connection was evaluated based on several criteria, including the secant stiffness to 0.8My of the CFT, maximum moment resistance, maximum drift, and the drift at which the resistance decreased to 80% of its maximum. The secant stiffness was determined when the moment resistance reached approximately 80% of the yield moment of the CFT. The stiffness of each specimen was expressed as the ratio of the measured stiffness to the theoretical stiffness of the CFT ($EI_{measured}/EI_{eff}$), calculated using the stiffness expression in AASHTO (2015). A value of $EI_{measured}/EI_{eff}$ greater than 1.0 indicated a larger stiffness than the theoretical stiffness of the CFT component, while a value less than 1.0 suggested a smaller initial stiffness.

In a similar manner, the moment resistance of each connection was assessed by determining the ratio of the maximum observed moment to the theoretical moment capacity of the CFT ($M_{max}/M_{p,\ CFT}$), calculated using the PSDM. A value of $M_{max}/ M_{p,\ CFT}$ greater than 1.0 indicated that the connection exceeded the theoretical plastic moment capacity of the CFT, while a value less than 1.0 suggested that the connection did not provide as much resistance as the

theoretical plastic capacity expected for the CFT component.

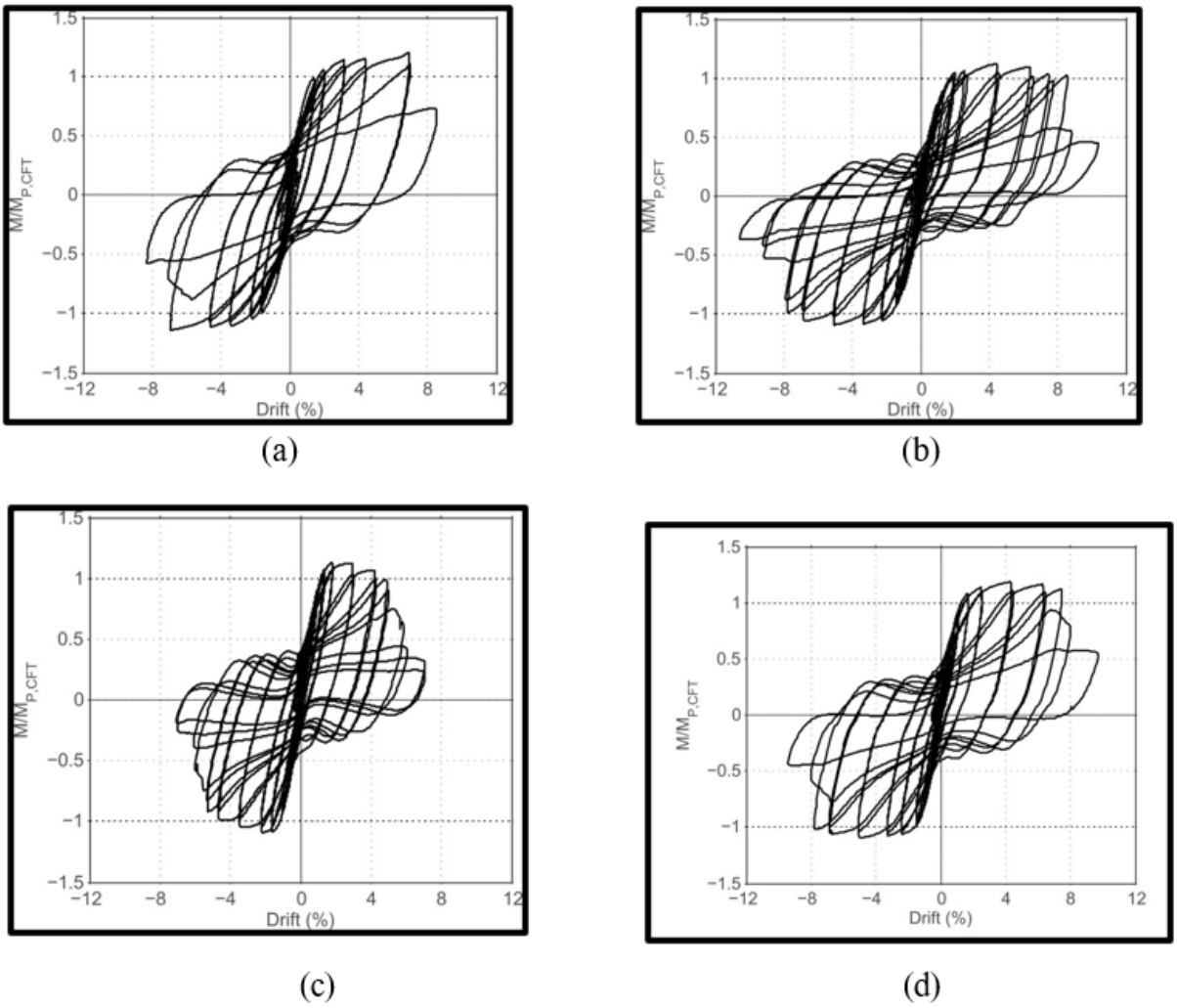

Figure 2.19. Moment-Drift Behavior of Specimen; (a)ER80T; (b) ER96T; (c) ER103L; (d) ER96L [14]

Table 2.7. Experimental results

Specimen	Initial stiffness ($EI_{measured}/EI_{eff}$)	$M_{max}/M_{P, CFT}$
ER80T	0.98	1.2
ER96T	0.77	1.12
ER103L	0.96	1.13
ER96L	0.6	1.19

The experimental results showed that this connection type exhibited significant strength, stiffness, and deformation capacity, and the predictions were accurate with a reasonable level of overstrength. All specimens utilizing this connection achieved the theoretical plastic moment capacity of the CFT component, as calculated using the PSDM. Additionally, the results indicated that the cap beam width could be twice the diameter of the column. Furthermore, reducing the external projection of the annular ring to eight times the thickness of the steel tube did not have an impact on the embedded connection. The design methodologies for a comprehensive design approach for this proposed connection are also provided in Section 4.2.1.

2.3.2 Column to reinforced concrete cap connection for punching resistance (X. Li et. al., 2017)

The research comprised experimental and analytical studies on the punching shear behavior of CFSTs bridge column to pile cap connections. Five different connections were proposed and tested under monotonic downward vertical loads. The study aimed to evaluate the effects of various connection details, such as column embedment depths, shear studs, face annular rings, and headed shear reinforcement, on the punching shear behavior.

Five connections, designated as Specimens PC1-PC5, were specifically designed, and subjected to punching shear loads to assess the behavior of CFST bridge columns connected to RC four-pile caps. Each specimen comprised four circular CFST piles, a PC-pile cap, and a circular CFT column. The design considerations for these connections encompassed several aspects: i) determining the appropriate embedment depths for the CFT columns, ii) incorporating shear studs, iii) utilizing face annular rings, and iv) incorporating double-headed shear reinforcement.

The detailed characteristics of each specimen can be found in Table 2.8 and Figure 2.20. Each pile in the specimens had a diameter of 6.26 in. and a thickness of 0.28 in., with an annular ring located at the column's tip. PC1 had an embedment depth of 12.61 in., while PC2 was similar to PC1 but had an embedment depth of 6.30 in. Specimens PC3, PC4, and PC5 were equipped with shear studs, a face annular ring, and headed shear bars, respectively. The pile caps, measuring 55 in. by 43 in. by 20 in., were reinforced with Φ0.47 bars spaced at 3.94 in. in two directions for the top bars. Likewise, it consisted of Φ0.70 bars spaced at 4.72 in. in the long direction for the bottom bars, and Φ0.55 bars spaced at 4.33 in. in the short direction for the bottom bars. Additionally, the vertical reinforcement in the pile cap consisted of approximately Φ0.4 bars spaced at 4.72 in., with one 180º hook at each end.

Table 2.8. Description of specimens

Specimen	f'_c (psi)	D (in.)	t (in.)	Anchorage	Embedment depth(in)	Remarks
PC1	4119.08	6.26	0.28	-	12.61	With end plate
PC2	3898.62	6.26	0.28	-	6.30	
PC3	4003.05	6.26	0.28	Shear studs	12.61	
PC4	4095.87	6.26	0.28	Face annular ring	12.61	
PC5	3747.78	6.26	0.28	Headed shear bars	12.61	

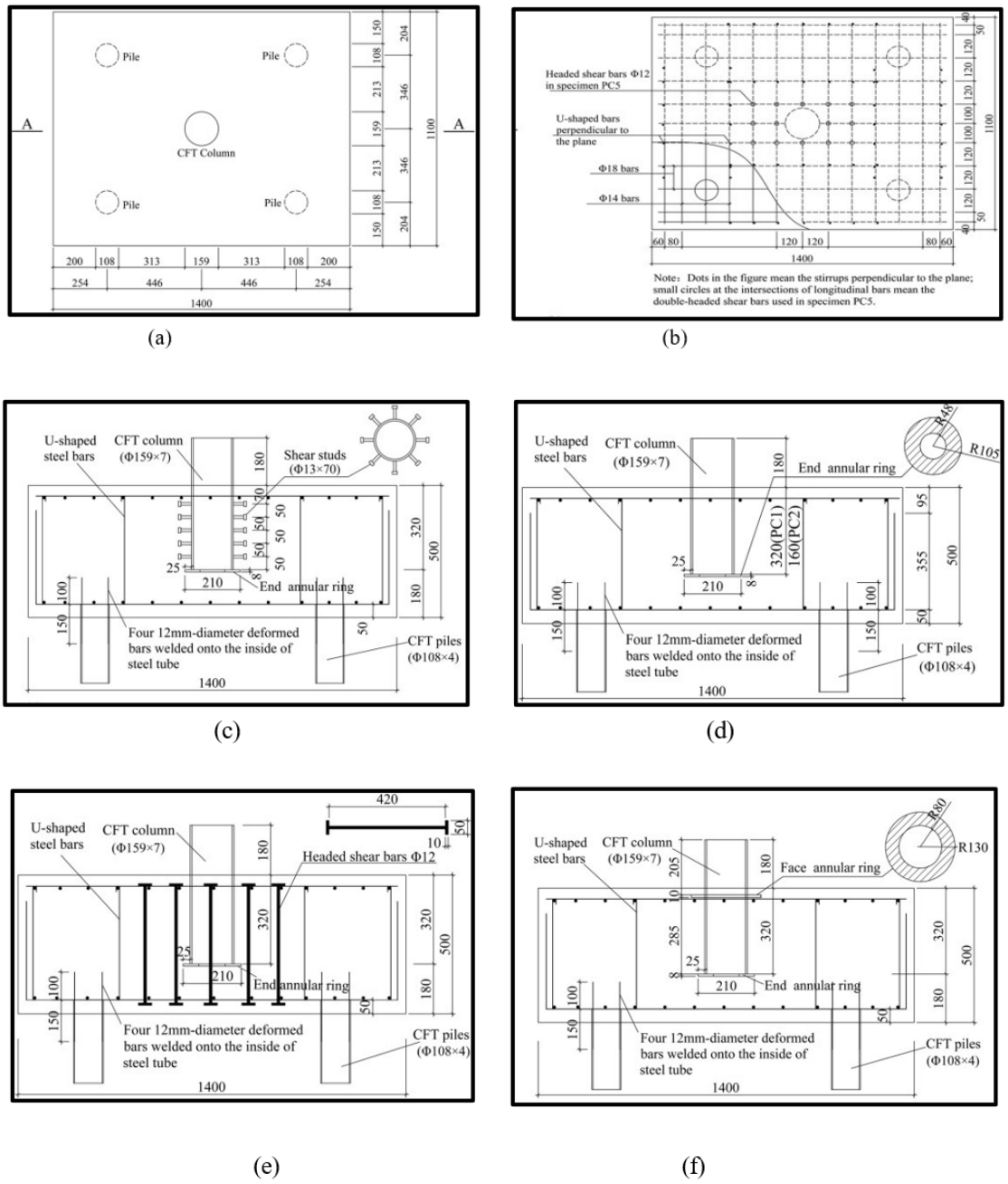

Figure 2.20. Details of specimens PC1-PC5(mm); (a) dimensions of pile caps; (b) steel reinforcement of pile caps; (c) A-A section of specimens PC3; (d) A-A section of specimens PC1 and PC2 with different embedment depths of column; (e) A-A section of specimen PC5; (f) A-A section of specimen PC4 [15]

(1 in. =25.4 mm)

Punching tests were conducted on each specimen, and the punching strength was calculated using the design methodologies discussed in Section 4.2.3. The experimental results, shown in Figure 2.21, indicated that for PC1 and PC2, the punching resistance increased as the embedment depth of the column decreased. Specimen PC4, with a double annular ring, exhibited the highest punching strength among all the specimens. PC3 also demonstrated a significant amount of strength. Furthermore, a comparison was made between the predicted results obtained using design codes and the actual test results, as presented in Table 4.1. It was observed that the design codes were inadequate in providing sufficient provisions for calculating punching strength, as they did not account for the contributions of embedment depth and shear studs.

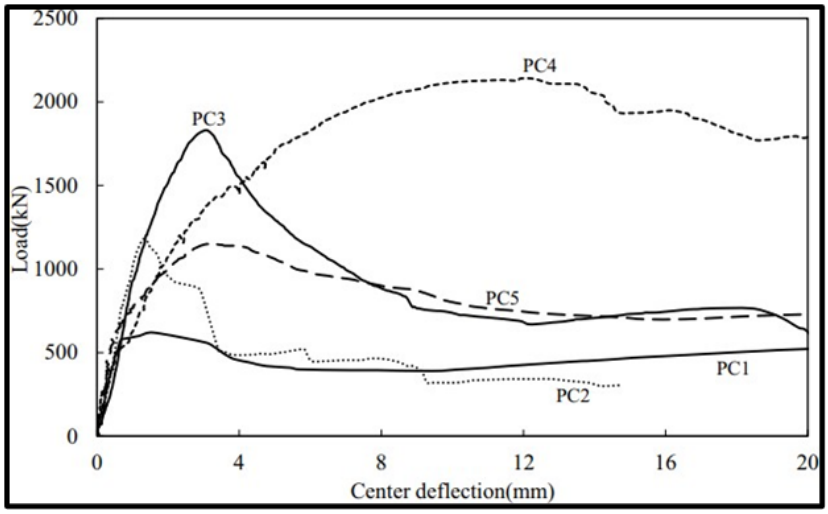

Figure 2.21. Load vs deflection [15]

(1KN=0.225 kips and 1mm= 0.0394 in)

Since the calculation methods provided by the code were insufficient to obtain accurate results, empirical formulas were derived based on the AASHTO LRFD specification, ACI 318-14 code, and a finite element analysis (FEA) model of specimen 1. These formulas were used to calculate the punching shear resistance of each specimen, as discussed in Section 4.2.3. The comparison between the test results and the empirical formulas is presented in Table 4.1. The

overall comparison revealed that the contribution of the embedment depth of the column must also be considered when calculating the punching resistance. It emphasized the importance of considering the embedment of the column in the punching resistance analysis.

The study concluded that reducing the embedment depth increased the punching resistance of the connection. The inclusion of an annular ring and shear studs had a substantial impact on the strength, and the type of connection influenced both the strength and failure pattern of the connection between CFSTs and the pile cap.

Chapter 3 STATE OF PRACTICE AND REVIEW

This chapter includes an overview of the current state of practice among state departments of transportation (DOT) regarding the use and experience of steel pipe piles for bridge structures. It provides a summary of a survey conducted to determine the prevailing practices and any variations in state standards and drawings related to the connection between pipe piles and reinforced concrete bent caps.

3.1 Introduction

A survey was conducted among state DOTs to investigate the utilization of steel pipe piles and their current design practices and methodologies. The main objective of the survey was to gather comprehensive data on the design and connection details used by different states for steel pipe piles connected to reinforced concrete bent caps, as well as to learn about their post-construction experiences with the use of steel pipe piles.

Bridge engineers from all states, except Alabama DOT, were contacted to gather their experiences and information regarding the use of steel pipe piles and the connection between the piles and bent caps. The bridge engineers were asked whether their respective states permitted the use of steel pipe piles. In states where steel pipe piles were used, additional questions were posed regarding the typical applications and sizes of commonly employed steel pipe piles. Furthermore, drawings, whether they were standard or specific to certain bridges, along with connection details and related design methodologies, were also collected from the bridge engineers.

Responses were obtained from engineers in 35 out of the 49 states that were contacted, while the remaining states did not respond. A summary of the responses received from each state is depicted in Figure 3.1. Among the contacted states, seven states indicated that they did not adopt

steel pipe piles for bridge structures and preferred other types of piles such as HP piles and concrete piles. The remaining twenty-eight states acknowledged the use of steel pipe piles in their state. Among those, seven states had standard drawings and details for the connection, while the other twenty-one states designed the connection based on the specific uses and applications of each bridge. Detailed information gathered from the responses is presented in Section 3.2.

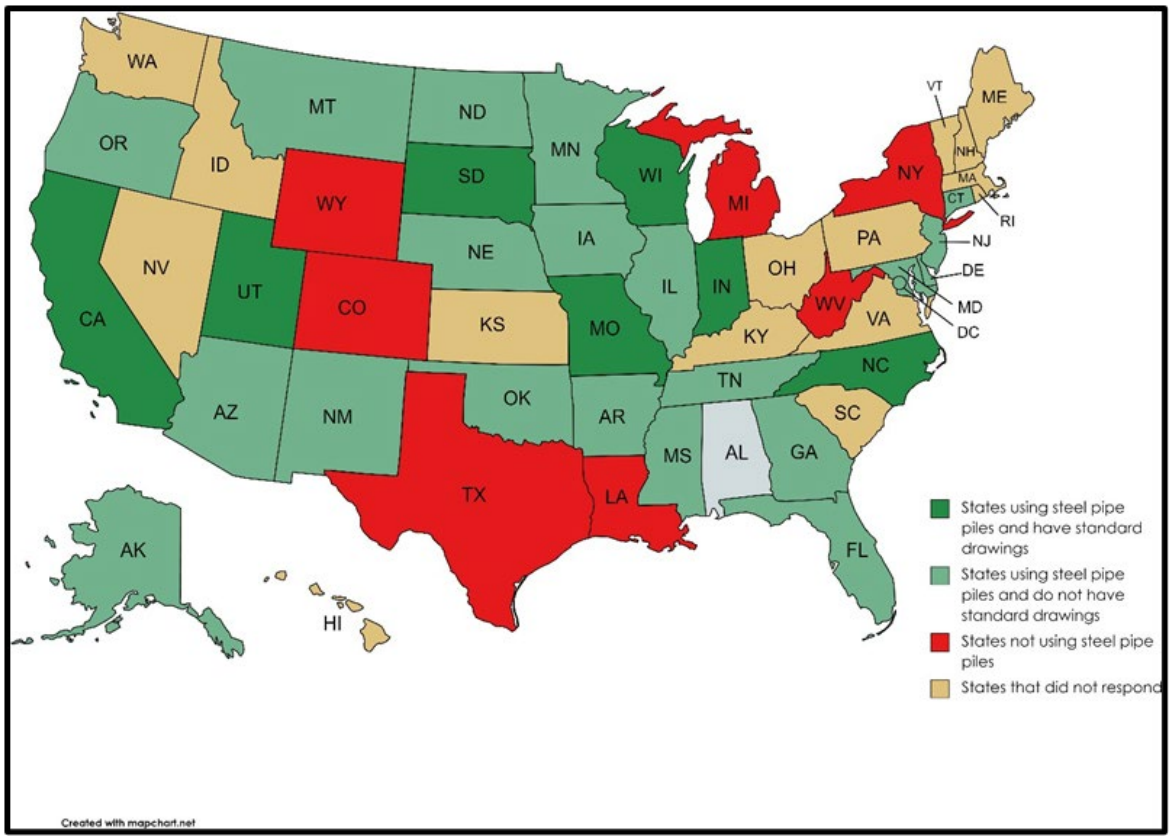

Figure 3.1. Map of response

3.2 Survey Results

3.2.1 General observations and information provided

Detailed design methodologies specifically used by state DOTs for the connection between steel pipe piles and reinforced concrete bent caps were not found. However, various states provided some information, standard drawings, and examples related to such connections. Table 3.1 below

serves as a master table summarizing the collected information on steel pipe pile connections used by different states. It includes parameters such as pile diameter, pile thickness, type of anchorage, pile embedment into the bent cap, pile type (hollow steel pipe or concrete-filled), concrete plug depth (if applicable), and references to drawings (standard or implemented example bridges). The elaboration of these parameters used by different states is documented below.

Table 3.1: DOT survey summary

State	Pile diameter (in)	Pile thickness (in)	Type of anchorage	Pile embedment	Pile type		Concrete plug	Implementation		Bridge Implementation Examples	Section
					Steel Pipe	CFT		Standard Dwg or Specifications	Permitted by DOT		
California	20, 24, 25.75 20	0.25	Annular ring Welded dowel Headed rebars	18", 20", 20.5" 1 inch below cap -	- - -	✓ ✓ ✓	-	✓	-	-	3.2.2.1
Delaware	14-18	min 0.1875	180º Hooked rebars	min 1'	-	✓	-	-	✓	-	3.2.2.2
Florida	24	0.5	90º Hooked rebars	-	-	✓	-	-	✓	Hicks road over west Pittman creek	3.2.2.3
Georgia	24	0.25-0.50	Rebars	1'	-	✓	-	-	✓	Bridges over Canooche river Dry Creek	3.2.2.4
Illinois	12-16, 36	-	90º, Headed Rebars	2'	-	✓		-	✓	-	3.2.2.5
Minnesota	42	-	Straight Rebars Shear studs	- -	✓ ✓	-	10' below bent cap -	-	✓ ✓	Lafayette Bridge Hastings Bridge	3.2.2.6
Mississippi	24-36	0.5-0.75	V-Rebars	min 1'	✓	-	1'-6" below bent cap	-	✓	Bridges over Cassidy Bayou Wolf River I-59	3.2.2.7
Missouri	14-24	0.5	180º Hooked rebars Shear studs Annular ring	1'-6"	-	✓	-	✓ - -	- ✓ ✓	- Champ Clark bridge Rocheport Bridge	3.2.2.8
Montana	16	0.5	Rebars & U-bars	1'-8"	-	✓	-	-	✓	Bridge over Swan River	3.2.2.9
Nebraska	42	-	180º Hooked rebars	min 1'	-	✓	-	-	✓	Freemont southeast beltway	3.2.2.10
New Mexico	16, 24	0.5	Studs	min 1' & max 2'	-	✓	-	-	✓	Yaple Canyon Bridge replacement Rio Puerco	3.2.2.11
North Carolina	14, 16, 18, 24, 30	0.5	90º Rebars	-	✓	-	Min 5' on top of pile	✓	-	-	3.2.2.12
Oklahoma	24	0.625	Annular ring	2'-6"	-	✓	-	-	✓	Bridge over pine creek	3.2.2.13
South Dakota	16	0.25	90º Hooked rebars	2'-3"	-	✓	-	✓	-	-	3.2.2.14
Tennessee	16	0.5	180º Hooked rebars	min 1'-6"	-	✓	-	-	✓	Over Norfolk southern railroad station	3.2.2.15
Utah	min 12.75	-	90º Rebars	2'	-	✓	-	✓	-	-	3.2.2.16
Washington	30,36	1	Headed rebars	3'6"-5'	✓	-	12'3"-14'	-	✓	Seatle Trestle Bainbridge island	3.2.2.17
Wisconsin	12.75, 14	0.375	Rebars	2'	-	✓	-	✓	-	-	3.2.2.18

3.2.2 Steel Pipe Pile to Bent Cap Connection Details for DOTs

Information regarding connection details and related drawings was collected from eighteen state DOTs that indicated the adoption of steel pipe piles. This section presents the responses received, which include the usage of steel pipe piles, sizes and types of commonly used steel pipe piles, design considerations for the connection, and associated drawings.

3.2.2.1 California (Caltrans)

Use of steel pipe piles

Steel piles are commonly used in accelerated bridge construction projects. Studies and research were conducted at the University of Washington (D. E. Lehman et al., 2015) in collaboration with Caltrans. These studies focused on the connection between concrete-filled steel tubes and precast reinforced concrete bent caps.

Size and types of commonly used pipes

Piles of various diameters, ranging from 20 in. to 25.75 in., were utilized in the conducted studies. These piles had a thickness of 0.25 in. Typically, these piles were filled with concrete to enhance their performance, especially for enhanced seismic design.

Connection design/Detailing consideration

Three types of anchorage were utilized in the study: i) Annular ring: An anchorage ring was welded on the top of the pile, and the pile was embedded 18 in. to 20 in. into the bent cap. ii) Welded dowel: Rebars were welded on the inside circumference of the pile, with an embedding depth of 12 times the diameter of the rebar ($12d_b$), into the bent cap. The pile itself was not embedded inside the bent cap. (iii) Headed rebars: A reinforcement cage was provided in the

concrete core of the piles, extending 12 times the diameter of the rebar ($12d_b$) into the bent cap and 30 times the diameter of the rebar ($30d_b$) into the column.

Connection Drawing

Figure 3.2, Figure 3.3, and Figure 3.4 illustrate the adopted details for the specimens of the annular ring, welded dowel, and headed rebars connections, respectively. These details were successfully employed in the experimental programs and yielded satisfactory results.

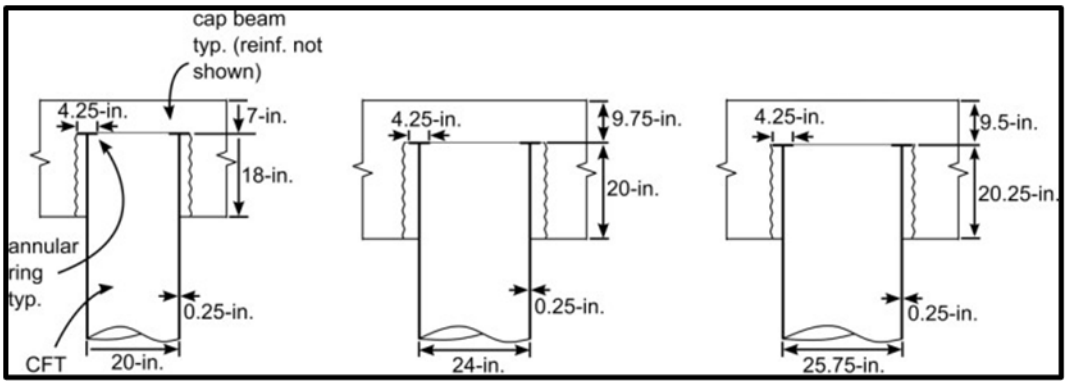

(a) Sectional elevation view

Figure 3.2. Caltrans: Annular ring detail for pile to bent cap connection for different diameter piles[14]

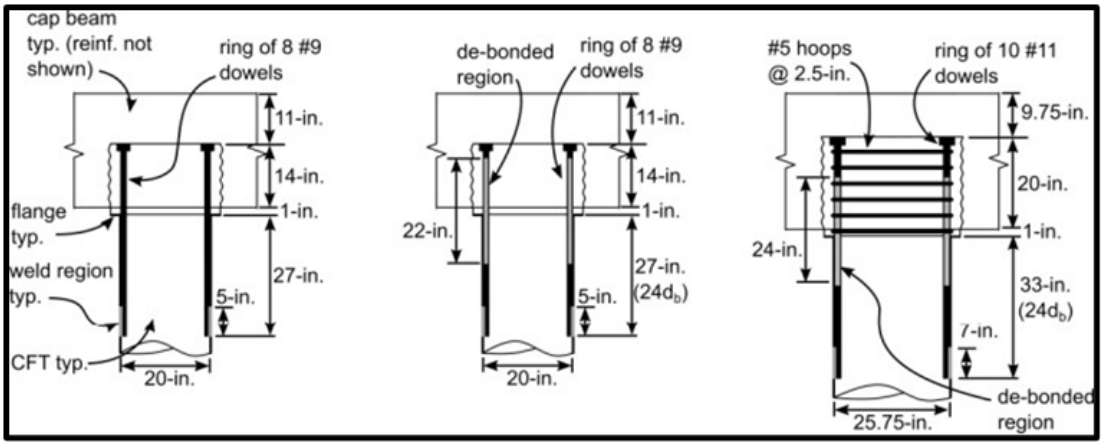

(a) Sectional elevation view

Figure 3.3. Caltrans: Welded dowel connection for pile to bent cap connection for different diameters[14]

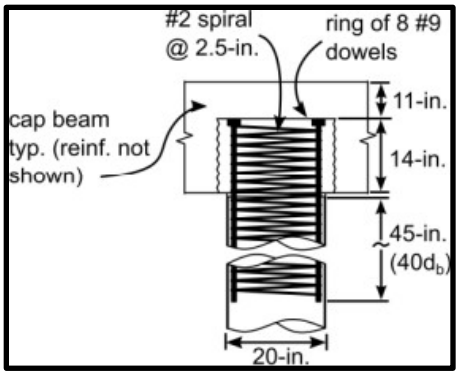

(a) Sectional elevation view

Figure 3.4. Caltrans: Welded dowel connection for a pile to bent cap connection for different diameters[14]

3.2.2.2 Delaware (DelDOT)

Use of steel pipe pile

Cast-in-place steel piles, which are essentially filled with concrete on-site, are commonly used by DelDOT.

Size and types of commonly used pipes

DelDOT predominantly utilizes small-diameter pipe piles and fluted pipe piles, ranging from 14 in. to 18 in. in diameter, with a minimum thickness of 0.1875 in. for bridge piers. These piles are typically filled with concrete to enhance their strength.

Connection design/Detailing consideration

The connection between the pile and cap is established using a combination of 180^o hooked rebars and straight rebars. To ensure a strong connection, a minimum of 1 ft. of pile embedment is required for the hooked bars. In the case of larger diameter steel piles, deeper bent caps can be employed, allowing for greater embedment of reinforcement into the cap and eliminating the need for hooked bars.

Example bridge

DelDOT does not have standard drawings for these details; however, they provide example details in their Bridge Design Manual, as depicted in Figure 3.5.

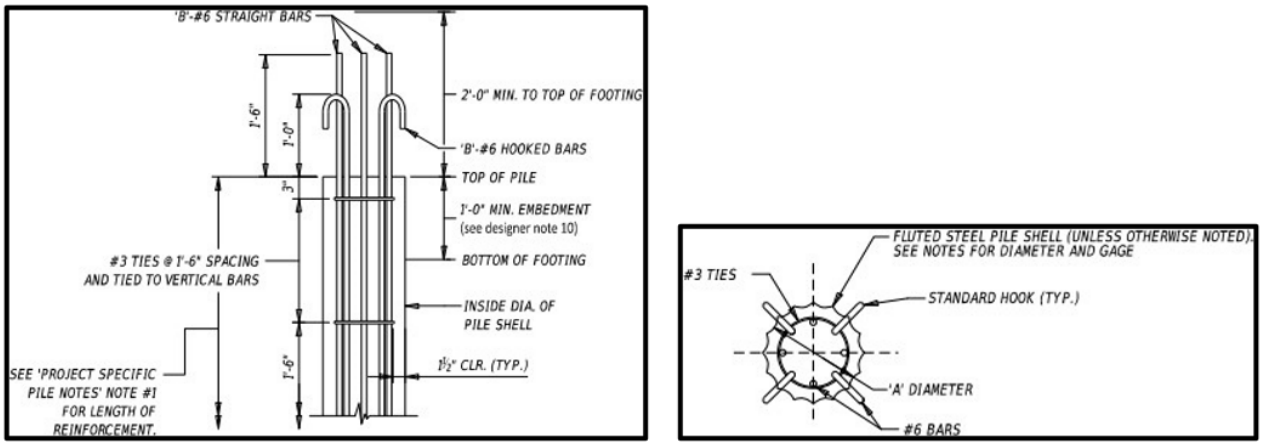

(a) Sectional elevation view (b) Pile plan view

Figure 3.5. DelDOT: Rebar detail for pile to bent cap connection

3.2.2.3 Florida (FDOT)

Use of steel pipe pile

According to FDOT, the state primarily utilizes closed-end steel pipe piles that are filled with concrete.

Size and types of commonly used pipes

The typical size of the piles used by FDOT is 24 in. in diameter and 0.5 in. in thickness. These piles are constructed with a cast-in-place concrete core that includes reinforcement details for permanent applications.

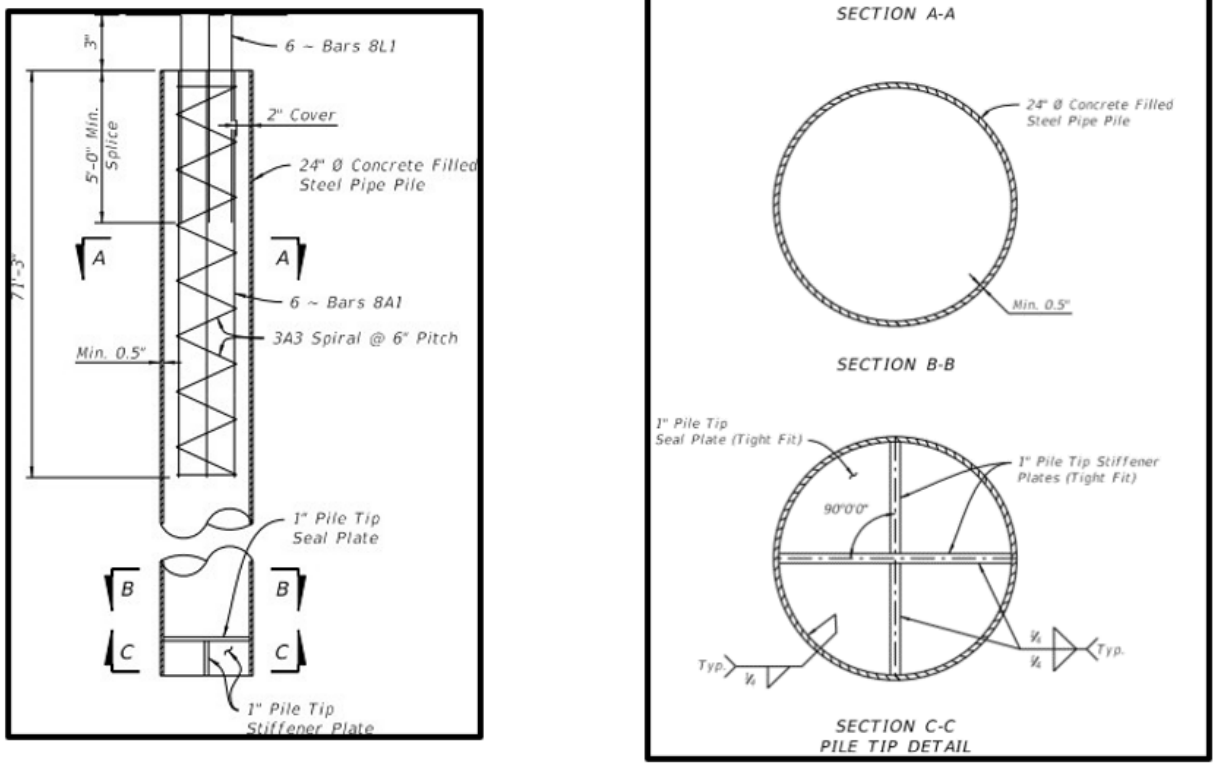

(a)Sectional elevation view (b) Sectional pile plan view

Figure 3.6. FDOT: Rebar detail for pile to bent cap connection, Hicks Road over west Pittman creek (Bridge No. 524219)

Connection design/Detailing consideration

The connection between the pile and bent cap is achieved by extending and hooking the reinforcing steel into the bent cap, making the connection easier. These rebars are also properly confined with spiral reinforcement to ensure their effectiveness. Additionally, an end stiffener plate is installed at the end of the pile to increase rigidity and enhance the structural integrity.

Example bridge

The details of the desired connection for Hicks Road over West Pittman Creek are shown in Figure 3.6.

3.2.2.4 Georgia (GDOT)

Use of steel pipe pile

GDOT frequently utilizes steel pipe piles, commonly referred to as metal shell piles.

Size and types of commonly used pipes

The largest diameter of metal shell piles used by GDOT is 2 ft., with thickness ranging from 0.25 in. to 0.5 in. These piles are filled with a concrete core to prevent pile failure.

Connection design/Detailing consideration

GDOT does not have standard details for the connections of metal shell piles, but they have certain considerations: i) The current practice is to embed the pile a minimum of 1 ft into the cap, ii) Placing a pile under the beam helps reduce moments, iii) Span lengths are typically limited to approximately 60 feet, iv) The fixity of the pile is maintained at a depth of 10 ft into the ground, the braced length, v) Piles exceeding a height of approximately 25 ft, including the braced length, tend to fail or plot outside the limits of the interaction diagram, vi) Lateral load is distributed based on tributary lengths and the stiffness of the bent, vii) A K (Effective length) value of 1.2 is used in the transverse direction, and a value of 2.1 is used in the longitudinal direction, viii) Rebar is not placed in the metal shell pile that supports an end bent, and ix) The metal shell itself does not contribute to the structural capacity.

Example bridge

They do not have standard drawing details, but the connection details of the bridge over the Canoochee River are shown in Figure 3.7.

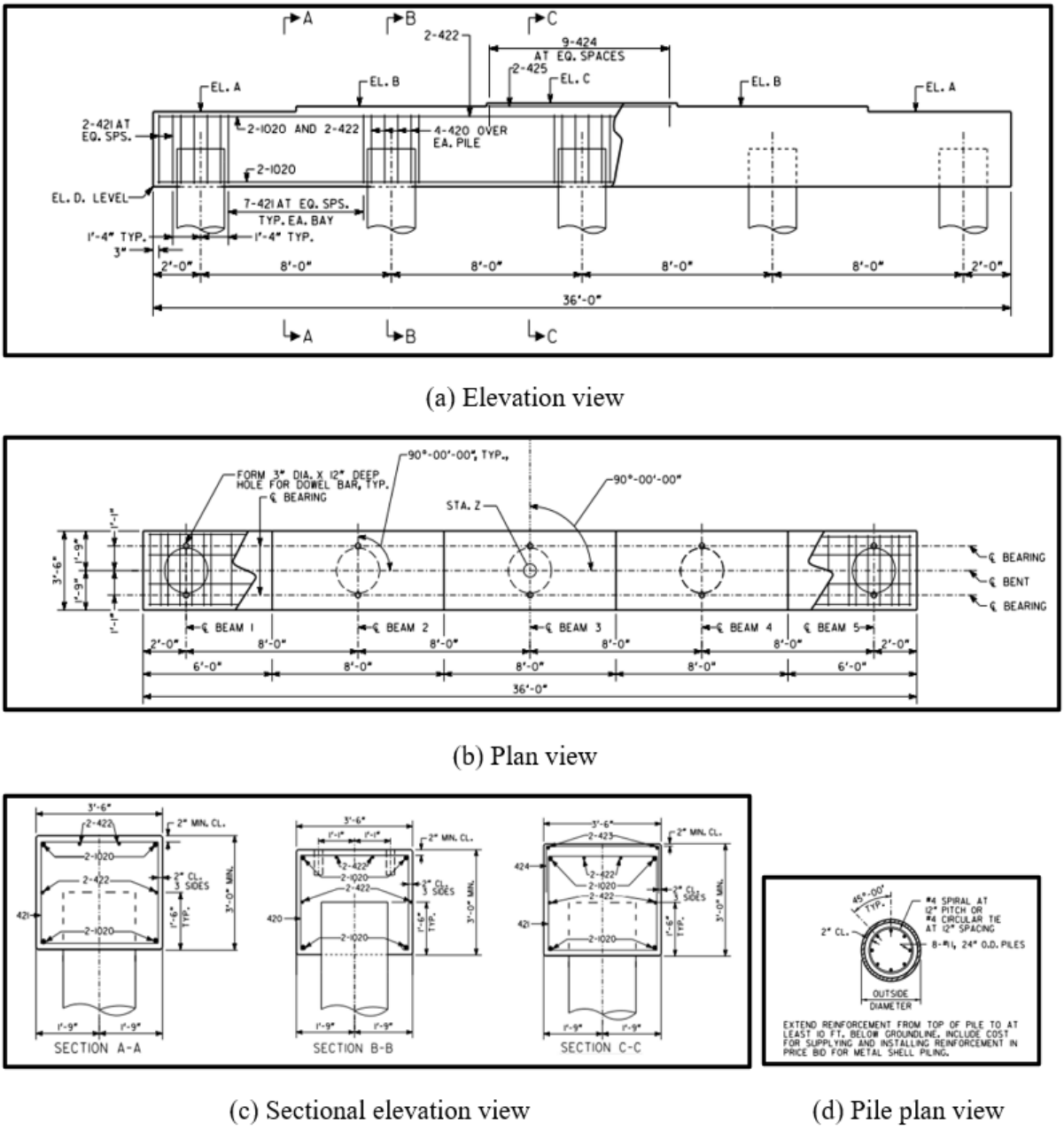

Figure 3.7. GDOT: Rebar detail for pile to bent cap connection, Canooche River

3.2.2.5 Illinois(IDOT)

Use of steel pipe pile

IDOT commonly utilizes steel pipe piles, also referred to as metal shell piles, for various bridge structures.

Size and types of commonly used pipes

Different diameter sizes, such as 12 in., 16 in., and 36 in., are used for the piles by IDOT. These piles are filled with a concrete core and reinforced with a reinforcement cage to enhance their strength.

Connection design/Detailing consideration

For the connection between the pile and cap, the standard practice for IDOT is to embed the pile 24 in. into the cap. This detail applies to large diameter pipe piles (36 in. and greater) as well. In the case of a cast-in-place pile cap, hooked reinforcement is utilized to extend into the cap. For a precast pile cap, the same connection details are used, but bar terminators are employed instead of hooks to minimize the size of the grout socket.

Example bridge

For metal shell piles, specifically those with encasement (12 in. – 16 in. in diameter, spiral-wound pipe), the connection detail is depicted in Figure 3.8. On the other hand, for metal shell piles without encasements, the corresponding detail can be found in Figure 3.9.

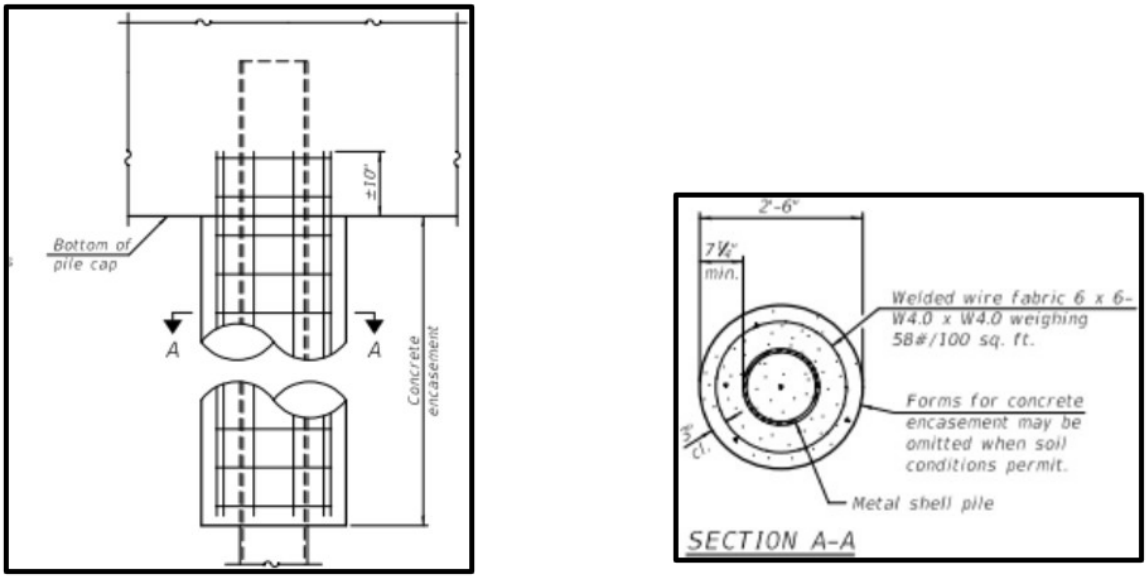

(a)Sectional elevation view (b) Pile plan view

Figure 3.8. IDOT: Rebar detail for pile to bent cap connection with concrete encasement

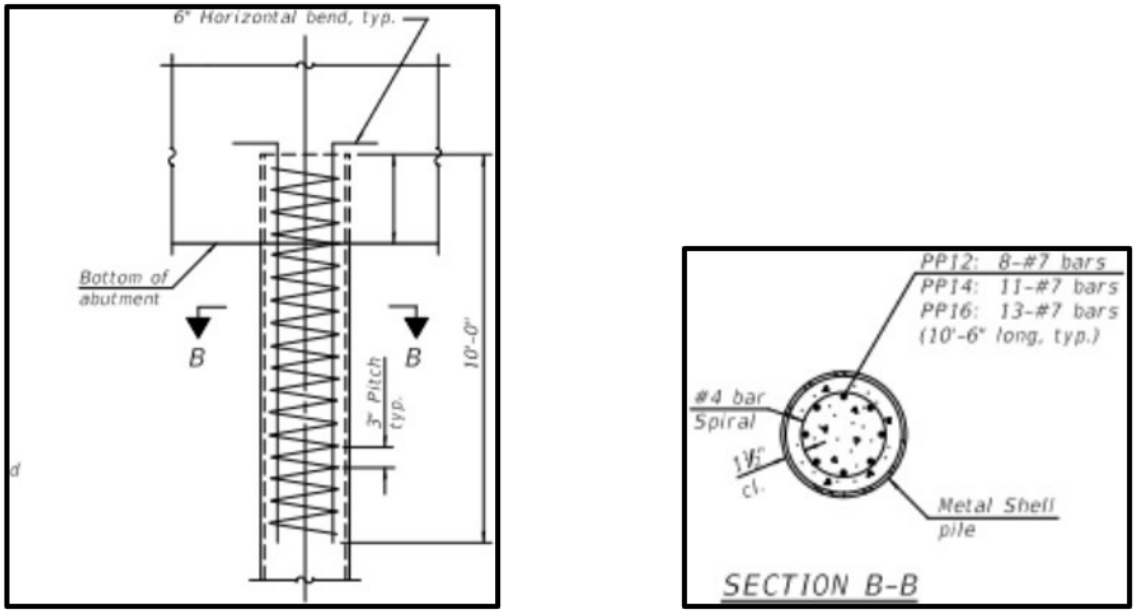

(a) Sectional elevation view (b) Pile plan view

Figure 3.9. IDOT: Rebar detail for pile to bent cap connection without concrete encasement

3.2.2.6 Minnesota (MnDOT)

Use of steel pipe pile

According to the 2015 NCHRP report [3], MnDOT commonly utilizes steel pipe piles with a foundation at the bottom. These piles are not directly driven into the soil.

Size and types of commonly used pipes

Large diameter piles, such as 42 in., are used in these cases. Due to the large diameter, a concrete core is not provided throughout the entire length of the pile.

Connection design/Detailing consideration

To ensure a strong connection, a concrete plug of approximately 10 ft. is placed below the bent cap. The piles are embedded within the bent cap, and two types of anchorage are used for the connection. Firstly, the longitudinal reinforcement of the piles extends into the pile cap, providing additional strength. Secondly, shear studs are welded to the steel pipe itself, enhancing the structural strength of the steel pipe at the connection point.

Example bridge

Figure 3.10 illustrates the connection details used in the Lafayette Bridge of Minnesota, which involves rebars for the connection. On the other hand, Figure 3.11 presents the connection details adopted by the Hastings Bridge, which utilizes shear studs for the connection.

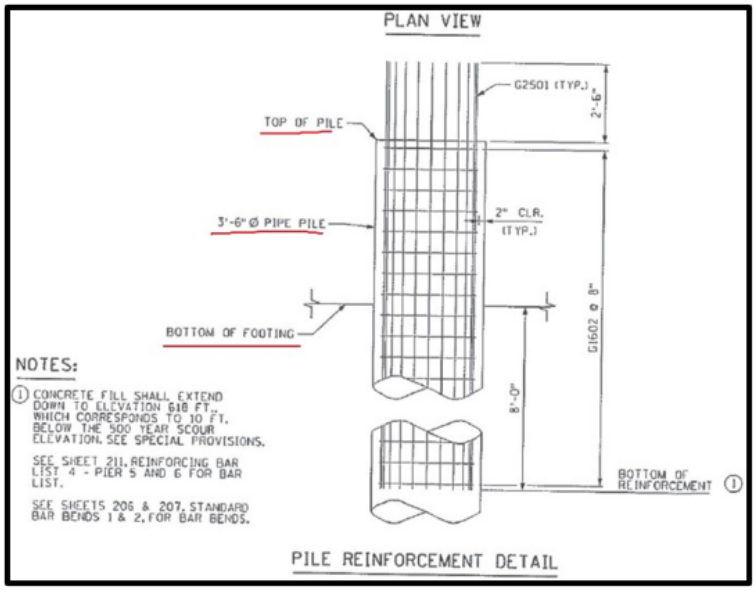

(a) Sectional elevation view

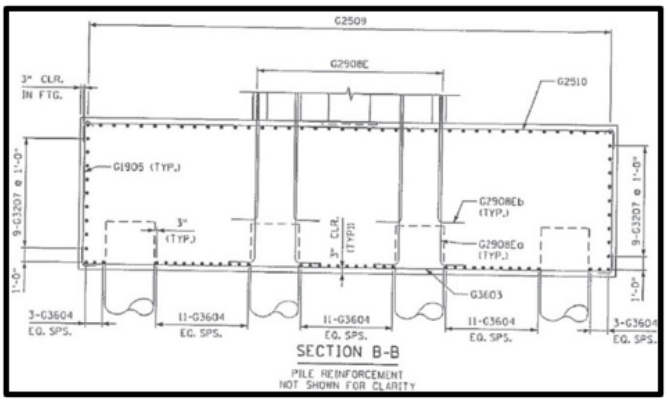

(b) Sectional elevation view

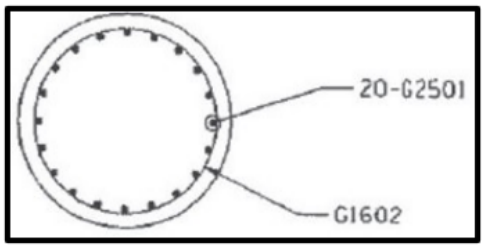

(c) Pile plan view

Figure 3.10. MnDOT: Rebar detail for pile to bent cap connection, Lafayette Bridge[3]

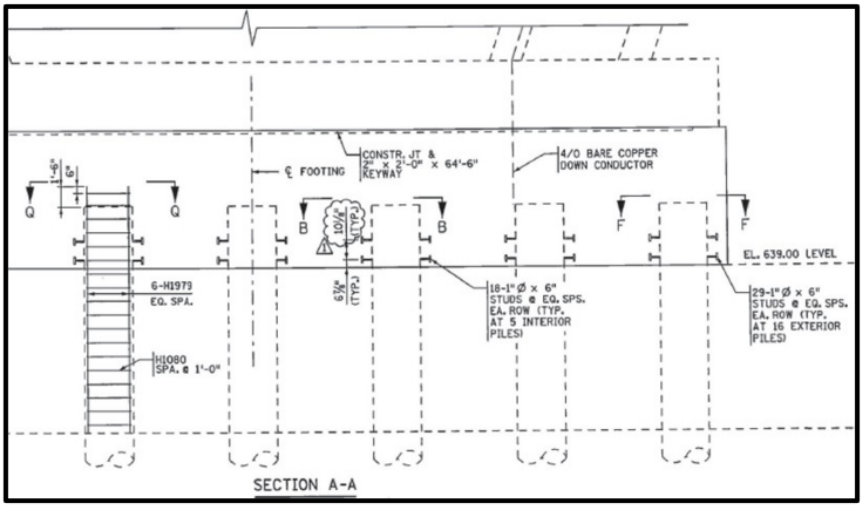

(a) Sectional elevation view

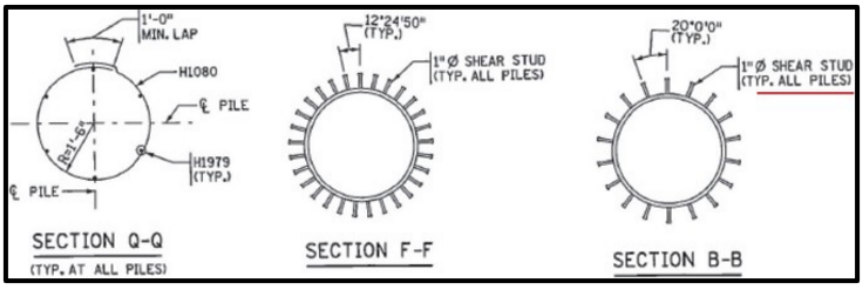

(b) Sectional pile plan view

Figure 3.11. MnDOT: Shear studs detail for pile to bent cap connection, Hastings Bridge[3]

3.2.2.7 Mississippi (MDOT)

Use of steel pipe pile

According to MDOT, steel pipe piles are commonly utilized in bridge structures.

Size and types of commonly used pipes

Piles with diameters ranging from 24 in. to 36 in. are used, with a thickness of 0.5 in. to 0.75 in. Due to their larger size, these piles do not have a concrete core.

Connection design/Detailing consideration

MDOT does not have standard design methodologies but has certain considerations. A minimum embedment of 1 ft. is provided for steel pipe piles inside the concrete bent cap. Additionally, through holes are provided in the piles to ensure that the embedment does not affect the layout of reinforcements in the bent cap. To enhance the strength of the connection between the bent cap and pile, a concrete plug of 1 ft. 6 in. is provided above and below the bent cap inside the steel pipe piles.

Example bridge

Figure 3.12 below depicts the details of the connection between the steel pipe piles and the concrete bent cap of the bridge over Cassidy Bayou. Figure 3.13 also illustrates the most commonly used details for the concrete plug.

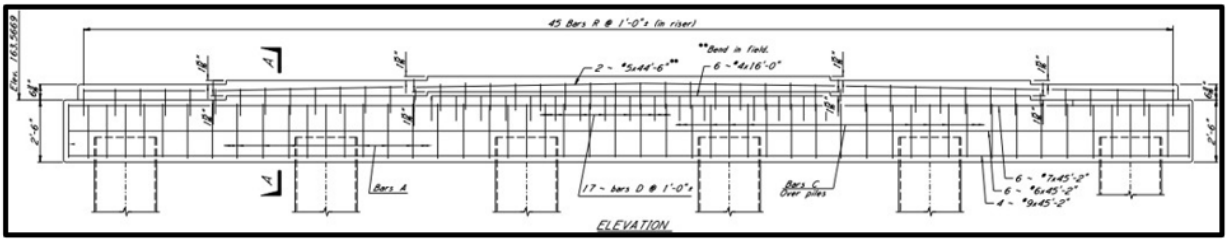

(a) Elevation view

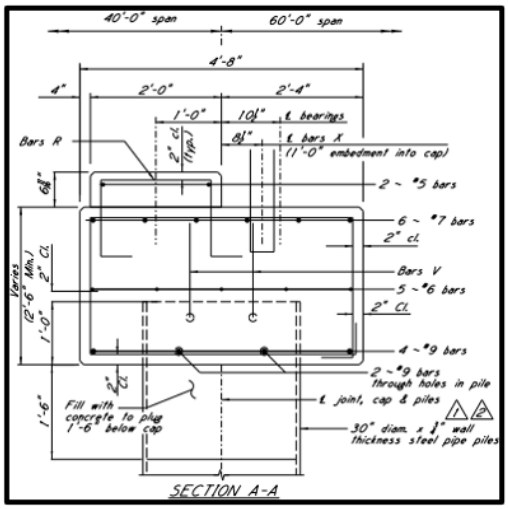

(b) Sectional elevation view

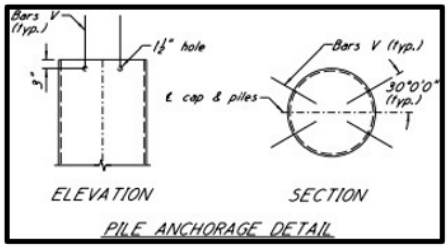

(c) Connection detail

Figure 3.12. MDOT-Rebar detail for pile to bent cap connection, Cassidy Bayou

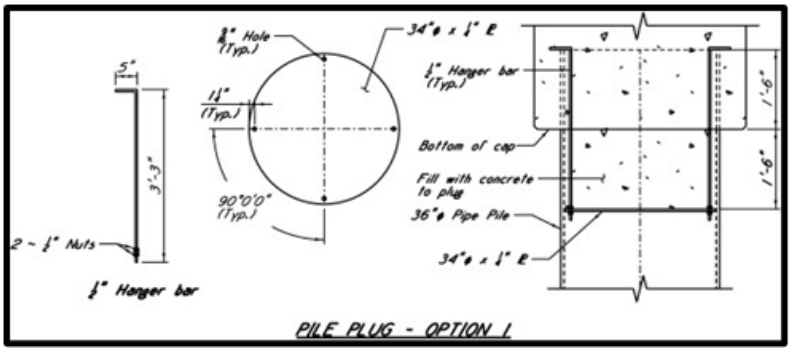

Figure 3.13. MDOT-Concrete plug detail, Wolf River

3.2.2.8 Missouri (MoDOT)

Use of steel pipe pile

Steel pipe piles, commonly referred to as Cast-In-Place (CIP) Piles, are utilized by MoDOT for intermediate bents in bridge construction.

Size and types of commonly used pipes

Missouri utilizes steel pipe piles with diameters ranging from 14 in. to 24 in. and thicknesses of 0.5 in. These steel shells are driven into the ground, either with a closed end or open end, and subsequently filled with concrete.

Connection design/Detailing consideration

The steel pipe piles are embedded within the reinforced concrete bent cap. Various anchorages, including hooked rebars, annular rings, and shear studs, are employed for the connection. To ensure a robust connection, a minimum embedment of 18 in. for the steel piles is required.

Standard/Example bridge

The standard drawings for the connection, as provided by the MoDOT, are depicted in Figure 3.14. Additionally, Figure 3.15 illustrates the specific details of the connection used in the construction of the Champ Clark bridge in Missouri. For the connection, shear connectors were welded inside the steel pipe piles. The details of the Rocheport bridge, constructed in Missouri, are presented in Figure 3.16. An annular ring was welded at the top end of the embedded steel pipe piles.

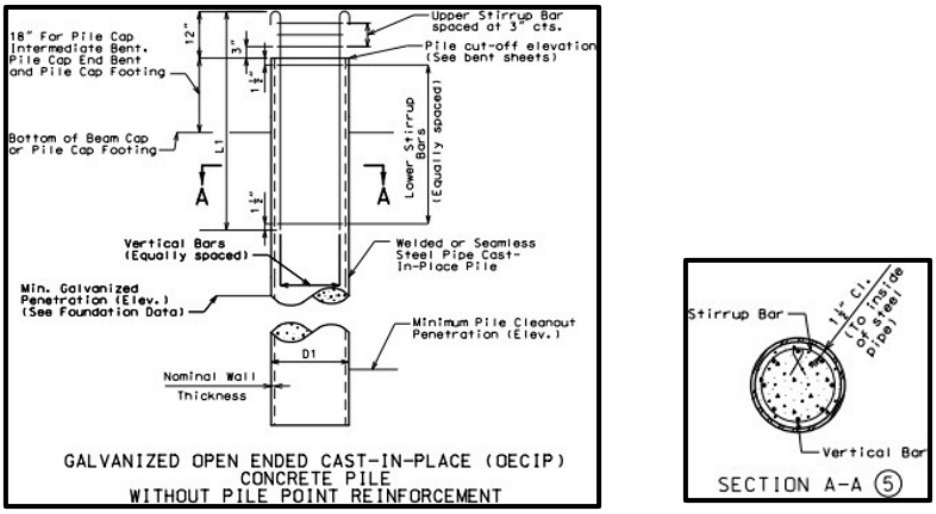

(a)Sectional elevation view

(b) Sectional Pile plan view

Figure 3.14. MoDOT: Rebar detail for pile to bent cap connection (Bridge No. PILE02)

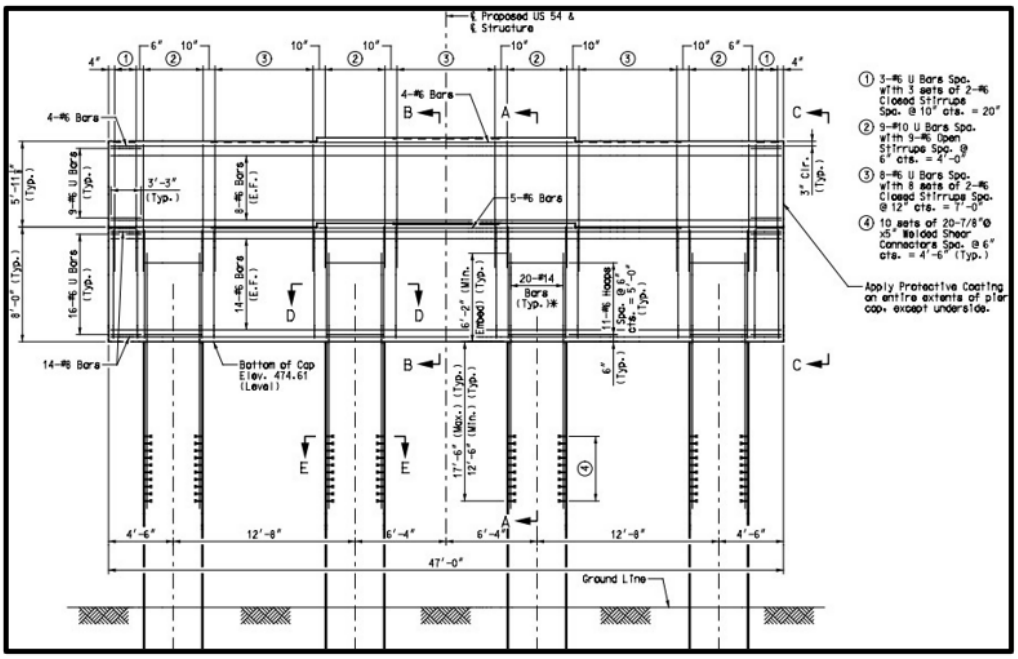

(a) Sectional elevation view

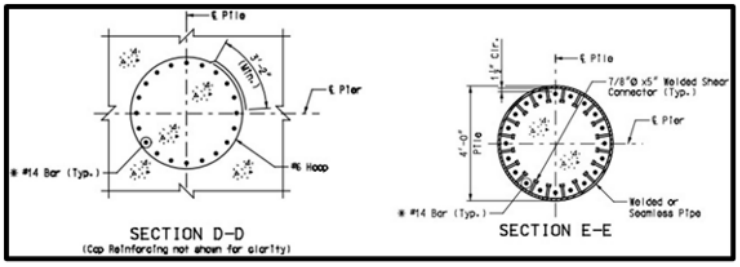

(b) Sectional Pile plan view

Figure 3.15. MoDOT: Shear studs detail for pile to bent cap connection, Champ Clark bridge

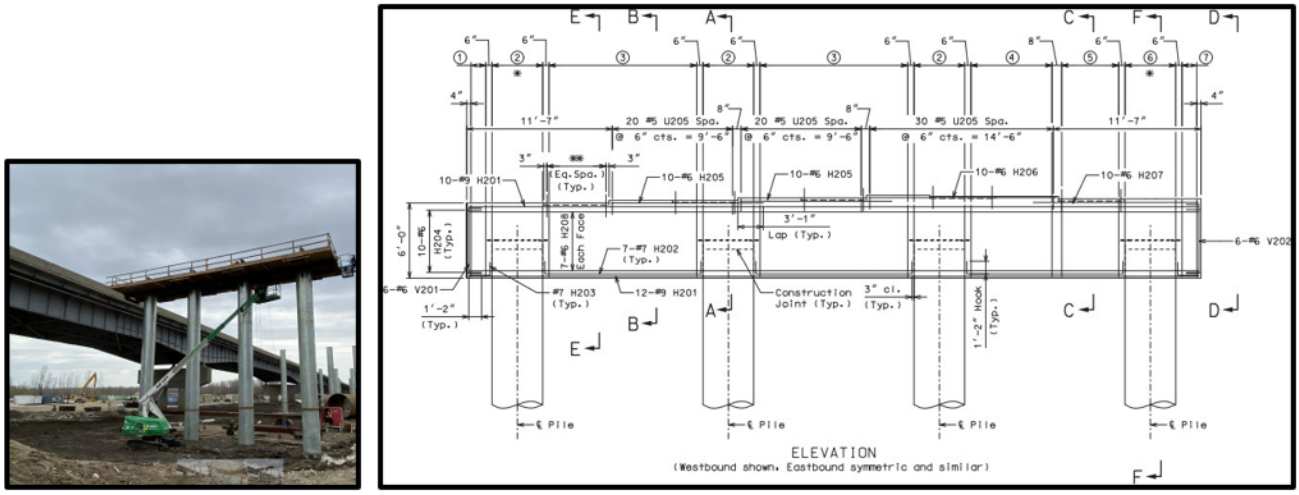

(a) Site view

(b)Elevation view

(c) Sectional elevation view

Figure 3.16. MoDOT: Annular ring detail for pile to bent cap connection, Rocheport Bridge

3.2.2.9 Montana (MDT)

Use of steel pipe pile

Steel pipe piles are commonly used by MDT. They are known to be simple, cost-effective, and relatively easy to construct, making them suitable for many situations.

Size and types of commonly used pipes

Piles with a small diameter of 16 in. and a thickness of 0.5 in. are used by MDT. These piles are filled with concrete to enhance their strength.

Connection design/Detailing consideration

The piles are embedded approximately 1 ft. 8 in. into the cap. To create the anchorage, special U-bars are installed in the bent cap around the pile.

Example bridge

The detailed connection used on the Swan River bridge is presented in Figure 3.17.

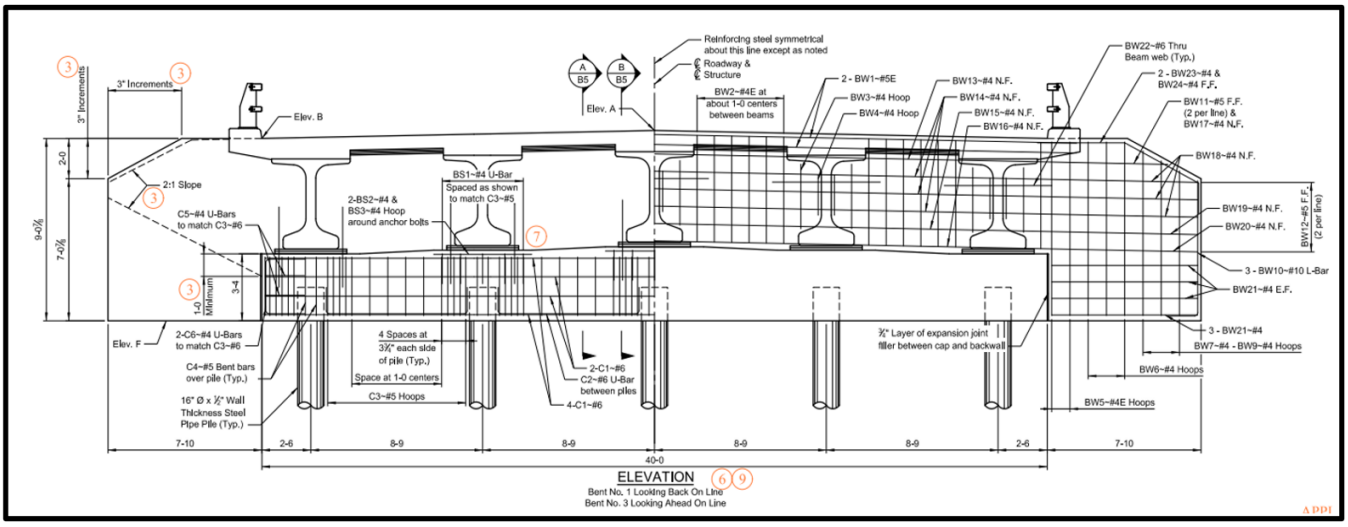

(a) Elevation view

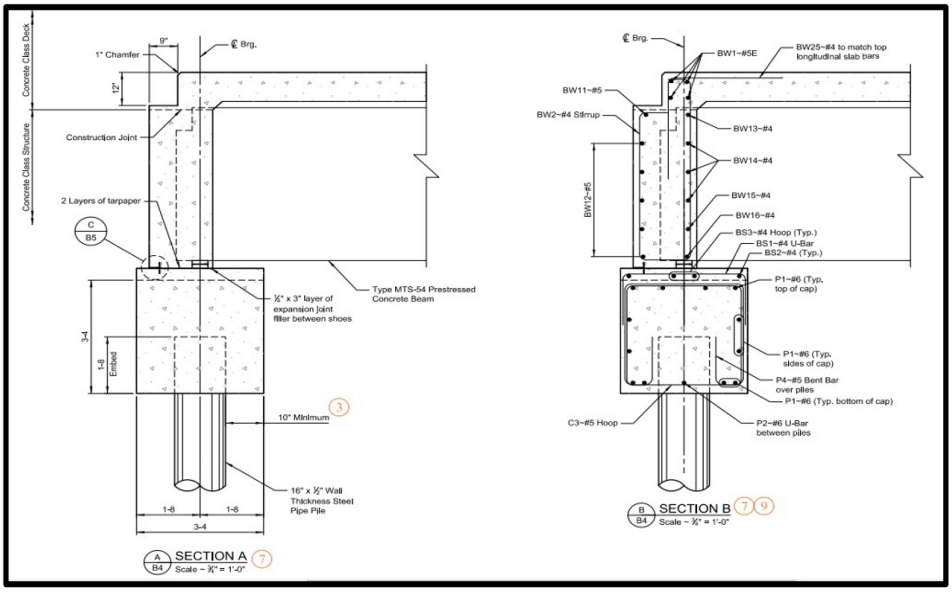

(b) Sectional elevation view

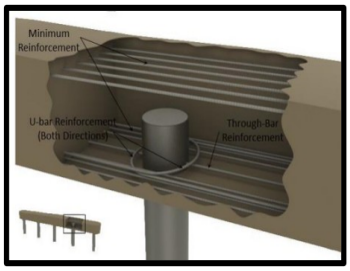

(c) Reinforcement details

Figure 3.17. MDT: Rebar detail for pile to bent cap connection, Swan River

3.2.2.10 Nebraska (NDOT)

Use of steel pipe pile

Steel pipe piles are utilized by NDOT when soil displacement bearing is required. In similar cases, HP-piles are also treated as substitutes. These piles are not directly driven into the soil; instead, a foundation is provided at the bottom of the pile.

Size and types of commonly used pipes

Steel pipe piles with a large diameter of 42 in. are used, and they are equipped with a concrete core and reinforcements.

Connection design/Detailing consideration

For the required connection, a minimum of 1 ft. of embedment is provided. The longitudinal rebars, which are hooked inside the cap, are placed within the concrete core of the piles.

Example bridge

Nebraska does not have specific connection details; however, Figure 3.18 provides an example of the connection details used at Fremont Southeast Beltway.

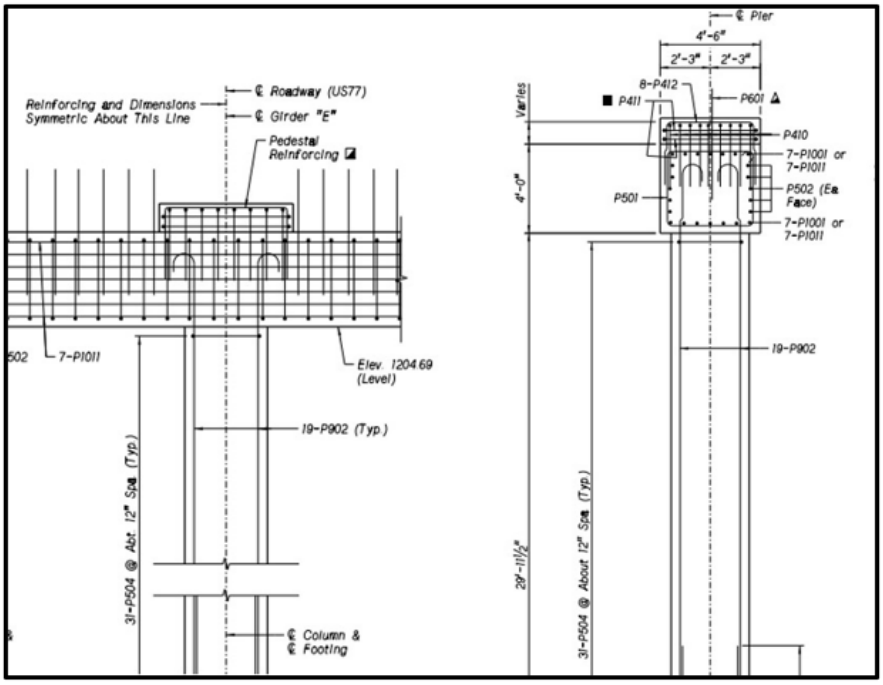

(a) Sectional elevation view

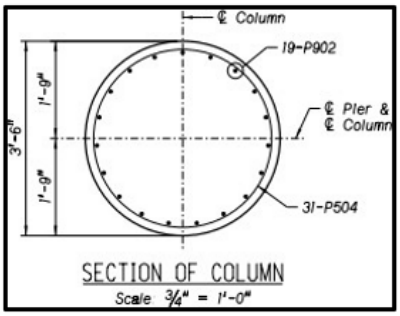

(b) Pile plan view

Figure 3.18. NDOT: Rebar detail for pile to bent cap connection, Freemont southeast beltway

3.2.2.11 New Mexico (NMDOT)

Use of steel pipe pile

NMDOT has a long history of frequently using and continues to utilize steel pipe piles for new bridge construction.

Size and types of commonly used pipes

In New Mexico, steel pipe piles of various diameters, such as 16 in. and 24 in., with a thickness of 0.5 in., are commonly used. These piles are filled with concrete for added strength and stability.

Connection design/Detailing consideration

For the connection, a minimum of 1 ft. and a maximum of 2 ft. of the pile are embedded inside the bent cap. Shear connectors are welded to the outer wall of the pile, which is embedded within the cap. This allows for the transfer of force and moment between the pile and the cap.

Example bridge

The detailed connection used in the replacement of Yaple Canyon Bridge is shown in Figure 3.19.

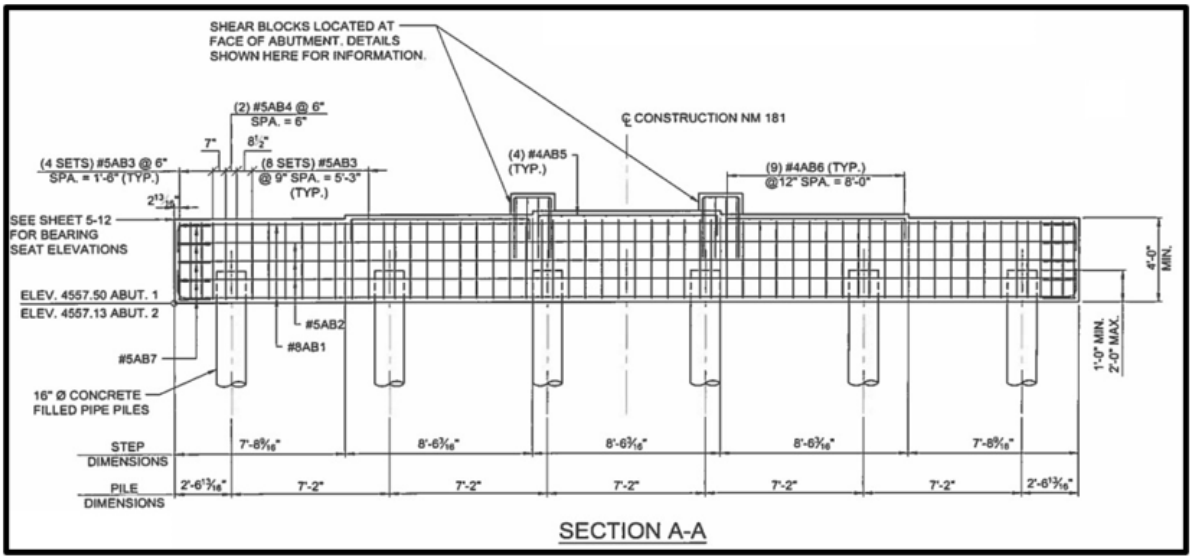

a) Sectional elevation view

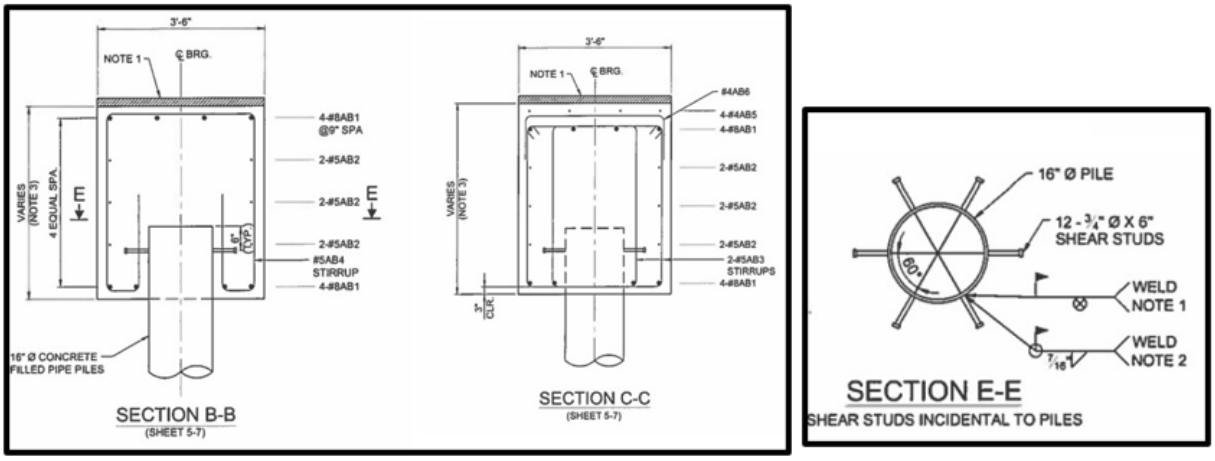

(b) Sectional elevation view (c) Pile plan view

Figure 3.19. NMDOT- Rebar detail for pile to bent cap connection, Yaple Canyon Bridge

3.2.2.12 North Carolina (NCDOT)

Use of steel pipe pile

According to NCDOT, steel pipe piles are commonly used in bridge structures.

Size and types of commonly used pipes

NCDOT utilizes steel pipe piles of various diameters, ranging from 14 in. to 30 in., with a thickness of 0.5 in. These piles, being of larger diameter, are hollow and do not have a concrete core.

Connection design/Detailing consideration

The pile is filled with concrete up to a minimum height of 5 ft. A concrete plug with a reinforcement cage is installed inside the pile, which facilitates the attachment with the bent cap. To minimize the required development length of the rebars inside the cap, they are hooked at a 90^0 angle. Additionally, transverse ties are incorporated to enhance the rebar confinement and overall strength.

Standard bridge

The standard drawings for steel pipe piles are presented in Figure 3.20.

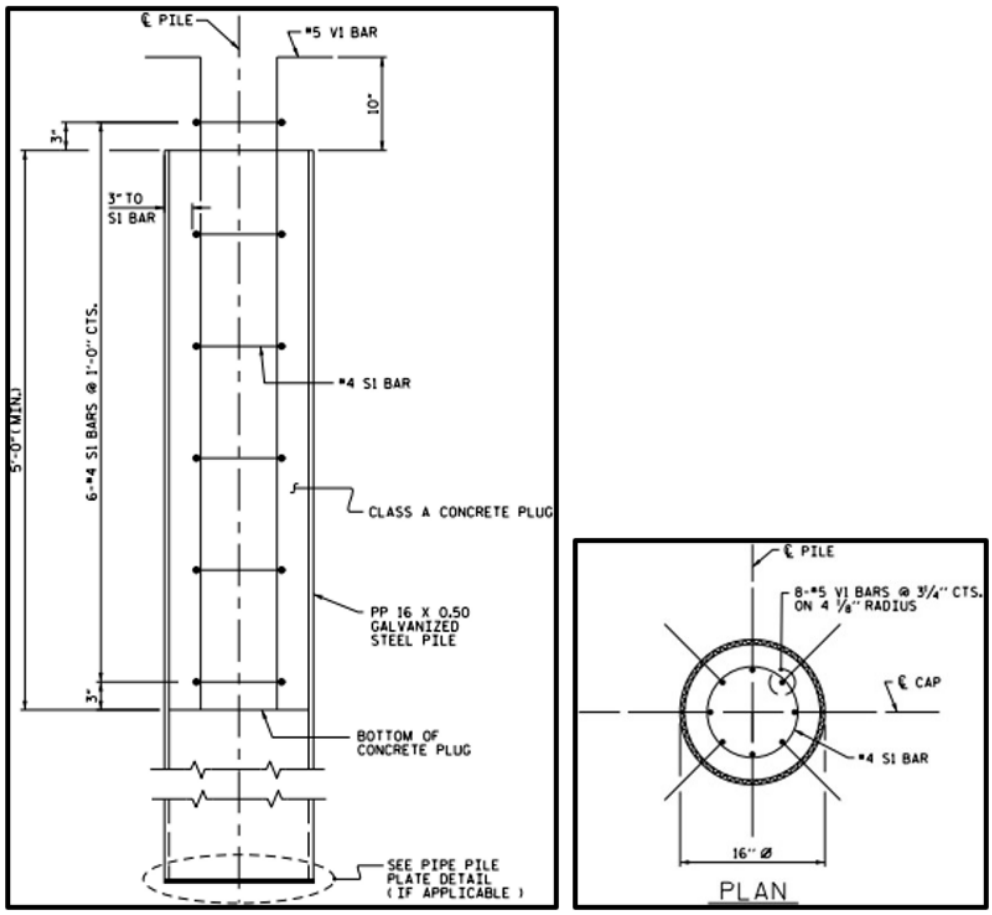

(a) Sectional elevation view (b) Pile plan view

Figure 3.20. NCDOT- Rebar detail for pile to bent cap connection (STD. NO. SPP2)

3.2.2.13 Oklahoma (ODOT)

Use of steel pipe pile

ODOT has utilized steel pipe piles at only one location, which is a couple of years old but remains in good condition. However, ODOT does not commonly employ such piles and lacks standardized details for their use.

Size and types of commonly used pipes

The commonly used size of steel pipe piles is 24 in., with a thickness of 0.625 in. Additionally, these piles are filled with concrete throughout their entire length.

Connection design/Detailing consideration

An anchorage ring is employed at the end of the embedded steel pipe pile for the connection. Such attachments enhance anchorage and establish a pathway for transferring forces, stresses, and moments from the concrete to the pile.

Example bridge

The connection details of the bridge structure over Pine Creek and the unnamed tributary are depicted in Figure 3.21.

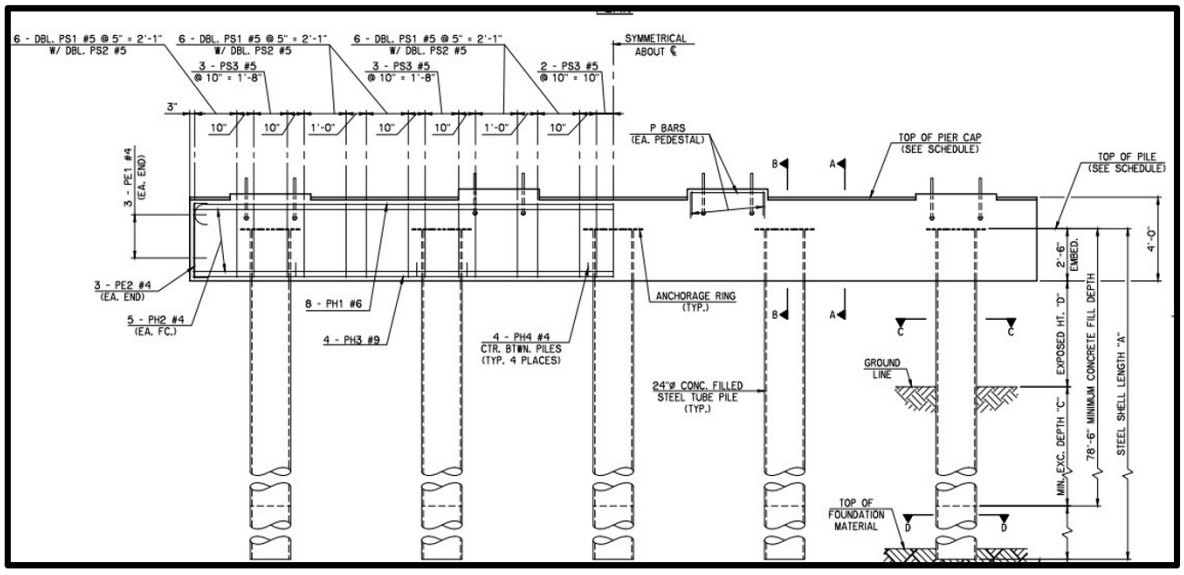

(a) Elevation view

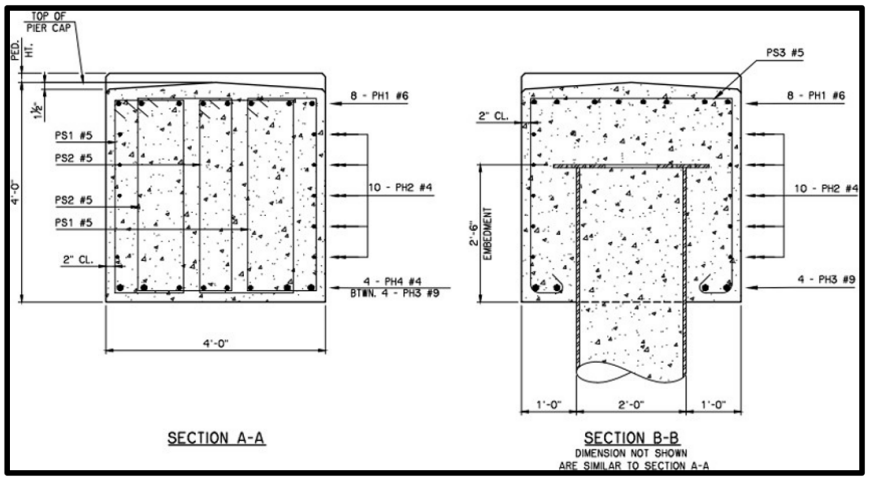

(b) Sectional elevation view

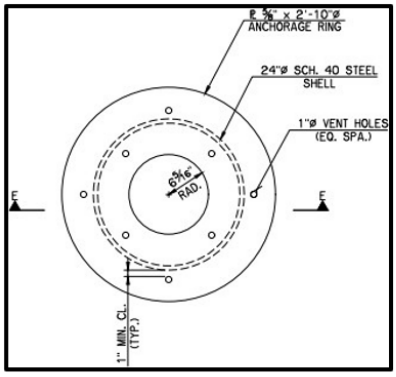

(c) Pile plan view

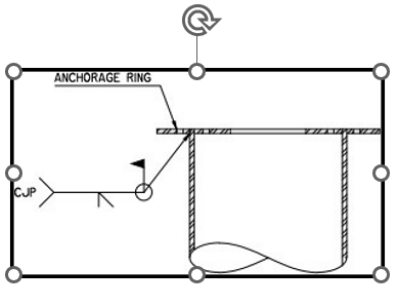

(d) Anchorage detail

Figure 3.21. ODOT: Annular ring detail for pile to bent cap connection, Pine Creek and unnamed tributary

3.2.2.14 South Dakota (SDDOT)

Use of steel pipe pile

Steel pipe piles are frequently utilized by SDDOT for relatively short concrete slab structures. In this scenario, the concrete slab serves as a bent cap, and the steel pipe piles are attached to the concrete slab.

Size and types of commonly used pipes

Steel pipe piles with a diameter of 16 in. and a thickness of 0.25 in. are utilized. These piles are filled with concrete to enhance their strength.

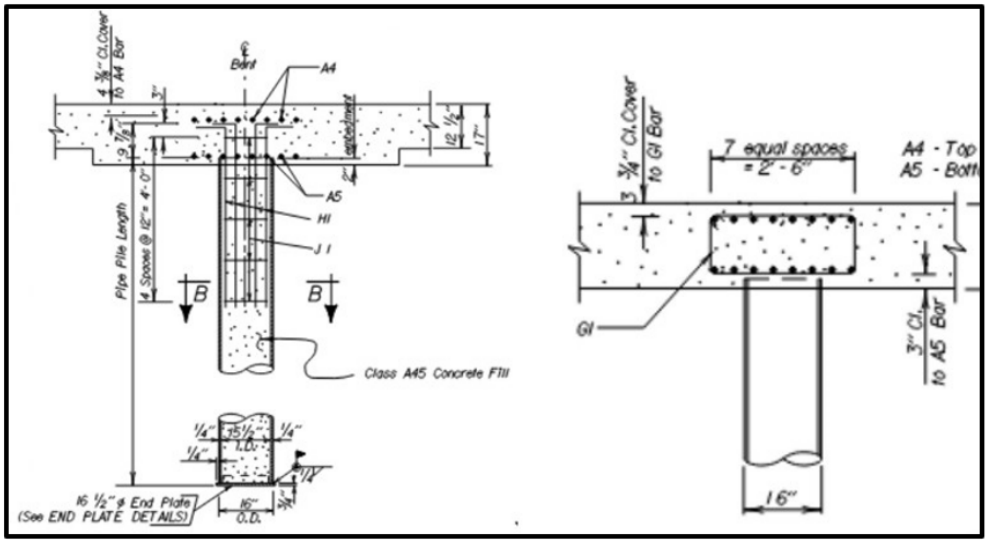

(a) Sectional elevation view

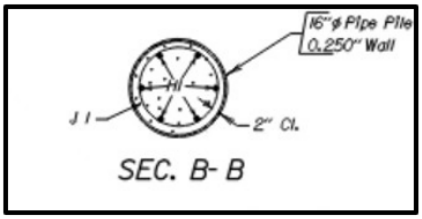

(b) Pile plan view

Figure 3.22. SDDOT: Rebar detail for pile to bent cap connection

Connection design/Detailing consideration

A pinned connection is typically assumed between the pipe pile and the slab. To achieve this connection, either 6 or 8 #6 bars are employed, depending on the diameter of the pipe pile. These bars are hooked at 90^0 angles and developed inside the cap for the connection. Additionally, the bars in the slab over the top of the pipe piles, acting as a "cap," vary depending on the spacing of the piles.

Standard bridge

The Base detail for the connection of the pile to the cap is illustrated in Figure 3.22.

3.2.2.15 Tennessee (TDOT)

Use of steel pipe pile

According to TDOT, steel pipe pile bents are commonly used in bridges, particularly in West Tennessee.

Size and types of commonly used pipes

TDOT typically utilizes small diameter (16 in.) steel pipe piles with a thickness of 0.5 in. These piles are filled with concrete due to their small dimensions.

Connection design/Detailing consideration

For the connection with the cap, longitudinal rebars are placed inside the concrete core of the steel pipe piles. These rebars are developed inside the cap and hooked at the end. However, they are not provided throughout the entire length of the pile. Additionally, a minimum embedment of 1 ft. 6 in. is required for the connection to the cap.

Example bridge

Figure 3.23 below illustrates an example of the details regarding the connection between the steel pipe pile and concrete bent cap at the Norfolk Southern Railroad Station.

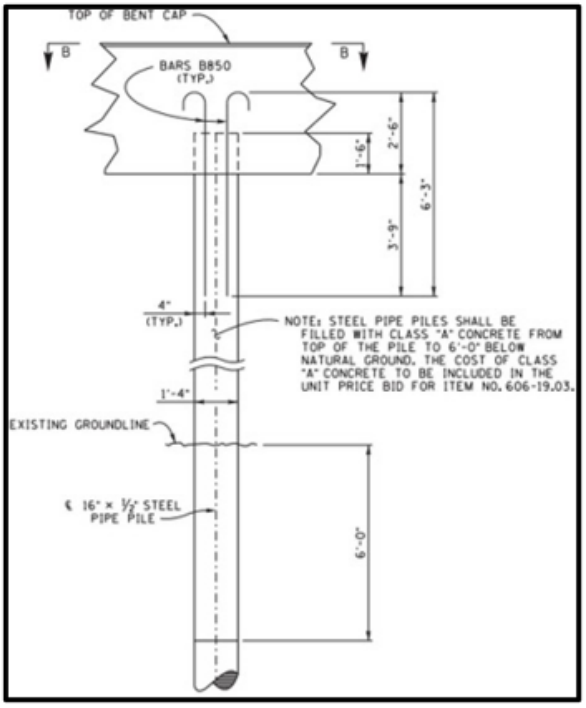

(a)Elevation view

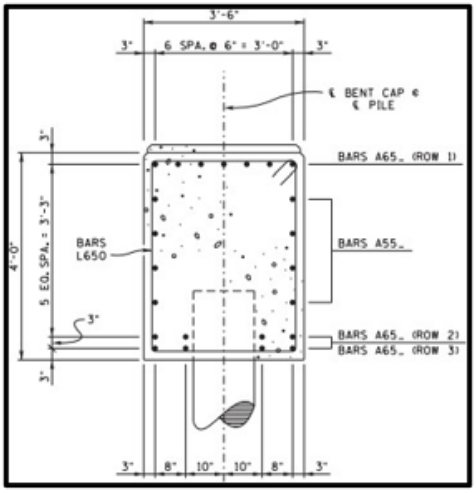

(b) Sectional elevation view

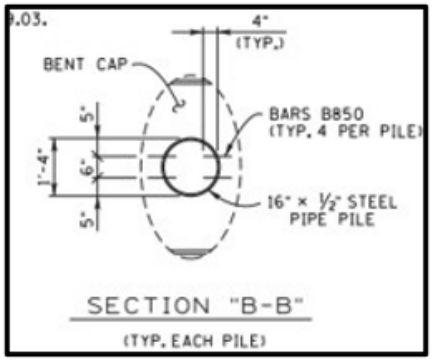

(c) Pile plan view

Figure 3.23. TDOT: Rebar detail for pile to bent cap connection, Norfolk southern railroad station

3.2.2.16 Utah (UDOT)

Use of steel pipe pile

According to UDOT, exposed pile bents are not commonly used in bridge structures, where the piles extend directly from the ground to the bent cap. However, in specific cases, this practice may be allowed but requires approval on a case-by-case basis. Typically, bents in bridge structures comprise the bent cap, columns, footings, and piles.

Size and types of commonly used pipes

UDOT utilizes piles of various diameters for their bridge structures. The commonly used pile diameter is 12.75 inches. Since these are smaller diameter piles, they are filled with concrete during the construction process.

Connection design/Detailing consideration

UDOT's standard details depict piles embedded in a pile cap, such as an abutment or column footing. The same detailing applies to an exposed pile bent. UDOT provides standard details for both pinned pile heads and fixed pile heads, with an embedment depth into the pile cap of 2 ft. A reinforcement cage is placed inside the steel pile and developed within the bent cap, with hooked ends for a strong connection. A railroad bridge constructed a couple of years ago followed this exact approach.

Standard bridge

Figure 3.24 depicts the bridge standard drawings associated with the pipe piles.

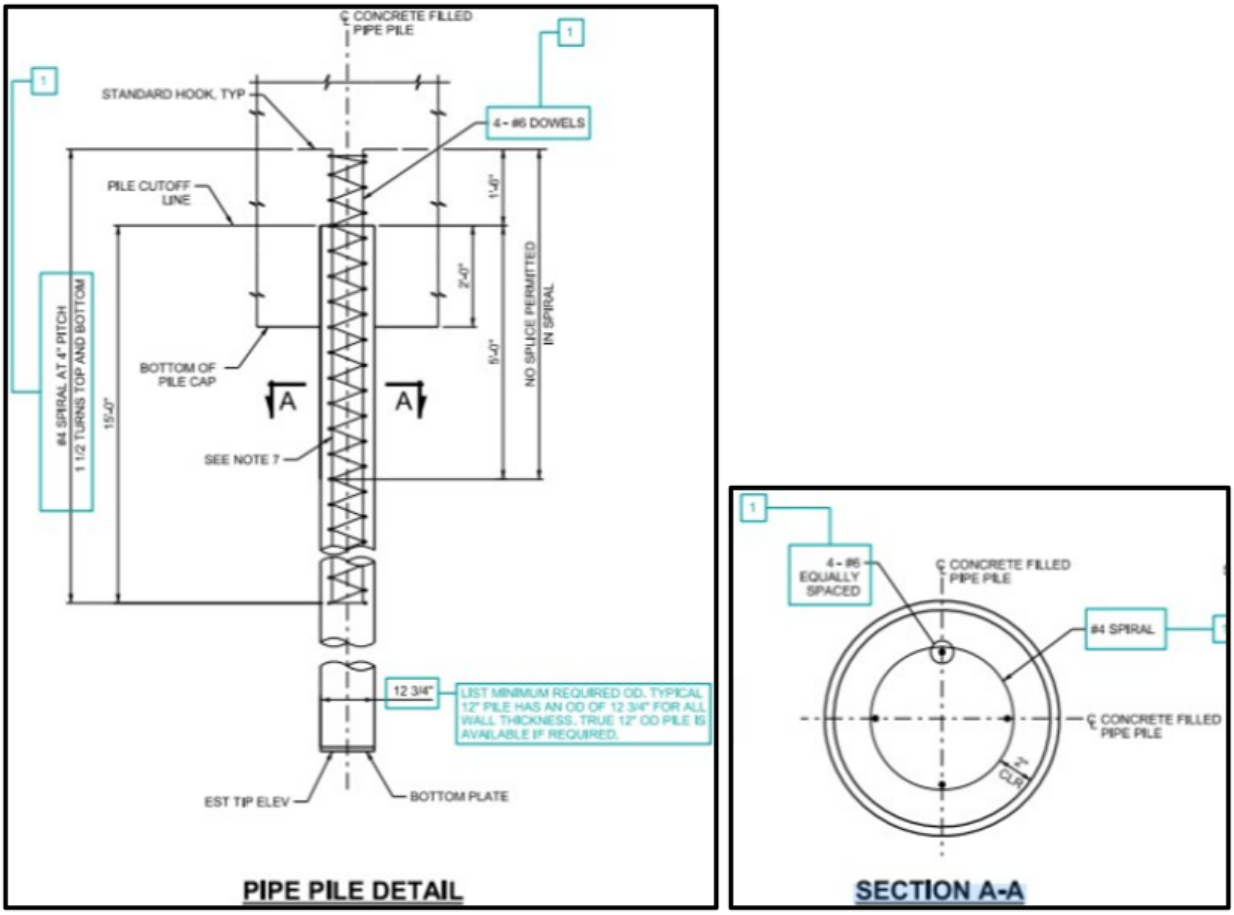

(a) Sectional elevation view (b) Pile plan view

Figure 3.24. UDOT: Rebar detail for pile to bent cap connection (Drawing No.: WS-2A)

3.2.2.17 Washington (WSDOT)

Use of steel pipe pile

According to WSDOT, steel pipe piles, and cast-in-place concrete caps are commonly employed in bridge structures. In the past, precast concrete piles were utilized to support terminal structures, but in the 1990s, a transition to steel piles occurred due to drivability and seismic considerations. The encountered soil is often highly dense and glacially consolidated, necessitating compliance with increasingly stringent seismic criteria, which include accounting for liquefaction and tsunami effects.

Size and types of commonly used pipes

Piles with larger diameters, such as 30 in. and 36 in., with a thickness of 1 in., are commonly used. Due to their larger size, hollow piles are often chosen for these applications.

Connection design/Detailing consideration

Since the piles are hollow, a concrete plug measuring 12 ft. 3 in. to 14 in. is placed on top of the piles. Longitudinal rebars are incorporated within the plug to enhance the strength of the connection. WSDOT has also implemented headed rebars, which are developed inside the cap. The purpose of these rebars is to reduce the depth of the bent cap while maintaining the same level of strength.

Example bridge

Figure 3.25 below displays an example of the connection details between the steel pipe pile and concrete bent cap at Bainbridge Island.

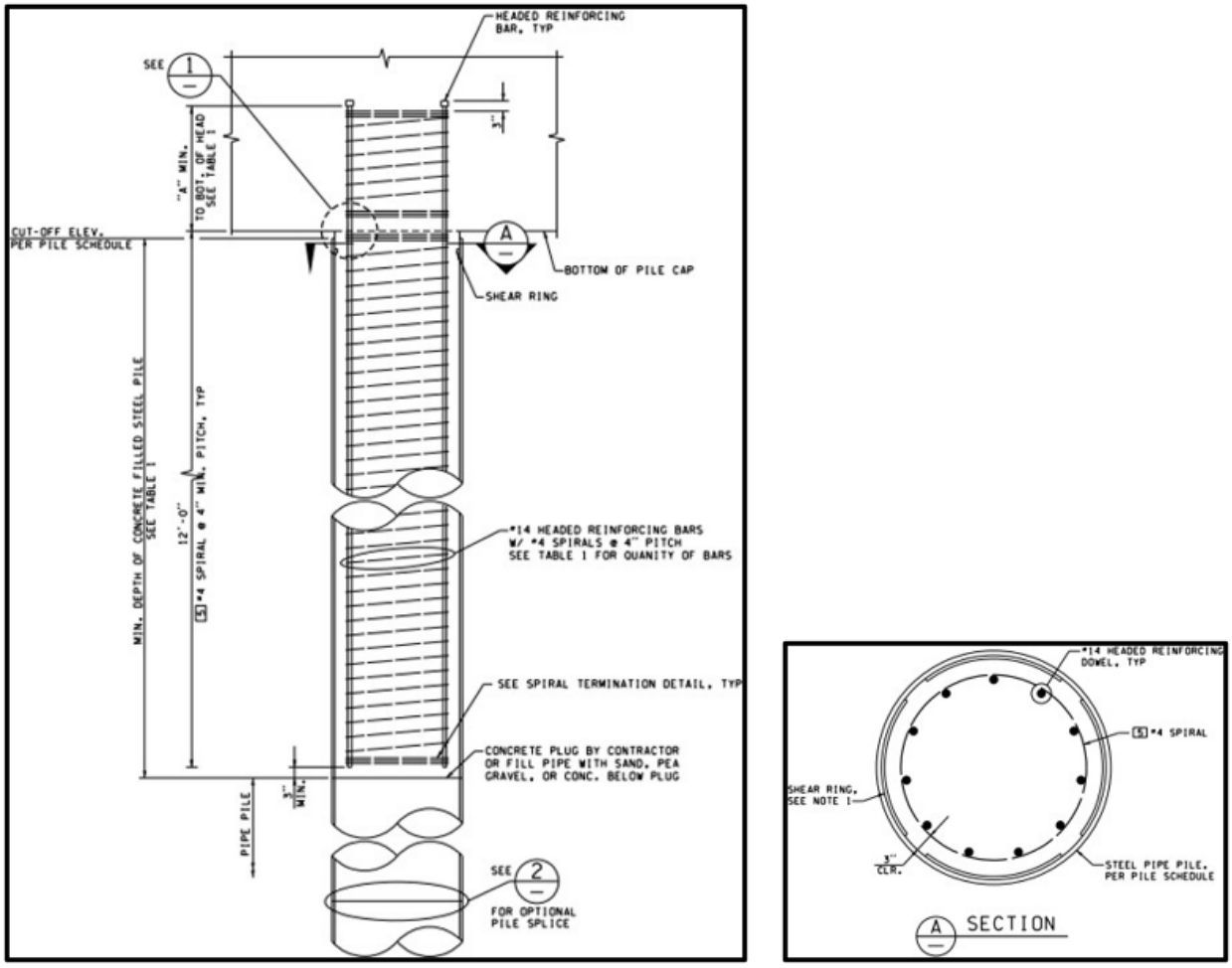

(a) Sectional elevation view (b) Pile plan view

Figure 3.25. WSDOT: Rebar detail for pile to bent cap connection, Bainbridge Island, Washington

3.2.2.18 Wisconsin (WisDOT)

Use of steel pipe pile

WisDOT commonly utilizes steel pipe piles (ASTM A252 Grade 3) that are filled with concrete to provide support for the substructures.

Size and types of commonly used pipes

WisDOT commonly employs steel pipe piles with various diameters, such as 12.75 in. and 14 in. The minimum thickness of these piles is 0.375 in. To enhance their load-bearing capacity, concrete is used to fill the steel piles. This concrete filling significantly increases the strength of the piles.

Connection design/Detailing consideration

The steel pipe piles used by WisDOT are internally reinforced with #7 bars, which are terminated 10 ft. below the groundline or streambed. For the necessary connection, a minimum pile embedment of 2 ft. is provided, and the longitudinal rebars extend up to 1 ft. 2 in. into the cap.

Standard bridge

Figure 3.26 displays the standard details of the connections used in Cast-In-Place piles.

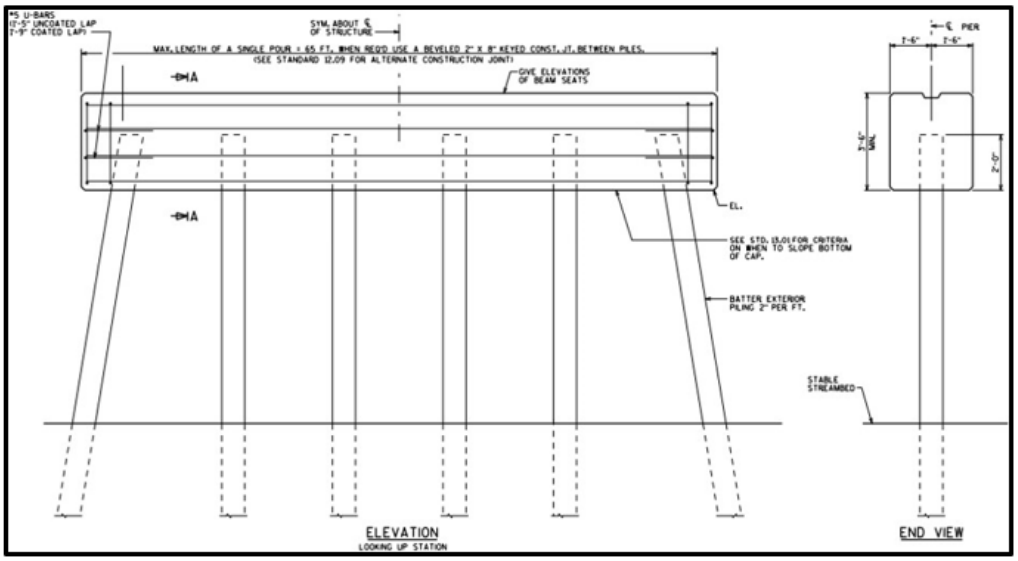

(a) Elevation view

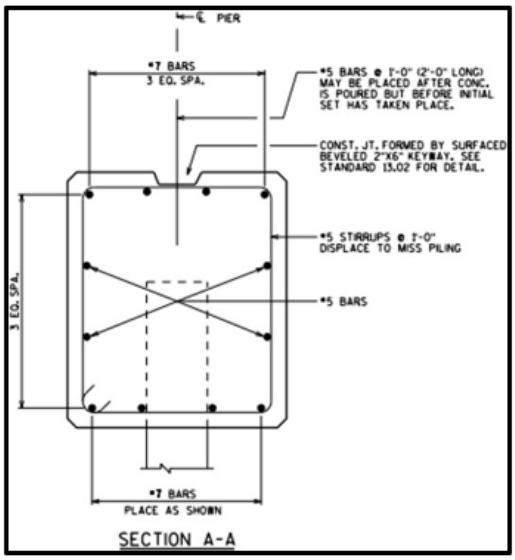

(b) Sectional elevation view

Figure 3.26. WisDOT: Rebar detail for pile to bent cap connection (STD. NO. 13.04)

3.2.3 Brief details of Steel pipe pile to Bent cap Connection for other DOTs

Several states, namely Iowa DOT, North Dakota DOT, Arkansas DOT, Maryland DOT, Oregon DOT, Connecticut DOT (3.2.3.1), Michigan DOT (3.2.3.2), and Alaska DOT, have indicated the use of steel pipe piles. However, these states do not have standard design

methodologies or example bridge drawings for the connection between steel pipe piles and concrete bent caps. On the other hand, Indiana DOT (3.2.3.3) also utilizes steel pipe piles and has a standard drawing for the connection details, which will be discussed.

3.2.3.1 Connecticut (CTDOT)

CTDOT rarely utilizes steel pipe piles; therefore, they do not have specific details regarding such piles. They do not have any provisions for steel pipe pile bents where the superstructure rests directly on a bent cap. However, the details concerning steel pipe piles with a wall pier on top of a pile cap are presented in Figure 3.27. Cast-in-place steel piles are employed, and they are embedded 1 ft. inside the cap.

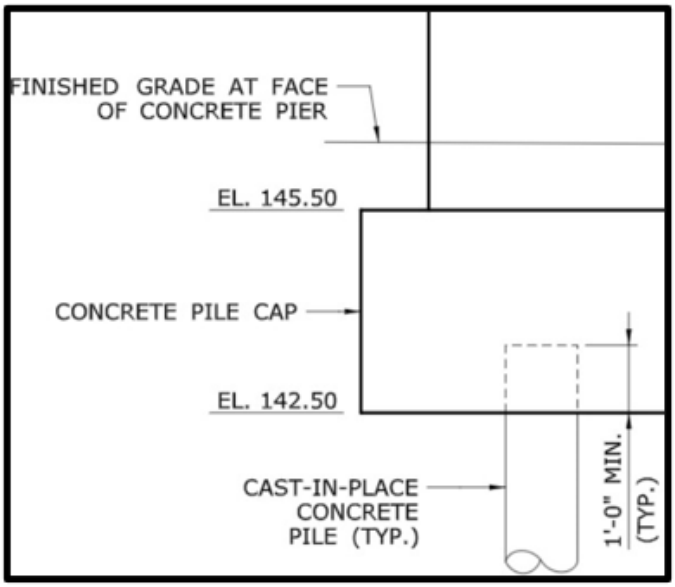

(a) Elevation view

Figure 3.27. CTDOT: Pile to cap connection

3.2.3.2 Michigan (MDOT)

MDOT utilizes steel pipe piles with footings on the bottom to design foundations that prevent uplift, and as a result, the piles are not typically anchored to the foundation. Moreover, MDOT does not possess any standard details specifically for this type of connection.

3.2.3.3 Indiana (INDOT)

Indiana also utilizes small diameter steel pipe piles filled with a concrete core. While they do not have specific details related to connection, a minimum embedment length of 2 ft. is required. Spiral reinforcement is provided around the steel piles to enhance the connection strength and transfer force, stress, and moment from the concrete to the piles. The standard details provided in the Indiana Bridge Design Manual are showcased in Figure 3.28.

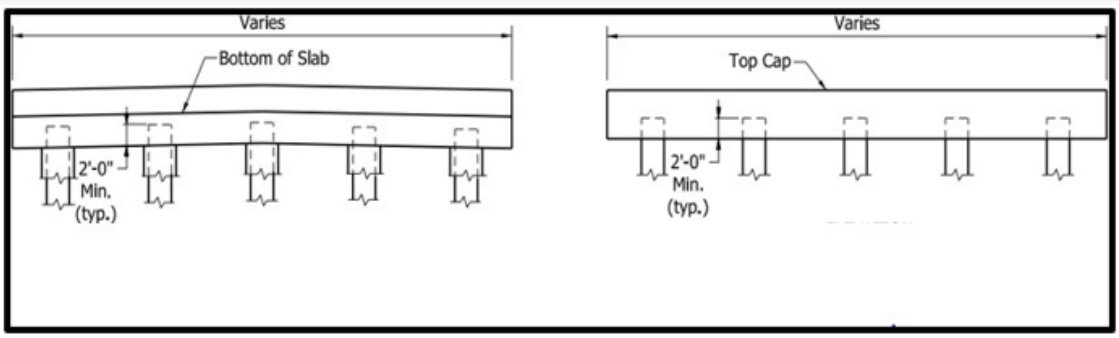

(a) Elevation view

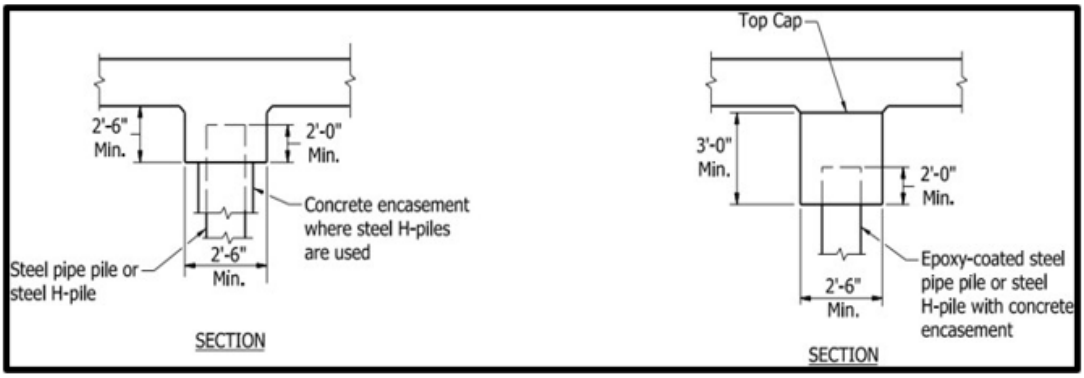

(b) Sectional elevation view

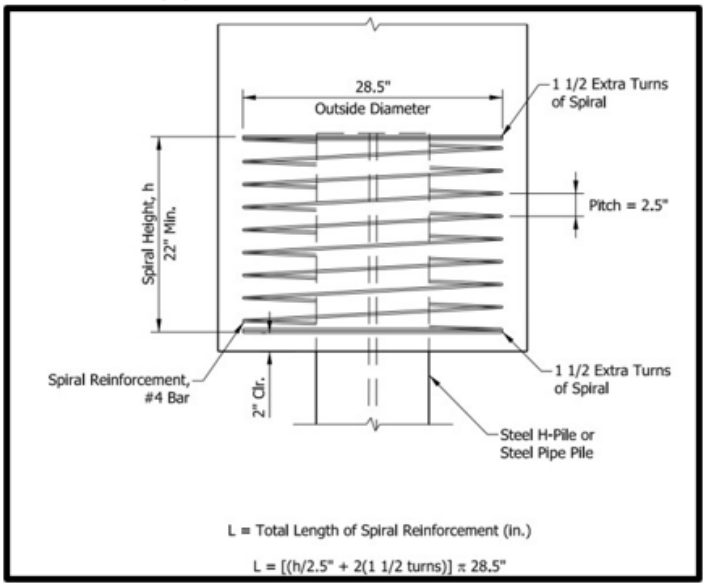

(c) Sectional elevation view

Figure 3.28. INDOT: Spiral rebar detail for pile to bent cap connection

3.2.4 Exceptional case

Louisiana Department of Transportation (LADOT) used steel pipe piles in the past and has several bridges in the state with exposed steel pipe piles supporting bent caps. All the bents were designed to be in compression, resulting in less critical connections. For connections requiring tension, studs were welded on the outside perimeter of the embedded pile. The steel pipe piles had an embedment length ranging from 6 in. to 9 in. inside the bent cap. A concrete plug was provided in the upper portion of the pile, and its length was determined based on the cohesion value between concrete and steel. For the connection, a reinforcement cage was implemented between the concrete plug and the bent cap. Unfortunately, standard details for these connections are not available. Lastly, it is worth noting that Louisiana no longer employs steel pipe piles for bridge structures.

3.3 Conclusions

Based on the electronically connected inquiry, it is evident that steel pipe piles are widely used by many states, and these states have extensive experience with such piles. The majority of states commonly utilize small diameter steel pipe piles, typically ranging from 14 in. to 24 in., which are filled with concrete. In certain states, a concrete plug is provided only on the top portion of the piles (usually around 1 ft. 6 in.) to enhance the connection's strength against buckling. Different states employ various methods to connect the steel pipe piles to the concrete bent cap, as discussed in the respective sections above. The piles are embedded inside the bent cap to a specific depth to establish a robust connection. The most commonly used method involves attaching the piles to the rebars, utilizing straight rebars, rebars with 180^0 hooks, or rebars with 90^0 hooks (as seen in Caltrans, DelDOT, FDOT, GDOT, IDOT, MnDOT, MDOT, MoDOT, MDT, NDOT,

NMDOT, NCDOT, SDDOT, TDOT, UDOT, WSDOT, WisDOT, INDOT). The longitudinal rebars of the piles are integrated into the concrete of the cap to ensure structural continuity. Moreover, in some states (such as Caltrans, MoDOT, and ODOT), an annular ring is welded to the top of the embedded pile to enhance anchorage, facilitating the transfer of stress, force, and moment to the surrounding rebars and concrete. Additionally, some states (MnDOT, MoDOT) utilize shear connectors that are welded to the outer perimeter of the embedded tube, providing strong resistance against applied forces, and ensuring robust punching resistance. These states have been employing steel pipe piles with various connection details for an extended period, and their structures have remained in good condition and performed well. Their extensive understanding and experience with these interconnections further support the suitability of steel pipe piles for bridge structures.

The online checks conducted to gather information on the provisions related to different states of the US had certain limitations. The study encountered challenges in reaching out to all the bridge engineers of the respective states due to the nature of communication through emails. As a result, responses from all the states were not obtained, which could be attributed to the constraints on engineers' time and personal circumstances. While the engineers who did respond were very helpful, the study was still somewhat constrained, and in-depth discussions were not feasible due to the chosen mode of communication. Moreover, the privacy concerns of certain states were taken into consideration, and some engineers expressed discomfort in sharing their standard data, details, and drawings. This further restricted the extent of information that could be obtained for the study. Despite these limitations, the available responses and insights from the participating engineers provided valuable information for the study. The findings and observations

derived from the obtained data still contribute to understanding the general practices and considerations related to steel pipe piles in bridge structures across different states.

Chapter 4 DESIGN PROVISIONS AND DESIGN METHODOLOGY DEVELOPMENT

This chapter provides a summary of the design provisions for various types of anchorages as specified in the AASHTO LRFD Bridge Design Specification (AASHTO, 2020), the American Concrete Institute (ACI, 318-19), and the AISC Steel Design Manual and Specification (AISC, 2016). It also includes an interpretation of the developed design procedures concerning the connection between piles and reinforced concrete foundations/bent caps, as discussed in Chapter 2. Within this chapter, those design methodologies are presented, explained, and compared with one another. Through these studies, a design methodology is proposed for the necessary connection, which is presented in detail in this chapter.

4.1 Design provisions

4.1.1 AASHTO LRFD Bridge Design Manual (2020) Design Provisions For Reinforcing Bars

The AASHTO LRFD Bridge Design Manual (AASHTO, 2020) provides provisions for the use of rebars in bridge structures and rules for the development of rebars within the concrete zone. These provisions can be applied to No. 11 bars, which have a yield strength of up to 100 ksi. Additionally, they can also be applied to smaller bars with normal weight concrete and compressive strength of up to 15.0 ksi, as well as lightweight concrete with compressive strength of up to 10.0 ksi.

The basic development length for straight rebars can be found in Section 5.10.8.2.1a, and it is given by Eq. (4.1).

$$L = 2.4d_b * \frac{f_y}{\sqrt{f'c}} \quad \textbf{(4.1)}$$

where, the variables f_y, f'_c, and d_b represent the yield strength of rebars, compressive strength of concrete, and nominal diameter of the reinforcing bar, respectively.

By incorporating spiral hoops and ties to provide a specific amount of confinement, the development length can be reduced by up to 40%. The modified development length can be determined using Eq. (4.2).

$$L_d = L\frac{\lambda_{rl}\lambda_{cf}\lambda_{rc}\lambda_{er}}{\lambda} \quad \textbf{(4.2)}$$

In the equation, various factors are involved: λ_{rl}, λ_{cf}, λ_{rc}, λ_{er}, and λ. These factors represent the reinforcement location factor, coating factor, reinforcement confinement factor, excess reinforcement factor, and concrete density modification factor, respectively. It is worth noting that all these factors, except for λ_{rc}, can be assumed to have a value of 1.

The confinement factor is crucial in reducing the development length. As per Section 5.10.8.2.1c, the value of λ_{rc} must meet the conditions specified in Eq. (4.3).

$$0.4 \leq \lambda_{rc} \leq 1.0 \quad \textbf{(4.3)}$$

in which

$$\lambda_{rc} = \frac{d_b}{c_b + k_{tr}}$$

$$k_{tr} = \frac{40A_{tr}}{sn}$$

where, c_b is the smaller of the distance from center of bar or wire being developed to the nearest concrete surface and one-half the center-to-center spacing of the bars or wires being developed, k_{tr} is transverse reinforcement ratio, A_{tr} is total cross-sectional area of all transverse reinforcement which is within the spacing s and which crosses the potential plane of splitting through the reinforcement being developed, s is maximum center-to-center spacing of transverse

reinforcement within L_d, and n is number of bars or wires developed along plane of splitting

Spiral reinforcement

Section 5.6.4.6 addresses the topic of spiral reinforcement in bridge structures. The ratio of spiral reinforcement to the total volume of the concrete core, ρ_s, measured from the outer edge of the spirals, can be determined using Eq. (4.4).

$$\rho_s = \frac{4A_{sp}}{d_c s} \geq 0.45\left(\frac{A_g}{A_c} - 1\right)\frac{f'_c}{f_y} \quad \textbf{(4.4)}$$

where, A_{sp} is area of cross-sectional area of spiral, d_c is core diameter of column measured to the outside diameter of spiral, s is pitch of spiral, Ag is gross area of section, and Ac is area of core measured to the outside diameter of the spiral

Due to the greater development length required for straight bars, there may be instances where there is insufficient space within the concrete zone. In such cases, Section 5.10.8.2.4a (AASHTO, 2020) provides provisions for using hook development length. According to Section 5.10.2.1, the standard hooks for longitudinal reinforcement, as depicted in Figure 4.1, should be one of the following:

a) A 180-degree bend, followed by a $4.0d_b$ extension, with the free end of the bar not less than 2.5 inches.

b) A 90-degree bend, followed by a $12.0d_b$ extension at the free end of the bar.

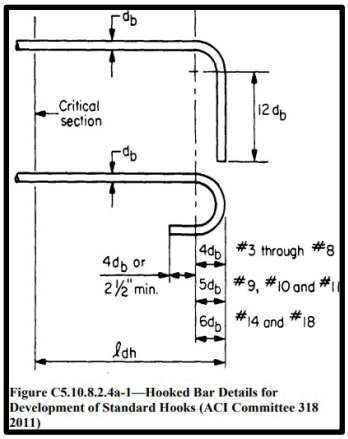

Figure C5.10.8.2.4a-1—Hooked Bar Details for Development of Standard Hooks (ACI Committee 318 2011)

Figure 4.1. Hooked rebar details[16]

The basic development length for hooked rebars can be determined by selecting the largest value among the following equations, as given in Eq. (4.5).

$$(a)\ L = \frac{38.0 * d_b * f_y}{60.0\sqrt{f'_c}} \quad \textbf{(4.5)}$$

(b) $8d_b$

(c) 6in

Furthermore, by implementing appropriate confinement through the use of spiral hoops and ties, the length can be adjusted by up to 80%, similar to straight rebars.

4.1.2 ACI (318-19) Design Provisions For Headed Rebars

Headed bars, depicted in Figure 4.2 can serve as effective alternatives to traditional straight and hooked rebars. These bars feature a coupler at the end, enhancing anchorage with concrete and facilitating stress transfer between steel and concrete. The advantages of using headed bars include straightforward bar replacement, reduced development length and congestion, simplified concrete placement, flexible design options, faster installation, and minimal detailing requirements.

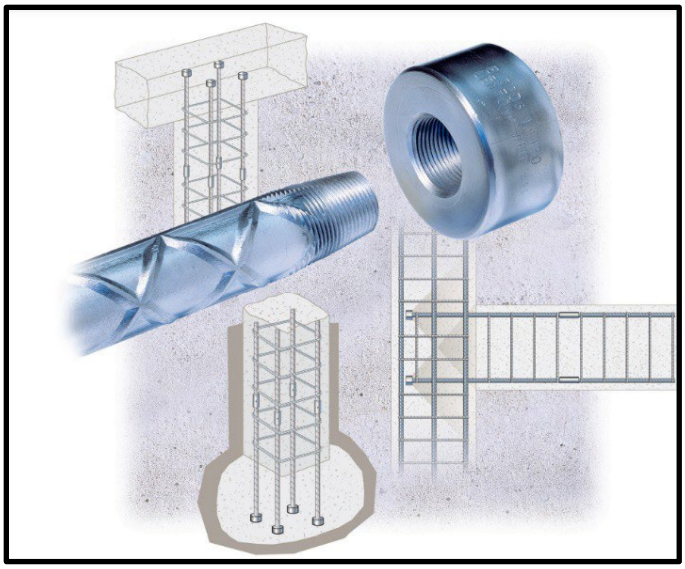

Figure 4.2. Headed Rebars[17]

While the AASHTO (2020) specifications include provisions for using mechanical anchorages in rebars, they do not specifically address the use of headed rebars. However, according to ACI (318-19), headed rebars, illustrated in Figure 4.3, can be utilized with certain limitations. These limitations are as follows:

i. the bar size should not exceed No. 11,

ii. the net bearing area of head should be at least 4 times of area of bar,

iii. the concrete should be of normal weight,

iv. the clear cover of the bar should be at least 2 times the diameter of the bar, and

v. the center to center spacing of bars should be at least 3 times the diameter of bar.

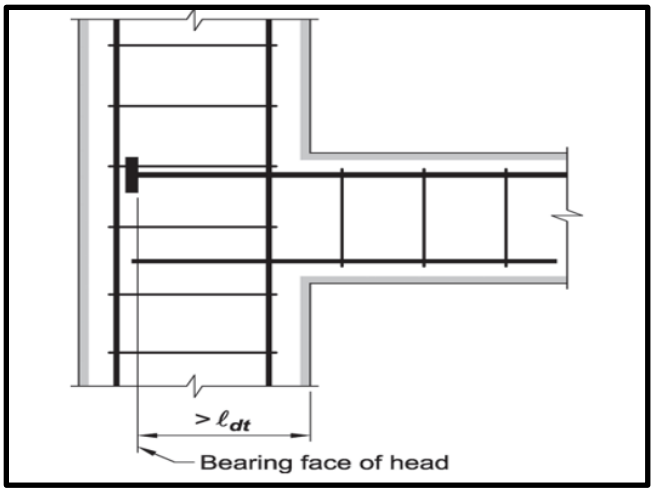

Figure 4.3. Detailing of Headed Rebars[18]

As per Section 25.4.4, the development length of the rebar can be determined by selecting the largest value among the following equations, as given in Eq. (4.6):

$$\text{(a) } L = \left(\frac{f_y \Psi_e \Psi_p \Psi_o \Psi_c}{75\sqrt{f'_c}}\right) {d_b}^{1.5} \quad \textbf{(4.6)}$$

(b) $8d_b$

(c) 6in

where, Ψ_e is Epoxy modification factor, Ψ_p is Parallel tie reinforcement factor, Ψ_o is Location factor, and Ψ_c is concrete strength factor and values are given in Table 25.4.2.5 of ACI.

4.1.3 Current AASHTO LRFD (2020) Design Provisions For Shear Studs

According to Section 6.4.4, welded stud shear connectors should meet all relevant requirements specified in the AASHTO/AWS D1.5M/D1.5 Bridge Welding Code. Additionally, they should have a minimum specified yield strength of 50.0 ksi and a minimum specified tensile strength of 60.0 ksi. These shear connectors should allow for thorough compaction of concrete to ensure full contact with all surfaces. Furthermore, the studs should be able to withstand horizontal and vertical movement between the concrete and steel. In Section 6.10.10.4.3, the nominal shear

resistance of a single stud shear connector is determined using Eq.(4.7).

$$Q_n = 0.5 * A_{sc} * \sqrt{f'c * E_c} \leq A_{sc} * F_u \quad \textbf{(4.7)}$$

where, A_{sc} is cross-sectional area of a stud shear connector (in^2), Ec is modulus of elasticity concrete (ksi), and Fu is specified minimum tensile strength of a stud shear connector (ksi)

Size of shear studs

As per Section 6.10.10.1.1 of AASHTO, the ratio of the height (H) to the diameter (d_{sc}) of a stud shear connector should be equal to or greater than 4.0.

Spacing of shear studs

Shear stud connectors should be spaced at a minimum distance of 4.0 stud diameters ($4d_{sc}$) center-to-center in a direction transverse to the longitudinal axis of the supporting member.

4.2 Design methodology

4.2.1 Connection between pile and foundation/bent cap

The connection design was based on the AASHTO LRFD Bridge Design Specification (AASHTO, 2015), AISC Steel Design Manual (AISC, 2010), and Caltrans Seismic Design Criteria (SDC, 2013), which governs bridge design in California. After conducting experimental programs and numerical analysis, as discussed in Section 2.2.1 (for the connection with the foundation) and Section 2.3.1 (for the connection with the bent cap), Caltrans developed a design process for the connection between CFST columns and the reinforced concrete bent cap, as outlined below:

1. The first step involved determining the factored load demands, including axial, bending, and shear forces, acting on the columns.
2. An initial estimation of the column diameter (D) and tube thickness (t) was performed to achieve a suitable D/t ratio ranging between 80 and 100. This ratio was chosen to ensure

that the column can sustain the axial load while maintaining a range of $0.1 < P/P_o < 0.2$ for the full loading spectrum.

3. The effective stiffness of the column was calculated using the guidelines provided by AASHTO.
4. By utilizing the effective stiffness, the moment magnification factor for the column was calculated.
5. The moment was amplified by the calculated magnification factor.
6. The required combinations of M_n (nominal moment capacity) and P_n (nominal compressive strength) were determined for each load case, representing M_u/ϕ (design moment capacity) and P_u/ϕ (design compressive strength). Here, the value of ϕ is taken as 0.75 for most live loads and 1.0 for seismic loads.
7. The P-M interaction curve was computed.
8. After completing all of these steps, the demands and capacities were compared, and the geometry of the column was finalized.
9. The annular ring was welded to the tube using complete joint penetration welds or fillet welds on both the inside and outside of the column. The full-strength connection was designed to ensure proper anchorage for stress transfer. The ring was made of steel with the same thickness and similar yield stress as the steel tube. To ensure adequate anchorage, the ring extended 16 times the tube thickness outside and 8 times the tube thickness inside the tube in the case of the foundation. However, in the bent cap, it extended 8 times the tube thickness both inside and outside. The size of the fillet weld should be sufficient to resist the tensile strength of the steel tubes, which was calculated using Eq. (4.8).

$$w \geq \frac{1.31tF_u}{F_{exx}} \quad \textbf{(4.8)}$$

where, t is thickness of steel tube, F_u is minimum tensile strength of steel tube, F_{exx} is minimum tensile strength of weld metal

10. For the designed CFST, the embedment depth was calculated based on the equilibrium relationship between the tensile strength of the steel tube and the shear strength of the concrete cone over that specific region (Figure 4.4). The necessary embedment depth, required to transfer the plastic moment capacity of the CFT component in the embedded connection, was derived using a cone pullout model depicted in Figure 4.5. This embedment depth should be sufficient to prevent potential foundation failure, known as conical pullout. The required embedment depth into the cap beam was determined using Eq. (4.9).

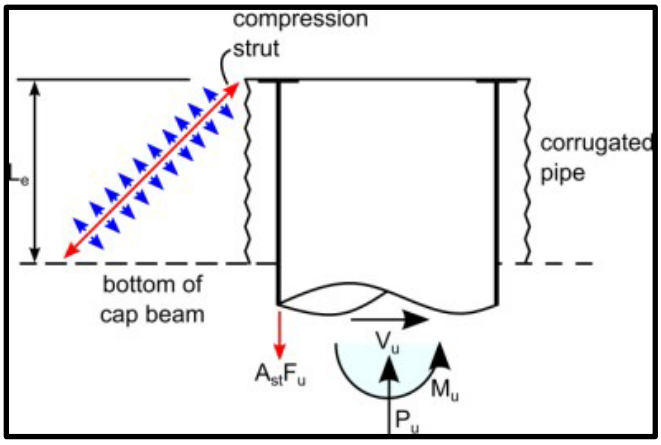

Figure 4.4. Transfer Mechanism for Calculating the Required Embedment Depth of the annular Ring Connection[14]

$$l_e = \sqrt{\frac{{D_o}^2}{4} + \frac{DtF_u}{6\sqrt{f'_c}}} - \frac{D_o}{2} \ (psi) \qquad \textbf{(4.9)}$$

where D_o is the outside diameter of the annular ring, D is the diameter of steel tube, and f'_c is the compressive strength of the foundation concrete in psi

11. The calculation was performed to determine the required concrete depth above or below the embedded CFST in the bent cap or foundation, respectively, to prevent punching shear failure during construction. The provisions outlined in ACI 318 (7) for footings in single shear served as the basis for developing an expression to determine the minimum foundation depth, d_f, necessary to avoid this failure mode. This expression is given in Eq. (4.10).

$$L_{pc} = \sqrt{\frac{D^2}{4} + \frac{C_c + C_s}{n\sqrt{f'_c}}} - \frac{D}{2} - l_e(psi) \quad \textbf{(4.10)}$$

where, the value of n is equal to 4 for the connection with the foundation and 6 for the connection with the bent cap. L_{pc} represents the depth above the embedded tube, and d_f represents the total sum of L_{pc} and l_e. C_c and C_s denote the compressive forces in the concrete and steel, respectively, resulting from the combined axial load and bending moment. These forces are calculated using the PSDM (Plastic Stress Distribution Method) as illustrated in Figure 4.6.

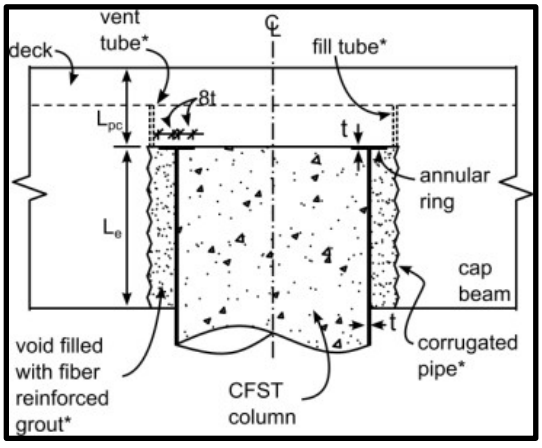

Figure 4.5. Punching shear depth for the connection between CFST and bent cap[14]

Based on the above Eq.(4.10), the punching resistance of the connection was summarized as Eq.(4.11).

$$V = [(L_{pc} + l_e + \frac{D}{2})^2 - \frac{D^2}{4}]n\sqrt{f'_c} \quad \textbf{(4.11)}$$

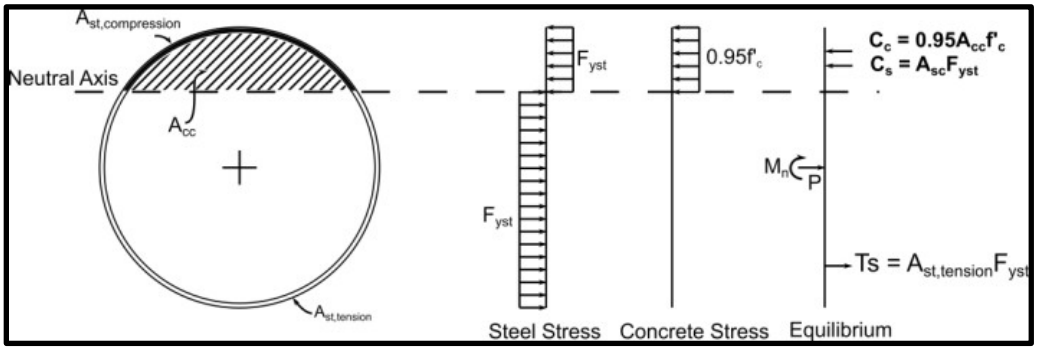

Figure 4.6. PSDM for the calculation of C_s and C_c[14]

12. Based on the aforementioned calculation, the depth of the foundation or beam cap was finalized.
13. Lastly, the cap beam was designed to accommodate the plastic moment capacity of the CFST. For the full-strength connection, the flexural capacity of the beam cap should exceed 1.25 times the plastic moment capacity of the CFSTs.

4.2.2 Punching resistance of CFSTs embedded inside the foundation

The punching resistance was calculated using three different codes: i) GB 50010-2010, ii) ACI 318-19, and iii) Eurocode 2. The results of these calculations, along with the findings from the experimental programs, are discussed in Section 2.2.2.

According to GB 50010–2010, the shear cone develops in a 45^0 direction towards the critical section, with the critical section's edge located h_o away from the column edge. Here, h_o is defined as the effective depth of the foundation, as shown in Figure 4.7(a). The punching resistance

is determined at the control perimeter, which is located at a distance of $0.5h_o$ from the column edge. The punching resistance of the connection is expressed by Eq. (4.12) and Eq. (4.13).

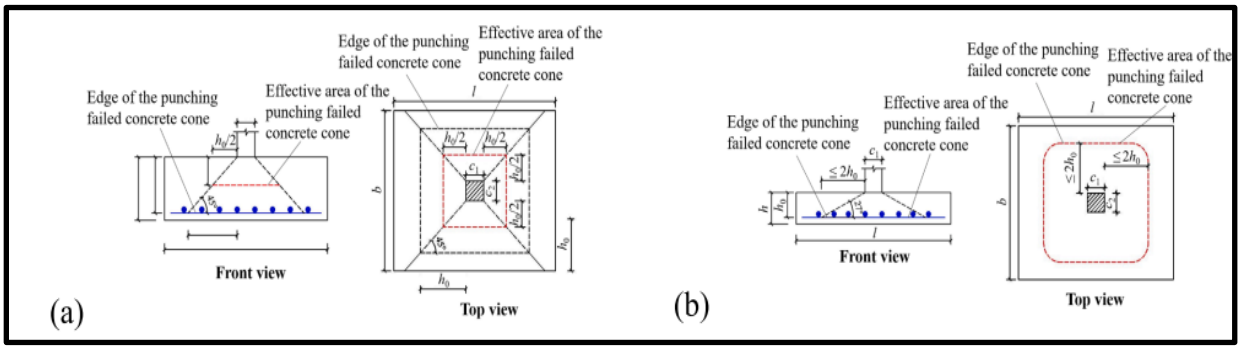

Figure 4.7. Critical punching section, According to (a) GB 50010-2010, and ACI 318-19, (b) Eurocode 2[13]

$$V = 0.5f_t \eta b_o h_o + 0.8f_y A_s \tag{4.12}$$

$$\eta = min(0.4 + 1.2/\beta_s, 0.5 + \alpha_s h_o/4b_o) \tag{4.13}$$

where, f_t is the tensile strength of the concrete, f_y is the yield stress of stirrups, b_o is the perimeter of the critical section, A_s is the area of stirrups, β_s is the length ratio of loading area, α_s is the coefficient of position for column

According to ACI, the assumption for the formation of a shear cone is similar to that of the previous code, as illustrated in Figure 4.7(a). The punching resistance of the connection is defined by equations Eq. (4.14) to Eq. (4.16).

$$V = 0.5V_c + f_y A_s \tag{4.14}$$

$$V_T \leq 6\sqrt{f'_c} b_o h_o \tag{4.15}$$

$$V_c = min\ of \begin{cases} \left(2 + \dfrac{4}{\beta s}\right)\lambda\sqrt{f'_c} * b_o * h_o \\ (2 + \dfrac{\alpha s * d}{u_m})\lambda\sqrt{f'_c} * b_o * h_o \\ 4\lambda\sqrt{f'_c} * b_o * h_o \end{cases} \tag{4.16}$$

where, λ is the coefficient of concrete density

According to Eurocode 2, unlike the previous two codes, the shear cone develops in an approximately 20^0 angles towards the critical section, which is located at a distance of h_o from the column edge. Similarly, the critical perimeter is defined within $2.0h_o$ from the column edge, as shown in Figure 4.7(b). The punching resistance is described by equations Eq. (4.17) to Eq. (4.22).

$$V = 0.75V_c + V_p \quad \textbf{(4.17)}$$

$$V_c = V_{Rd,c} h_o b_o \quad \textbf{(4.18)}$$

$$V_p = 1.5(h_o/s_r)A_s f_y sin\alpha \quad \textbf{(4.19)}$$

$$V_{Rd,c} = C_{Rd,c} k(100\rho * f'_c)^{1/3} \quad \textbf{(4.20)}$$

$$C_{Rd,c} = \frac{0.18}{\Upsilon_c} \quad \textbf{(4.21)}$$

$$K = min(2.1 + \sqrt{200/h_o}) \quad \textbf{(4.22)}$$

where, ρ is the flexural reinforcement ratio, Υ_c is the partial coefficient for concrete and the units are in SI system

Since these design codes did not account for the bonding strength and shear resistance offered by studs, the calculated values were significantly different from the experimental results, as illustrated in Figure 2.16. As a result, a new empirical formula was developed based on GB 50010-2010, which includes the contribution of bond strength and shear studs. This formula is explained in Eq. (4.23) to Eq.(4.26). Considerations were made to ensure that the calculated results fell within the range of experimental results. Specifically, the parameter h_o was adjusted differently based on the contribution of shear studs, as depicted in Figure 4.8.

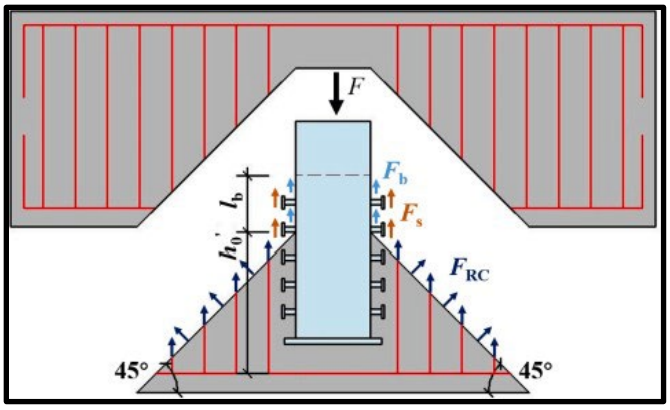

Figure 4.8. Illustration of calculation principles for punching shear resistance[13]

The bond stress between the outside of the steel tube and the concrete contributes to the punching resistance, which is expressed in Eq. (4.23). Similarly, the contribution of shear studs and the RC foundation is presented in Eq. (4.24) and Eq. (4.25), and Eq. (4.26), respectively.

$$F_b = \tau_u \pi D l_b \tag{4.23}$$

$$F_o = min\,\{0.43 A_s \sqrt{Ec * f'c}, 0.7 A_{ss} f_u \tag{4.24}$$

$$F_s = \sum_{i=1}^{n} F_{si} \tag{4.25}$$

$$F_{RC} = 0.5 f_t \eta b_o h'_o + 0.8 f_y A_s \tag{4.26}$$

where, F_b represents the bond force and τ_u denotes the bond stress, which was determined to be 1.1 MPa. l_b refers to the effective length of bonding, while F_o, A_{ss}, and f_u represent the ultimate shear resistance, cross-sectional area, and tensile strength of a single shear stud, respectively. F_{si} represents the shear force of the i^{th} row of shear studs, and n denotes the number of rows of studs above the critical section

Finally, the total punching resistance provided by the connection was calculated by summing Eq. (4.23), Eq. (4.25), and Eq. (4.26). The result, as shown in Figure 2.17, indicated that

the bond strength between the concrete-filled steel tube and the surrounding concrete, as well as the shear resistance provided by the shear studs, should also be taken into account when calculating the punching resistance of such connections.

4.2.3 Punching resistance of column to reinforced concrete bent cap

The provisions of the ACI 318-14 code and the AASHTO LRFD Bridge Design specifications include calculations for punching shear resistance. The 2012 AASHTO LRFD specifications and the ACI 318-14 code provide methods to calculate the punching shear strength of footings for reinforced concrete (RC) columns. However, no code specifically addresses the design methods for RC footings for CFST columns. In this paper, the design requirements are based on the provisions of the AASHTO LRFD Bridge Design specifications and the ACI 318-14 code. The results, considering both the codes and the experimental programs, are discussed in Section 2.3.2.

In the 2012 AASHTO LRFD code, the punching resistance (V_c) for two-way shear action without shear reinforcement is given by Eq. (4.27). For two-way action with shear reinforcement, it is expressed in Eq. (4.28). Additionally, the ACI 318-14 code provided an additional restraint for punching capacity, which is given by Eq. (4.29). Similarly, for two-way action with shear studs, the punching resistance inside the shear reinforced zone is calculated using Eq. (4.30).

$$V_c = \Phi 2\left(1 + \frac{2}{\beta_c}\right)\sqrt{f'_c}\, b_o d_v \leq \Phi 4\sqrt{f'_c}\, b_o d_v \tag{4.27}$$

$$V_c = \Phi\left(2\sqrt{f'_c} b_o d_v + \frac{f_y A_v d_v}{s}\right) \leq \Phi 6\sqrt{f'_c}\, b_o d_v \tag{4.28}$$

$$V_c = \Phi\left(\frac{\alpha_s d_v}{b_o} + 2\right)\sqrt{f'_c} b_o d_v \tag{4.29}$$

$$V_c = \Phi\left(3\sqrt{f'_c}b_o d_v + \frac{f_y A_v d_v}{s}\right) \leq \Phi 8\sqrt{f'_c}\, b_o d_v \quad \textbf{(4.30)}$$

b_o represents the perimeter of the critical section located at a distance of $0.5d_v$ from the column face. d_v refers to the effective shear depth of the footings. ϕ represents the strength reduction factor. α_s is a parameter with values of 40 for interior columns, 30 for edge columns, and 20 for corner columns. c represents the ratio of the long side of the column to the short side of the column. s denotes the spacing of the peripheral lines of shear reinforcement in the direction perpendicular to the column face.

Some initial assumptions were made for the calculation of punching strength. The strength reduction factor, ϕ, was assumed to be 1.0. Annular rings welded on top of the column were used to increase the perimeter of the critical section for punching shear. For PC2, U-shaped bars in the long direction were considered. For PC3 and PC4, U-shaped bars in both the long and short directions were considered. For PC5, contributions of double-headed shear bars were considered. The effective shear depth, d_v, was determined as the distance from the end annular ring to the centroid of the tension reinforcement. Since the column was considered to be interior, α_s was taken as 40. The critical section for a circular column was permitted to be defined assuming a square column with an equivalent area. The calculation of the critical section was based on Figure 4.9.

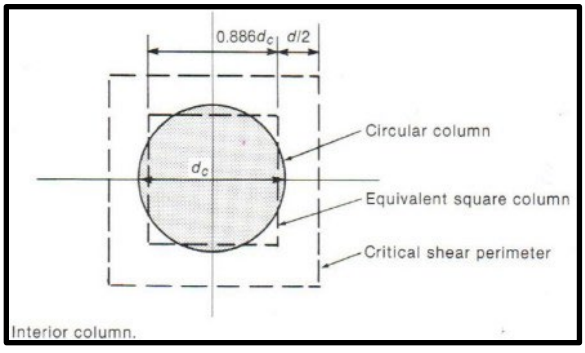

where, dc= D, d= d_v, and b_0= 4*(0.886*D+d_v)

Figure 4.9. Conversion of circular column to equivalent square column[15]

Table 4.1 demonstrates that the calculation methods prescribed by the code were insufficient to yield accurate results. In this paper, empirical formulas were derived by incorporating the AASHTO LRFD specification, ACI 318-14 code, and FEA model of specimen 1 to accurately calculate the punching shear resistance of each specimen. The comparison between the test results and the empirical formulas is presented in Table 4.1. These formulas are provided in Eq. (4.31) to Eq. (4.33).

1. Without shear reinforcement

$$V = \Phi\,[2\sqrt{f'_c}\,b_o d_v + 12\sqrt{f'_c}\pi D\,L_e(\frac{d_v}{L_e})^{0.5}] \quad \textbf{(4.31)}$$

2. With shear reinforcement

   a. Stirrups

$$V = \Phi\,[2\sqrt{f'_c}\,b_o d_v + 0.8\frac{f_y A_v d_v}{s} + 12\sqrt{f'_c}\pi D L_e(\frac{d_v}{L_e})^{0.5}] \quad \textbf{(4.32)}$$

   b. Double headed shear reinforcement

$$Vc = \Phi\,[3\sqrt{f'_c}b_o d_v + 0.8\frac{f_y A_v d_v}{s} + 12\sqrt{f'_c}\pi D L_e(\frac{d_v}{L_e})^{0.5}] \quad \textbf{(4.33)}$$

Based on the study, the following conclusions were drawn: i) The incorporation of shear studs and face annular rings with appropriate embedment significantly enhanced the punching shear resistance of the embedded CFSTs in the RC cap. ii) The contribution of the embedded CFSTs should be considered when calculating punching shear resistance. iii) The calculations based on AASTHO and ACI design codes for embedded CFSTs were insufficient, as they did not consider the bond strength. iv) The bond between the steel tube and the concrete in the concrete cap played a crucial role in the punching resistance.

4.3 Comparison of design methodologies

Different papers discussed various design procedures for determining the punching strength of the connection. To assess the effectiveness of these methodologies and existing design codes, the punching resistance was evaluated using experimental programs from two research studies mentioned in Sections 2.2.2 and 2.3.2, respectively. To establish a suitable design process, these methodologies were interpreted and presented based on fundamental principles and understanding.

Table 4.1 presents a comparison between the design procedures provided by existing design codes and the developed empirical formulas. It also includes the evaluation of the ratio between the test results and the predicted results based on different proposed formulas. Values less than 1 indicate that the predicted result was lower than the actual result, while values greater than 1 indicate that the predicted result was higher than the actual result.

4.3.1 Conclusion

As shown in Table 4.1, the calculated values did not align with the experimental values. The discrepancies can be attributed to the limitations in considering the embedded CFSTs. The design codes failed to account for the contributions of bond strength and shear studs, resulting in inaccurate predictions. Furthermore, the existing methodologies only considered the contributions of concrete and shear stirrups within the shear depth of the cap. The design approach proposed by Washington University solely focused on the contribution of concrete within the effective depth of the cap. Similarly, the other two studies considered both the contribution of shear studs and bond strength, yet the results still deviated from the experimental values.

An improved empirical formula needs to be developed to accurately calculate the performance of embedded large diameter steel piles and bent cap connections. This formula should

consider the significant contributions of concrete, stirrups, bond strength, and shear studs to provide more accurate results.

4.4 Proposed Design Method

The proposed connection between large diameter steel pipe piles and reinforced concrete bent cap should be designed as an over-strength connection that can withstand punching failure, pullout failure, and lateral moment. Therefore, it is essential to calculate the strength of the connection before proceeding with the design. Empirical formulas were developed to calculate the punching strength, pullout strength, and moment capacity of the connections, considering the specifications of the AASHTO LRFD bridge design, ACI 318 building code, AISC steel manual, and the studies mentioned above. The required strengths are summarized below:

Table 4.1: Comparison of design methodologies for punching resistance based on different studies carried out

Specimens (2.3.2)	Test I kips	Design codes (ACI) (Eq.(4.27)-Eq.(4.30)) II kips	CFST and Foundation (D. E. Lehman et. al) (Eq.(4.10)) III kips	CFST and Bent cap (D. E. Lehman et.al.) (Eq.(4.10)) IV kips	Embedded column base in CFST (S.Tan et.al.) (Eq.(4.23)-Eq.(4.26)) V kips	CFSts to RC pile cap (X. Li et.al.) (Eq.(4.31)-Eq.(4.33)) VI kips	Test/Prediction				
							I/II	I/III	I/IV	I/V	I/VI
PC1	139.9	59.49	105.11	156.44	79.82	144.08	2.35	1.33	0.89	1.75	0.97
PC2	265.5	169.04	102.26	152.20	210.90	269.70	1.57	2.60	1.74	1.26	0.98
PC3	411.8	404.25	103.62	154.22	482.52	481.53	1.02	3.97	2.67	0.85	0.86
PC4	481.5	413.03	209.63	308.49	385.37	505.54	1.17	2.30	1.56	1.25	0.95
PC5	258.8	85.97	100.26	149.22	190.50	263.92	3.01	2.58	1.73	1.36	0.98
Average							1.82	2.56	1.72	1.29	0.95
Specimens (2.2.2)	I	GB 50010-2010 (Eq.(4.12)-Eq.(4.13)) II	III	IV	V	VI	I/II	I/III	I/IV	I/V	I/VI
P-900/P-500	64.13	20.69	79.89	117.66	53.36	95.23	3.10	0.80	0.55	1.20	0.67
P-SD-10-3-50-I/II	161.1	24.05	79.89	117.66	238.76	98.59	6.70	2.02	1.37	0.67	1.63
P-SD-10-3-100-I/II	137.7	24.05	79.89	117.66	238.76	98.59	5.73	1.72	1.17	0.58	1.40
P-SD-10-5-50-I/II	169.4	24.05	79.89	117.66	219.39	98.59	7.05	2.12	1.44	0.77	1.72
P-SD-16-3-100-I/II	172.1	24.05	79.89	117.66	273.79	98.59	7.16	2.15	1.46	0.63	1.75
Average							5.95	1.76	1.20	0.77	1.43

4.4.1 Punching Strength

In the connection between a bent cap and piles, punching resistance refers to the ability of the connection to withstand concentrated loads and resist the formation of shear failures or cracks around the point of load application. It specifically relates to the capacity of the connection to resist the punching shear forces that act perpendicular to the plane of the connection.

Punching resistance is crucial to ensure the structural integrity and safety of the connection. It is influenced by several factors, including the strength of the concrete, the presence of shear reinforcement (such as stirrups or shear studs), and the bond strength between the piles and the concrete.

Accurate evaluation and consideration of punching resistance ensure that the connection between the bent cap and piles can effectively resist the applied loads and maintain the structural integrity and stability of the entire system. Therefore, the development of an empirical formula to accurately calculate the punching strength of the connection becomes essential. The punching strength was determined by considering the contributions of concrete strength, shear reinforcement, and bond strength which is summarized below:

Contribution of concrete(V_c)

The calculation of punching strength was based on the provision in ACI 318-19 for one-way shear strength of non-prestressed members, as described in Section 22.5. According to Section 22.5.5.1.1, the contribution of concrete is limited by the value specified in Eq. (4.34). The critical section for one-way shear is depicted in Figure 4.10, where the width (b_w) was taken as the sum of L_{pc} and D_o, and d was equal to L_{pc}. An n factor can be considered as 2 for the contribution of concrete on both sides of the critical section. In the empirical formula, a factor of $5n$ was assumed

to be 7. With these assumptions, Eq. (4.34) was modified as Eq. (4.35) to express the contribution of concrete for shear resistance.

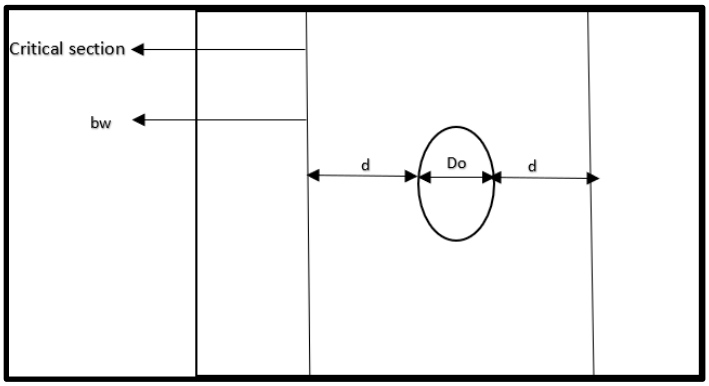

Figure 4.10. Critical section due to one way shear

$$V_c = 5n\sqrt{f'c} * b_w * d \quad \textbf{(4.34)}$$

$$V_c = 7\sqrt{f'c} * ((L_{pc} + \frac{Do}{2})^2 - \frac{Do^2}{4}) \quad \textbf{(4.35)}$$

Contribution of reinforcement

a) Stirrups(V_s)

The stirrups in the bent cap serve the purpose of carrying the vertical shear force and preventing diagonal shear cracks. Additionally, these stirrups play a role in enhancing the punching resistance of the connection. According to Section 22.5.8.5.3 of ACI 318-19, the contribution of stirrups can be calculated using Eq.(4.36).

$$V_s = f_y * A_v * \frac{L_{pc}}{s} \quad \textbf{(4.36)}$$

b) Shear studs(V_{ss})

Shear studs are essential shear connectors used to facilitate the transfer of forces between steel and concrete in composite sections. In accordance with Section 6.10.10.4.3 of AASHTO LRFD Bridge Design Specification, the nominal shear resistance of a single

shear stud connector can be determined using Eq. (4.7). The total resistance provided by the shear studs welded on the steel pile (V_{ss}) was calculated by multiplying Q_n by the total number of studs (n), as shown in Eq. (4.37). It should be noted that only 80% of the total strength was considered, as not all the studs yield during their service.

$$V_{ss} = 0.8n * Q_n \quad \textbf{(4.37)}$$

Where, A_{sc} is cross-sectional area of a stud shear connector (in^2), E_c is modulus of elasticity concrete (ksi), and F_u is specified minimum tensile strength of a stud shear connector (ksi)

Contribution of bond length(V_b)

The bond stress between the outside of the steel pipe pile and the surrounding concrete was considered a contributing factor to the punching resistance of the connection. In accordance with Section I6 (3c) of the AISC specification (AISC, 2016), which addresses force transfer in a filled composite member through direct bond interaction, the available bond strength between the steel and concrete should be determined. This bond strength is represented by Eq. (4.38). The critical section resulting from the bond stress is illustrated in Figure 4.11.

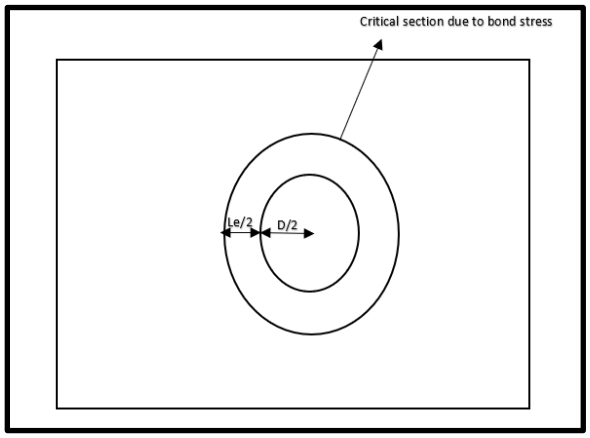

Figure 4.11. Proposed critical section due to bond stress

$$V_b = P_b L_{in} F_{in} \quad \textbf{(4.38)}$$

Where, the nominal bond stress (F_{in}) is calculated as $30t/D^2 \leq 0.2$ ksi, L_{in} is equal to the effective embedment length (l_e), and P_b represents the perimeter of the steel-concrete bond interface at the critical section.

The punching resistance offered by the bond stress between the steel pipe and concrete is represented by Eq.(4.39).

$$V_b = 0.5\pi(D + L_e)F_{in}L_e \quad \textbf{(4.39)}$$

The total punching resistance (V_p) was calculated by summing up the contributions from Eq. (4.35), Eq. (4.36), Eq. (4.37), and Eq. (4.39), and it is summarized in Eq. (4.40).

$$V_p = V_c + V_s + V_{ss} + V_b \quad \textbf{(4.40)}$$

4.4.2 Calculation of punching strength

The punching strength of the specimens used in the experimental programs of the studies discussed above was calculated using the proposed formulas. Table 4.2 presents the calculation of punching resistance for the connection in study Section 2.2.2 for P specimens and study Section 2.3.2 for PC specimens, respectively. The total punching resistance(V_p) included the contributions from concrete strength (V_c), stirrups(V_s), shear studs(V_{ss}), and bond stress(V_b).

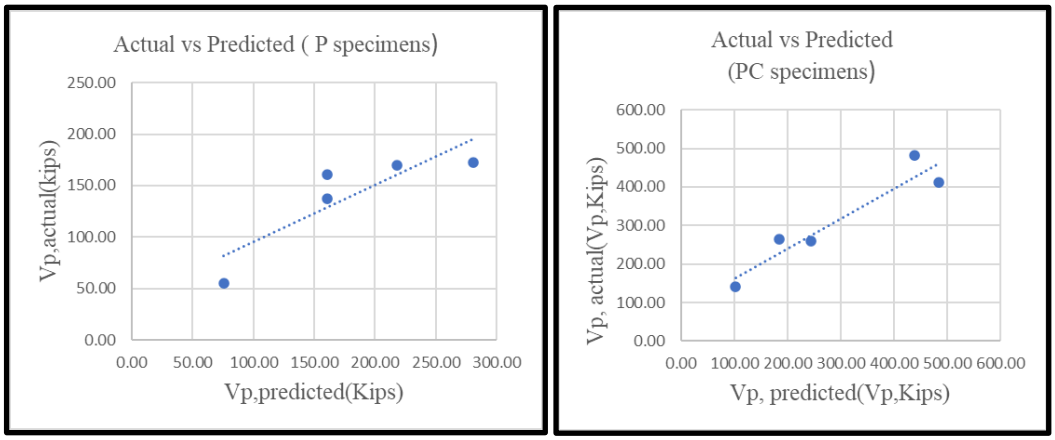

Figure 4.12. Comparison of the predicted and Experimental results; (a) P specimens; (b) PC specimens

The ratio of test results to predicted results based on different proposed formulas was evaluated. Values less than 1 indicated that the predicted result was lower than the actual result, while values greater than 1 indicated that the predicted result was higher than the actual result. Figure 4.12 presents the comparison between the predicted results and the test results. It is evident that the proposed empirical formulas performed well and were closely aligned with the experimental results.

Table 4.2: Calculation of punching resistance based on proposed formulas for paper

Specimens	V_c	V_s	V_{ss}	V_b	Total (V_p) kips	Test (V_p) kips	Ratio
P-900	15.20	4.20	-	56.25	75.65	54.90	1.38
P-SD-10-3-50	15.20	4.20	85.25	56.25	160.90	161.10	1.00
P-SD-10-3-100	15.20	4.20	85.25	56.25	160.90	137.70	1.17
P-SD-10-5-50	15.20	4.20	142.00	56.25	217.65	169.43	1.29
P-SD-16-3-100	15.20	4.20	205.25	56.25	280.90	172.13	1.63
Average							1.29
PC1	28.25	-	-	75.00	103.25	139.95	0.74
PC2	94.14	66.13	-	25.00	185.27	265.50	0.70
PC3	27.85	-	381.94	75.00	484.80	411.75	1.18
PC4	205.90	158.72	-	75.00	439.62	481.50	0.91
PC5	26.95	142.76	-	75.00	244.71	258.75	0.94
Average							0.89

4.4.3 Pullout resistance

In the connection between a bent cap and piles, the pullout resistance refers to the capacity of the connection to resist the upward or horizontal forces that may try to pull the piles out of the bent cap. It is a measure of the ability of the connection to prevent the displacement or failure of the piles due to applied loads or external forces. Therefore, it is necessary to develop an empirical formula that accurately calculates the pullout strength of the connection.

The pullout resistance includes the contributions from the concrete and the stirrups in the connection. The concrete strength plays a significant role in resisting the pullout forces, as the interaction between the piles and the surrounding concrete determines the overall stability and integrity of the connection. Additionally, the presence of stirrups further enhances the pullout resistance by providing additional confinement and preventing the development of cracks or failure in the concrete. The contribution of various factors to the pullout resistance is summarized below:

Contribution of concrete(V_c)

Based on the provisions of ACI 318-19 for one-way shear strength, which is equivalent to punching resistance, the calculation of pullout resistance followed a similar approach. In this case, the parameter b_w was determined by summing the values of l_e and D_o, and the value of d was taken as L_{pc}. Since the contribution of concrete was considered on both sides of the critical section, the value of n is taken as 2. For the empirical formula, a factor of $5n$ was assumed to be 6. Taking all these assumptions into account, Eq. (4.41) is used to express the contribution of concrete in calculating the pullout resistance.

$$V_c = 6\sqrt{f'c} * ((l_e + \frac{Do}{2})^2 - \frac{Do^2}{4}) \quad \textbf{(4.41)}$$

Contribution of stirrups(V_s)

The stirrups that are located within the pullout cone play a significant role in contributing to the pullout resistance of the connection. The calculation of their contribution was similar to that of the punching resistance, and it was determined using the same method. The equation representing this calculation is Eq. (4.42).

$$V_s = f_y * A_v * \frac{l_e}{s} \quad \textbf{(4.42)}$$

The total pullout resistance (V_{po}) was obtained by summing up the contributions from the equations mentioned above. The resulting equation is Eq. (4.43), which summarizes the calculation of the total pullout resistance.

$$V_{po} = V_c + V_s \quad \textbf{(4.43)}$$

4.4.4 Lateral moment resistance

A concrete bent cap is subjected to various loads, including loads from superstructures, dead loads, live loads, and lateral loads. These loads generate a significant moment at the bent cap,

which must be effectively transferred to the ground through steel pipe piles. In the connection between the bent cap and pile, the lateral moment resistance is crucial. It determines the connection's capacity to withstand applied moments or forces that act perpendicular to the longitudinal axis of the pile. The lateral moment resistance assesses the connection's ability to resist rotational or bending forces induced by lateral loads or moments.

The connection should be strong enough to resist the lateral moment subjected to the connection. Since the connection proposed was an overstrength connection, the moment capacity of attachment between the steel pile and bent cap should be greater than the moment demand calculated using AASHTO LRFD Bridge Design Provisions (AASHTO, 2020) at the point of connection. The proposed connection must be strong enough to withstand the moment loads to ensure the sustainability and structural integrity of the bridge.

Chapter 5 COMPARISON OF STEEL PIPE PILE TO CONVENTIONAL PILE OPTIONS

This chapter focuses on the utilization of large diameter steel pipe piles as replacements for RC drilled shaft piles and HP-piles. The analysis and design of these various pile types considered for use by ALDOT are included herein. Furthermore, the chapter delves into the rationale behind selecting steel pipe piles as a superior alternative to existing options.

5.1 Analysis of bent cap with drilled shaft bridges

The design details were derived from a general bridge with drilled shafts (refer to APPENDIX I) commonly used by ALDOT. The drawings of this particular bridge were utilized as a reference for analyzing the bridge and calculating the load demands.

The typical elevation of the bridge, as shown in Figure 5.1, had a length of 40 ft., and included rail barriers on both sides. A 7 in. thick slab was present, supported by six equally spaced beams in each span. Additionally, there were two drilled shafts located 24 ft. apart from each other, center-to-center.

5.1.1 Calculation of load demands in bent cap

The connection between the steel pipe pile and bent cap must possess sufficient strength to effectively transfer the load demands from the bent cap to the pile connection. It is imperative to have a full-strength or overstrength design that is developed in accordance with the capacity of the pile or the load demand, respectively. However, considering the significantly high capacity of the proposed pile, the connections were designed based on the load demands exerted on top of the pile.

The load demands on the bent cap were calculated using the analysis and design tool used by the Florida Department of Transportation (FDOT) [19] . This tool is based on the Structural Design Guidelines of Florida [20] , which adhere to the AASHTO LRFD standards. FDOT has developed a comprehensive flowchart for the design of the bent cap, encompassing the load generator, frame analysis, and design of the bent cap. The details of these components are discussed below.

5.1.1.1 Load generator

The initial step in the process involved calculating various loads, including dead load, live load, braking load, centrifugal force load, wind load, and wind load on live load, applied to the bridge structures. Certain fundamental assumptions were made during this calculation process, which is summarized below:

1. Bridge beams should be simply supported.
2. The cap should be symmetrical.
3. Uniform spacing should be maintained between beam and column.
4. While the span lengths may vary, the number of beams in each span should remain the same.
5. WA and TU loads should not be considered.
6. Eccentric loading resulting in torsional forces (due to live load and dead load on unequal span) on cap should not be considered.
7. Live load distribution to beams should be determined using lever rule.

These assumptions established a basis for the subsequent design and analysis of the bridge components.

The load generator utilized basic geometric parameters obtained from drawings provided by ALDOT, as shown in APPENDIX I. A general description of the load parameters is presented in Table A.1, which includes DC, DW, BR, CE, WS, WL, WA, LL, and TU. BR loads are applied to the superstructure and subsequently transferred to the substructure. The total load is distributed to bent caps based on superstructure continuity and the relative stiffness of the bent cap. This distribution was calculated using the bridge's length, typically the length of the continuous deck. For CE, the maximum specified design speed of 70 mph from the AASHTO publication, "A Policy on Geometric Design of Highways and Streets," [21] was conservatively selected. The design wind speed was determined using the ASCE 7 Hazard tool [22] . WS was then calculated based on the design wind speed and bridge structure's elevation. The miscellaneous dead load was estimated based on the Structural Design Guidelines of Florida [20].

Section 3.4.1 and Table 3.4.1-1 of the AASHTO LRFD Bridge Design Specifications (AASHTO, 2020) outline various load factors and load combinations, along with 13 limit states. These load combinations encompass 5 related to strength limits, 2 for extreme events such as earthquakes, 4 for service limits associated with prestressed concrete elements, and 2 for fatigue limits. Among these limit states, Strength-III was the most applicable for the analysis of the bent cap, considering the bridge's location exposed to a design speed of 105 mph. A general description of load combinations and load factors specific to Strength-III limit state is provided in Table A.2. It is important to note that vehicles become unstable at higher wind velocities, which effectively prevents the presence of significant live load on the bridge. Additionally, WA was not considered since the flood elevation was below the bottom of the bent cap. Furthermore, TU was assumed to be 0 for the analysis.

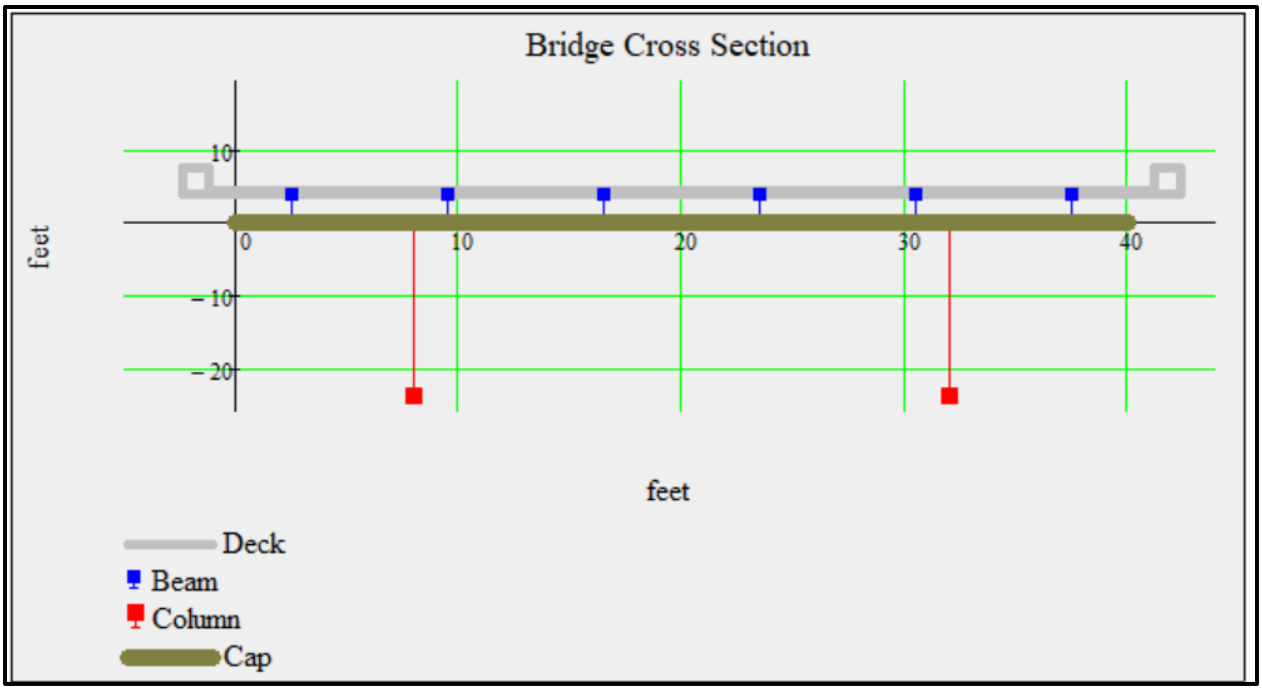

Figure 5.1. Cross section of bridge at Cedar Creek Station

After entering the input parameters to the load generator tool, the factored loads applied were calculated as follows: a wind load of 41 kips applied parallel to the bent cap, a wind load of 17 kips applied perpendicular to the bent cap, a self-weight of the cap of 3.42 klf, and a vertical superstructure load of 135.3 kips per beam line. The corresponding loads used for each load type is summarized in Table A.3.

5.1.1.2 Frame Analysis

The analysis of the bent cap aimed to determine the load demands, which were crucial for designing the connection between the pile cap and the proposed piles. Several basic assumptions were made during this process, and they are explained below.

1. Pile to bent cap connections were fixed.

2. Beam loads were applied to the bent cap as a distributed line load (length of bearing pad + 2 * height of pedestal by default).
3. Full gross section stiffness of all bent-cap components was used for a simplified and conservative analysis.

The load generated from the first step was utilized to analyze the bent cap. Following the analysis, the envelope derived from the Strength-III limit state was used to calculate the load demands at bent cap and top of the piles. Figure 5.2 and Figure 5.3 depict the shear diagram and moment diagram, respectively, which illustrate the shear demand (V_{ub}) of 345 kips and flexural demand (M_{ub}) of 1266 kips-ft in the bent cap. The asymmetrical figures observed were a consequence of the asymmetric wind loads applied at the end of the bent cap. These loads were subsequently resolved into vertical, longitudinal, and transverse components resulting in asymmetric load demands along the length. The analysis also revealed the axial demand (P_{up}) and flexural demand (M_{up}) at the top of the pile, which were determined to be 530 kips and 292 kips-ft, respectively. Additionally, the shear demand for the pile in both the longitudinal (V_{upx}) and transverse (V_{upz}) directions of the bent cap was calculated to be 21 kips and 9 kips, respectively.

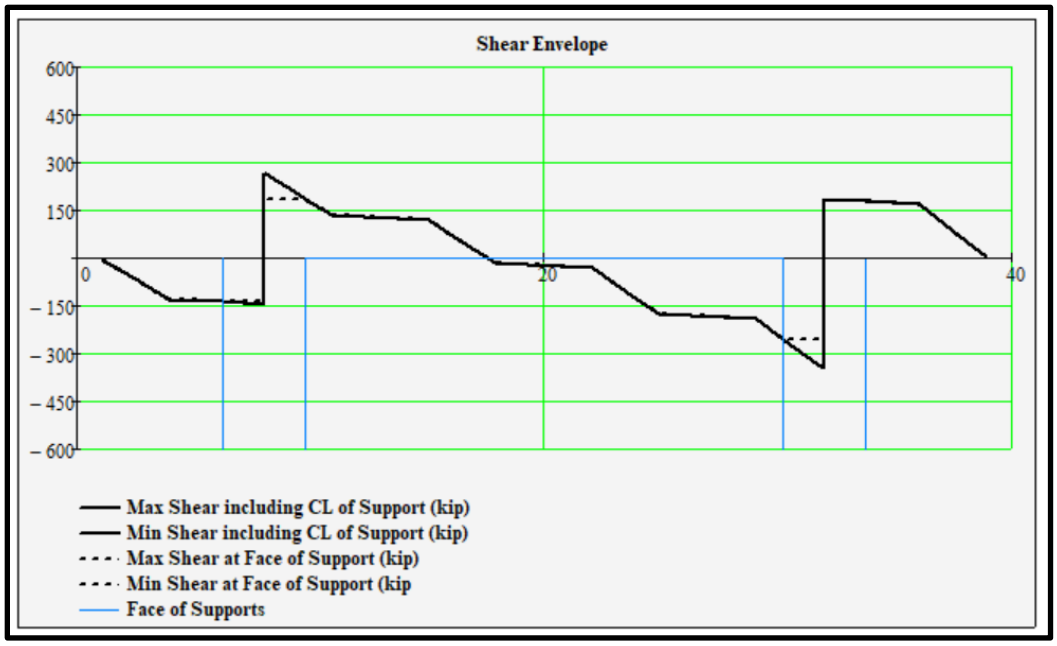

Figure 5.2. Shear Diagram of bent cap with drilled shafts

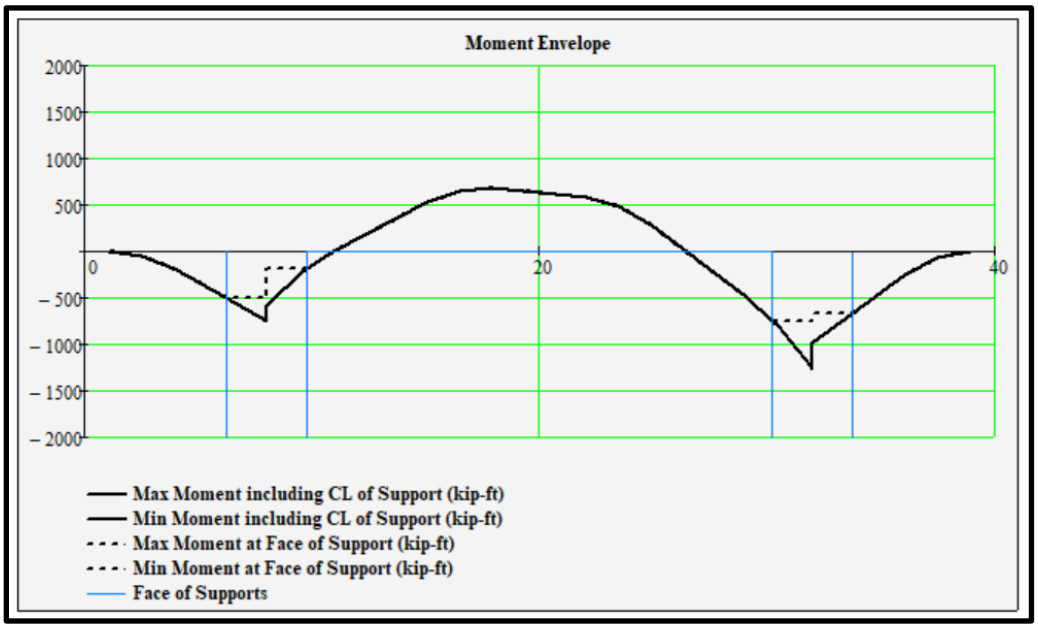

Figure 5.3. Moment diagram of bent cap with drilled shafts

5.2 Analysis of bent cap with HP-Piles

The design details for the HP-piles were also adopted from the same bridge with drilled shafts (APPENDIX I) used by ALDOT. However, in this case, the two shafts were replaced with

six HP-piles, with each girder supported directly above a single pile. The drawings of the reference bridge were utilized to determine the load demands and calculate the dimensions of the piles and bent cap, as well as the reinforcement details for the bent cap.

The typical elevation of the bridge, illustrated in Figure 5.4, spanned a length of 40 ft. and included rail barriers on both sides. Supporting the structure was a 7 in. thick slab, which rested on six equally spaced beams in each span. In contrast to the previous case, where two drilled shafts were utilized, the current design featured six piles placed at a center-to-center spacing of 7 ft. Since placing the piles below the girders typically leads to a smaller bent cap, a preliminary assumption was made for a trapezoidal bent cap, which was also used in the study by Marshall et. al.[5] as a representative bridge with HP-piles. The base of the bent cap was assumed to have a smaller width of 2 ft., a larger width of 3 ft., and a height of 2 ft.

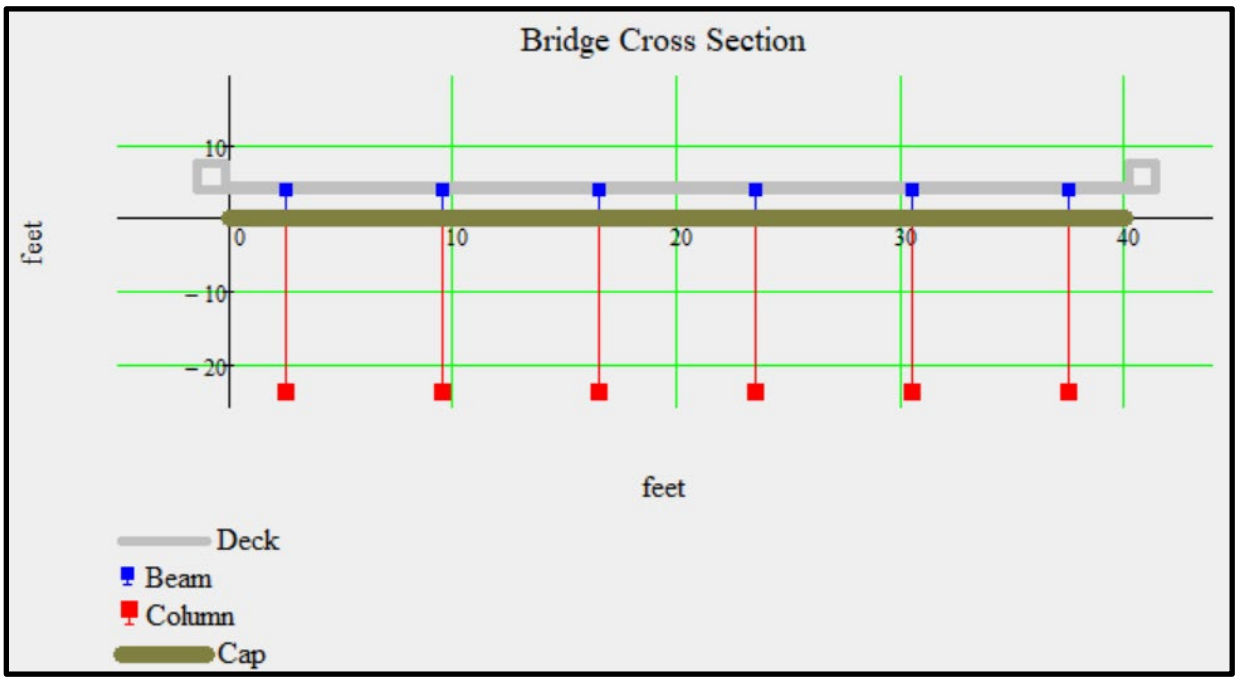

Figure 5.4. Typical cross section of bridge with HP-piles

5.2.1 Calculation of load demands on bent cap

Similar to the analysis conducted for drilled shafts, a series of steps were followed to determine the load exerted on the bent cap due to various factors, including dead load, live load, and wind load. The loading conditions were comparable to those of the previous case, making Strength-III limit state the most appropriate for the bent cap analysis. After running the load generator tool, the factored loads were computed. The wind load applied parallel to the cap was 41 kips, the perpendicular load was 17 kips, the self-weight of the cap was 0.98 klf, and the vertical superstructure load from each beam line was 135.3 kips, which are also summarized in Table A.3.

The load generated from the first step was utilized to analyze the bent cap. Following the analysis, the envelope derived from the Strength-III limit state was used to calculate the load demands at bent cap and the pile tip. Figure 5.5 and Figure 5.6 depict the shear diagram and moment diagram, respectively, which illustrate the shear demand (V_{ub}) of 98 kips and flexural demand (M_{ub}) of 138 kips-ft on the bent cap. The analysis also revealed the axial demand (P_{up}) and flexural demand (M_{up}) at the tip of the pile, which were determined to be 179 kips and 81 kips-ft, respectively. Additionally, the shear demand for the pile in both the longitudinal (V_{upx}) and transverse (V_{upz}) directions of the bent cap was calculated to be 7 kips and 3 kips, respectively.

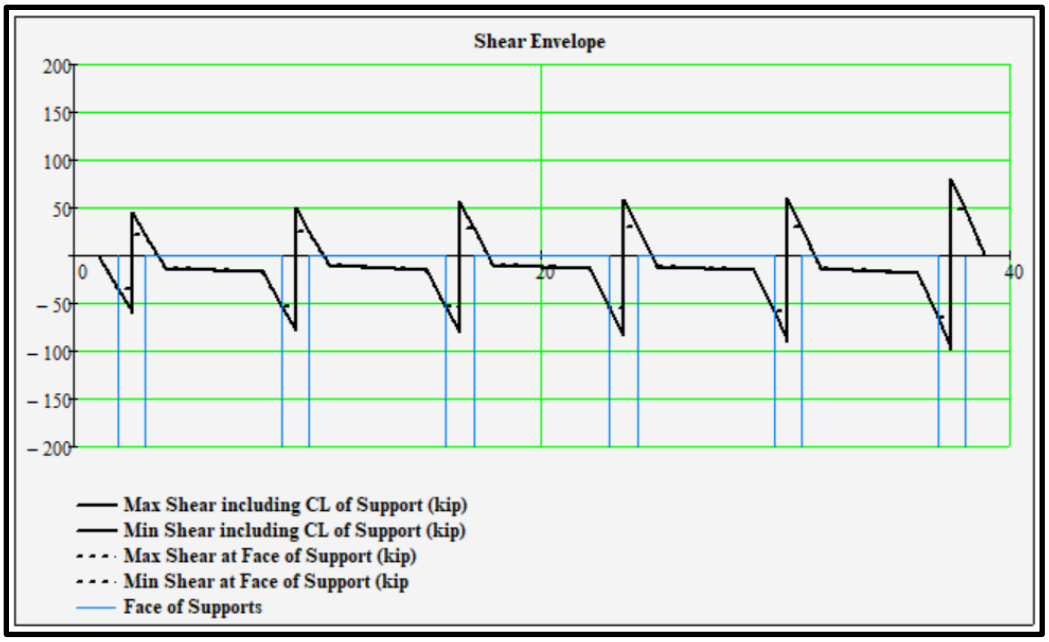

Figure 5.5. Shear diagram of bent cap with HP-piles

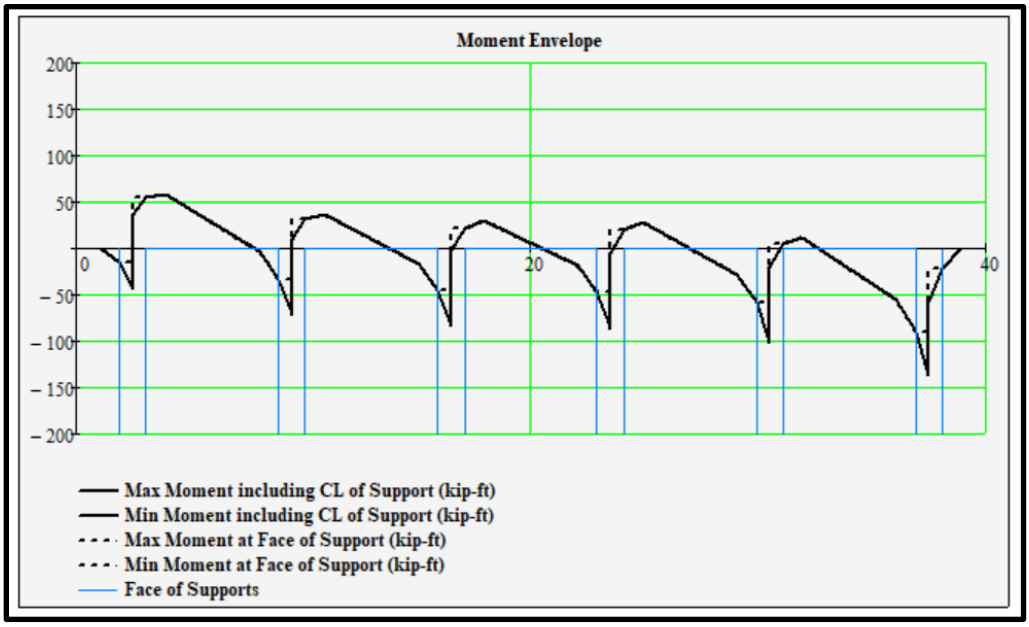

Figure 5.6. Moment diagram of bent cap with HP-piles

5.2.2 Design of bent cap

A trapezoidal bent cap, a standard bent cap adopted by ALDOT bridges for HP-piles, was selected for the design. Figure 5.7 illustrates this bent cap design. The details of the proposed bent

cap design, including the calculation of moment capacity and shear capacity, can be found in APPENDIX B.

The calculated moment capacity of the bent cap was determined to be 436 kips-ft, which significantly exceeded the moment demand in the cap (138 kips-ft). This indicates that the depth of the bent was able to accommodate the moment demands in the bent cap. However, it was also important to ensure that the shear capacity was adequate. The design shear capacity of the bent cap was calculated to be 136 kips, surpassing the shear demand in the cap (98 kips). This confirms that the proposed bent cap was capable of meeting the load demands placed on it. The reinforcement of the bent cap included equally spaced #11 rebars, three on the top as tension reinforcement and three on the bottom as compression reinforcement. Additionally, two-legged shear stirrups made of #5 rebars, spaced at 12 in. were incorporated to enhance the shear resistance. The rebars had yield strength of 60 ksi, while the compressive strength of the concrete was 4 ksi.

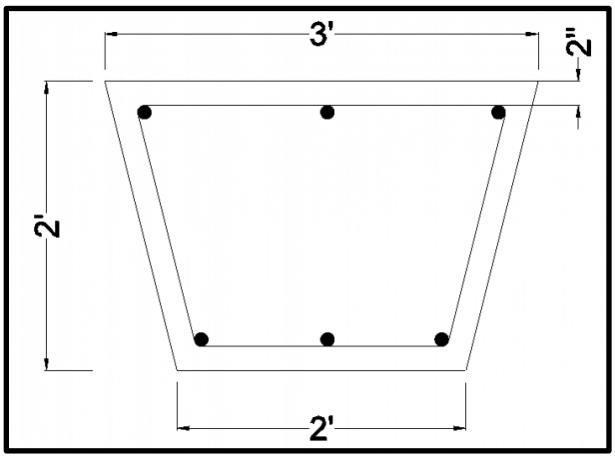

Figure 5.7. Cross section of bent cap with HP-piles

5.2.3 Design of HP-pile

Based on the AASHTO LRFD Bridge Design Manual (AASHTO, 2020), the HP-piles were designed to withstand the load demands calculated after the bent cap analysis. The load

demands on the top of the pile can be summarized as follows:

Axial load demand(P_{up}): 179 kips

Flexural demand (M_{up}):81 kips-ft

Shear demand parallel to bent cap (V_{upx}): 7 kips

Shear demand perpendicular to bent cap (V_{upz}): 3 kips

The calculation for the design of the pile is presented in APPENDIX C. The HP 12x63 section was selected, which had a design compressive strength of 820 kips and flexural strengths of 279 kips-ft. and 123 kips-ft., respectively, in the directions parallel and perpendicular to the bent cap. These values are relatively higher than the axial load demand (P_u) and flexural demand (M_u) at the bottom of the pile, respectively.

5.3 Study of bent cap with large diameter steel pipe pile

Since the steel pipe piles were considered as a replacement for RC drilled shaft piles and HP-piles, the design details for the pipe piles were also derived from a previous bridge structure with drilled shafts. This previous structure served as a reference to determine the overall dimensions of the pipe piles and bent cap, as well as the reinforcement details for the bent cap.

Table 5.1 provides a comparison of the capacity between existing RC drilled shaft piles, proposed HP-piles, and large diameter steel pipe piles. The capacity of the drilled shaft was calculated using spColumn software for a balanced condition, while the capacity of the HP-pile and steel pipe pile was determined using the AASHTO LRFD Bridge Design Manual (AASHTO, 2020), as shown in APPENDIX C and APPENDIX D respectively. Based on the comparison of pile capacities, it was recommended to replace the traditional piles with 3 ft. steel pipe piles with a wall thickness of 0.5 in. Since the steel pipe piles had a larger diameter, the construction layout

included six girders and two steel piles, similar to the layout for drilled shafts.

Table 5.1. Comparison of capacity of piles

SN	Piles	Size	P_n (kips)	M_n (kips-ft)	Remarks
1	Drilled shaft	3'6"	1785	2270	-
2	HP piles	12x63	920	136	-
3	Hollow steel pile	3'	2828	2377	Thickness=0.5 in.

5.3.1 Comparing bent cap of pipe pile against drilled shafts

The original bent cap had a depth of 4 ft. 6 in. and a width of 4 ft. It was reinforced with 8 #11 rebars on the top and bottom for tension and compression reinforcement respectively, with a clear cover of 2 in. Additionally, four-legged shear stirrups made of #5 rebars with a yield strength of 60 ksi were provided, spaced at 12 in. To assess whether the depth of the bent cap could be applicable to steel pipe pile, the moment capacity and shear capacity were checked against the demands calculated in the bent cap analysis (as described in Section 5.1). The calculation related to the flexural and shear capacity of the bent cap can be found in APPENDIX E. The design moment capacity of the bent cap was determined to be 4700 kips-ft, which significantly exceeded the flexural demand in the cap (1266 kips-ft). This indicated that the depth of the bent cap could meet the load demands. However, it was also important to consider the shear capacity of the bent cap. The design shear capacity of the bent cap was calculated to be 574 kips, which was greater than the shear demand in the cap (345 kips). This confirmed that the original bent cap was adequately designed to withstand the load demands.

5.4 Weight estimation of different piles

After considering identical bridges layout with a 40 ft. long bent cap and six girders, the design of piles and their respective bent caps was carried out. The details of the reinforced concrete bent cap and the corresponding piles are presented in Table 5.2. The table reveals that the bent cap with HP-piles had a smaller size compared to the other two options. This was due to the lower axial and moment load demands, which resulted from the placement of each pile directly beneath a single girder. In contrast, the other options involved only two large diameter piles.

Table 5.2. Description of typical bent

Elements			Types of piles			Unit weight
			Drilled shaft	HP	Steel pipe	
Bent cap	Length(ft)		40	40	40	
	Cross-section (ft x ft)	Reinforced concrete	4.5 x 4	2.5x2	4.5 x 4	150 pcf
	Rebars	Top	8#11	3#11	8#11	5.32 plf
		Bottom	8#11	3#11	8#11	5.32 plf
		Skin	4#5	-	4#5	1.04 plf
		Stirrups	4-legged #5 @ 12 in. o.c.	2-legged #5 @ 12 in. o.c.	4-legged #5 @ 12 in. o.c.	1.04 plf
No. of piles			2	6	2	
Pile	Size	Reinforced concrete	3.5 ft.	-	-	150 pcf
		Hp-steel		12 x 63	-	63 plf
		Steel pipe (ft x in)		-	3 x 0.5	490 pcf
	Rebars	Longitudinal	12#11	-	-	5.32 plf
		Spiral ties	#5	-	-	1.04 plf
	Encasement (ft x ft)	Reinforced concrete		2 x 2	-	150 pcf
Remarks	Size of encasement in HP-piles is assumed					

The estimation of the weight for each of the three bents was performed, considering the weight of the bent cap, piles, and other miscellaneous details. The unit weights used for the bent caps, drilled shafts, encasements (reinforced concrete), steel, and rebars were 150 pcf, 490 pcf, and as per ASTM standards, respectively, as indicated in Table 5.2. The detailed calculations for the different bents are summarized in Table 5.3. The total weights of the bents with drilled shafts, HP-piles, and steel pipe piles were determined to be 5910 lb./ft., 1846 lb./ft., and 3729 lb./ft., respectively.

Table 5.3. Estimation of weight of bent

Structural Elements		Types of piles		
		Drilled shaft	HP	Steel pipe
Bent cap (Lb/ft)	Concrete	2700	750	2700
	Top rebars	42.52	15.95	42.52
	Bottom rebars	42.52	15.95	42.52
	Stirrups	171.05	85.5	171.05
	Side face	4.17	-	4.17
Pile (Lb/ft)	Concrete	2886.34	600	-
	Steel	-	378	769.69
	Rebars	63.78	-	-
Total (Lb/ft)		5910.38	1845.4	3729.25

5.5 Comparison of different piles

The qualitative inspection of HP piles and drilled shafts is discussed in Section 1.2.1 and Section 1.2.2, respectively, while the quantitative analysis is summarized in Table 5.3. From a construction and economic standpoint, steel pipe piles have the potential to be a viable alternative to drilled shafts and driven piles. The main reasons for considering the replacement of existing piles with large diameter steel piles are summarized in the respective sections below.

5.5.1 Advantages of Steel pipes over H-piles

1. Unlike H-piles, steel pipes can be utilized for long-span bridges.
2. The exterior piles do not require battering.
3. Lateral bracing is not necessary to resist lateral loads.
4. The estimation of weight has shown that the initial construction cost for steel pipe piles may be higher than that of HP-piles. However, according to the report submitted to ALDOT (Marshall et al., 2017), cracks were discovered on the bent cap, particularly at the exterior piles (battered piles), leading to failure in the connection between the pile and bent cap. In this context, these piles need to be replaced, and steel pipe piles would be more cost-effective in the long term.

5.5.2 Advantages of Steel pipes over Drilled shafts

1. Steel pipe piles can be driven deeper into the soil.
2. Steel piles can be utilized in deep weak soil and marine water conditions, whereas drilled shafts require a strong bearing stratum.
3. They can be employed for supporting heavy structures.
4. The installation process is easier as it does not involve boring the ground, using reinforcement casing, or pouring concrete, making it less time-consuming.
5. The estimation of weight demonstrated that steel pipe piles are more cost-effective than drilled shafts.

All the qualitative and quantitative analyses of different existing and proposed bents have demonstrated that steel pipe piles can be highly effective both in terms of construction and

economics. Additionally, these piles can also be utilized for accelerated bridge works, leading to reduced time and labor costs too.

Chapter 6 PROPOSED CONNECTION DETAILS

Based on the different connection designs proposed by the state DOTs and the experimental research studies discussed in the previous chapters, this chapter discusses five types of connection details for connecting large diameter steel tubes to the reinforced concrete bent cap.

6.1 Design Considerations

After studying various bents, several design considerations had been developed to ensure robust connections between the pipe pile and reinforced concrete bent cap. These considerations were applicable to all five proposed connections and are summarized below:

1. The steel pipe pile to have a diameter of 3 ft. and a wall thickness of ½ in. The construction layout consists of six girders and two steel piles.
2. The pipe pile extends into the bent cap and have through holes to allow the bottom longitudinal reinforcement in the bent cap to pass through without obstruction.
3. A concrete plug to be provided at the top of the pile to facilitate force transfer between the pipe pile and the bent cap and prevent hollow pipe buckling near the connection region. A steel end plate to be installed at the bottom of the concrete plug to act as formwork and create a transition from the hollow to the concrete-filled region.
4. The size of the bent cap is designed based on the load demands determined through analysis, which was calculated to be 4 ft. x 4 ½ ft.

6.2 Proposed Anchorages and Connection Details

Five different types of anchorages, namely straight rebars, hooked rebars, headed rebars, annular rings, and shear studs, were proposed for the required connection between large diameter

steel pipe piles and the reinforced concrete bent cap. These anchorages were developed based on the load demands on top of the pile, which are calculated in Section 5.1. The load demands can be summarized as follows:

Axial load demand(P_{up}): 530 kips

Flexural demand (M_{up}):292 kips-ft

Shear demand perpendicular to bent cap (V_{upz}): 9 kips

Shear demand parallel to bent cap (V_{upx}): 21 kips

6.2.1 Non-Contact Lap Splice Anchorage

In non-contact lap splice connections, the upper part of the steel pipe is filled with a concrete plug, and a series of reinforcing bars extend into the bent cap. Various end anchorage types can be utilized for these connection types, including straight bars with transverse confining reinforcement (Figure 6.1), hooked bars with 90° or 180° bend hooks (Figure 6.2), and headed bars using mechanical anchors or terminators (Figure 6.3). The development length for the hooked and headed bars is expected to decrease due to improved anchorage resistance between the rebar and concrete. These connections are commonly employed in various reinforced concrete designs using rebars with established design approaches, offering easier and more cost-effective construction methods.

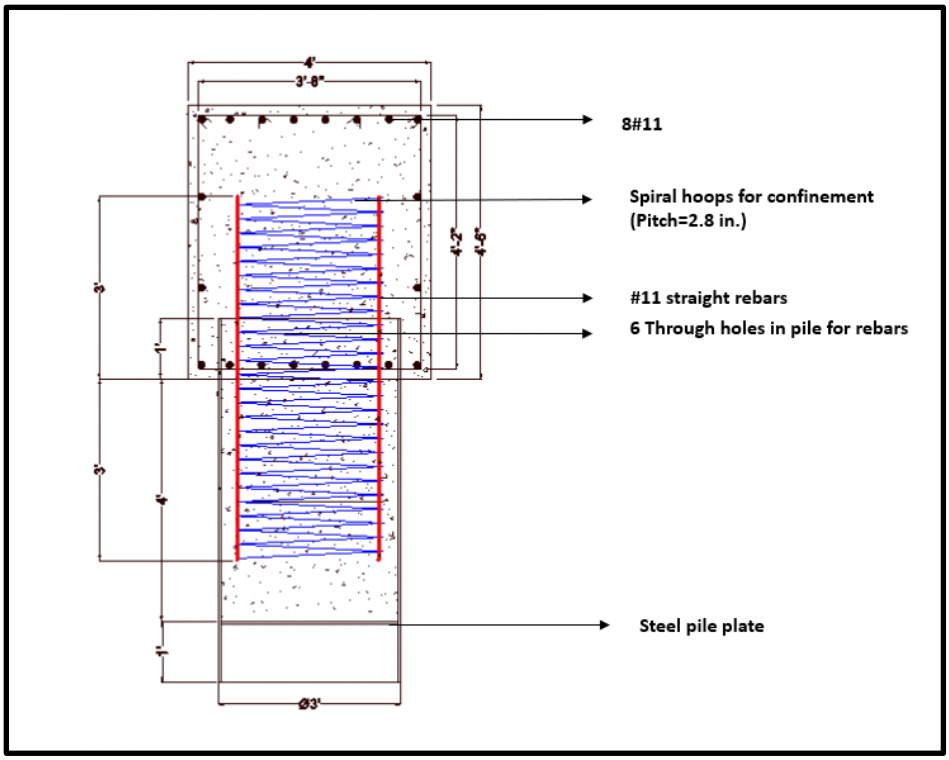

Figure 6.1. Typical Specimen With Non-Contact Lap Splice Connection; O1: Straight Rebars

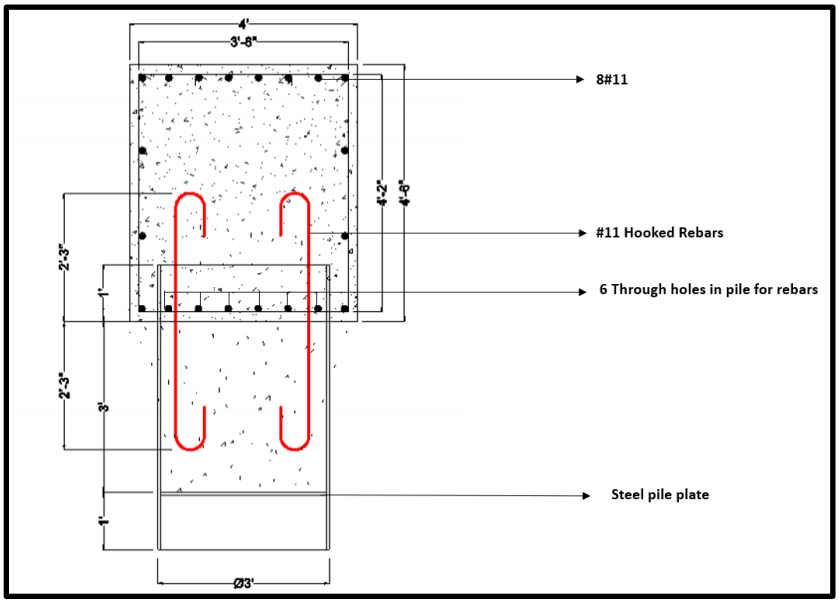

Figure 6.2. Typical Specimen With Non-Contact Lap Splice Connection; O2: Hooked rebars

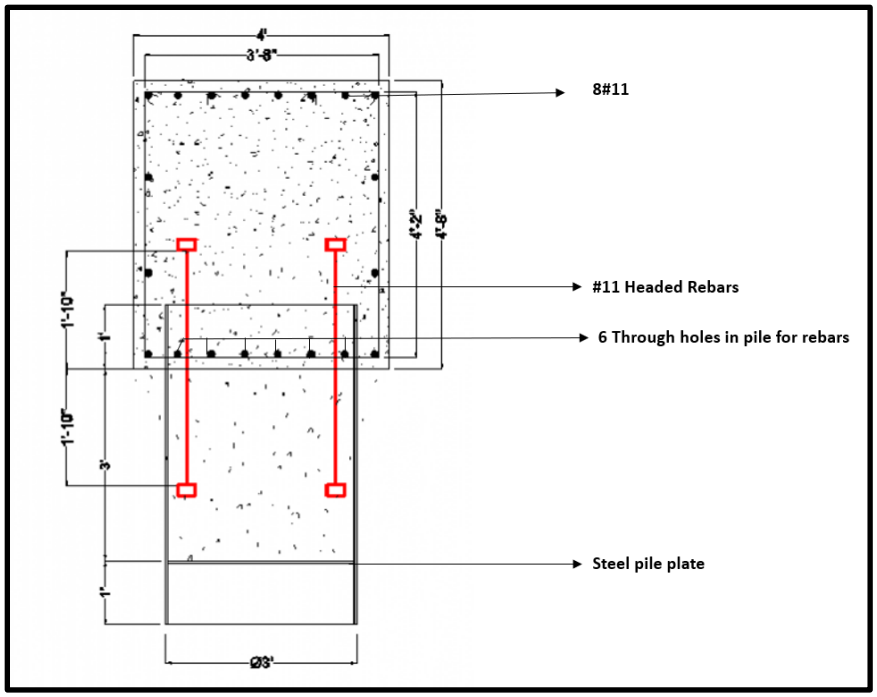

Figure 6.3. Typical Specimen With Non-Contact Lap Splice Connection; O3: Headed Rebars

6.2.2 Annular ring

In this type of connection, an annular ring is welded to the top of the pile, which is then embedded into the bent cap, as depicted in Figure 6.4. The annular plate can be welded to the end of the pipe pile at a fabrication shop, eliminating the need for reinforcing cages that extend from the pipe pile into the bent cap. This approach maximizes off-site fabrication and simplifies on-site efforts by enabling monolithic concrete casting. The annular ring provides anchorage for axial and shear stresses and facilitates moment transfer to the surrounding reinforcement and concrete.

According to a study conducted by Washington University, the annular ring should have a thickness equal to that of the steel tube, with a yield stress equal to or greater than that of the steel tube. The ring extends 8 times the thickness of the tube in both the outside and inside directions, resulting in a total diameter of the annular ring of $16t + D$ (where t is the thickness of the tube and

D is the diameter of the steel tube). The size of the fillet weld should be sufficient to resist the tensile strength of the steel tubes, as given in Eq. (4.8). The embedment depth of the annular plate, or the extension of the pile into the bent cap, is calculated based on the equilibrium relation between the tensile strength of the steel tube and the shear strength of the concrete cone below the ring plate, as given by Eq. (4.9). Furthermore, the effective depth of the bent cap is ensured to resist the axial compressive forces in the pile, as summarized in Eq. (4.10).

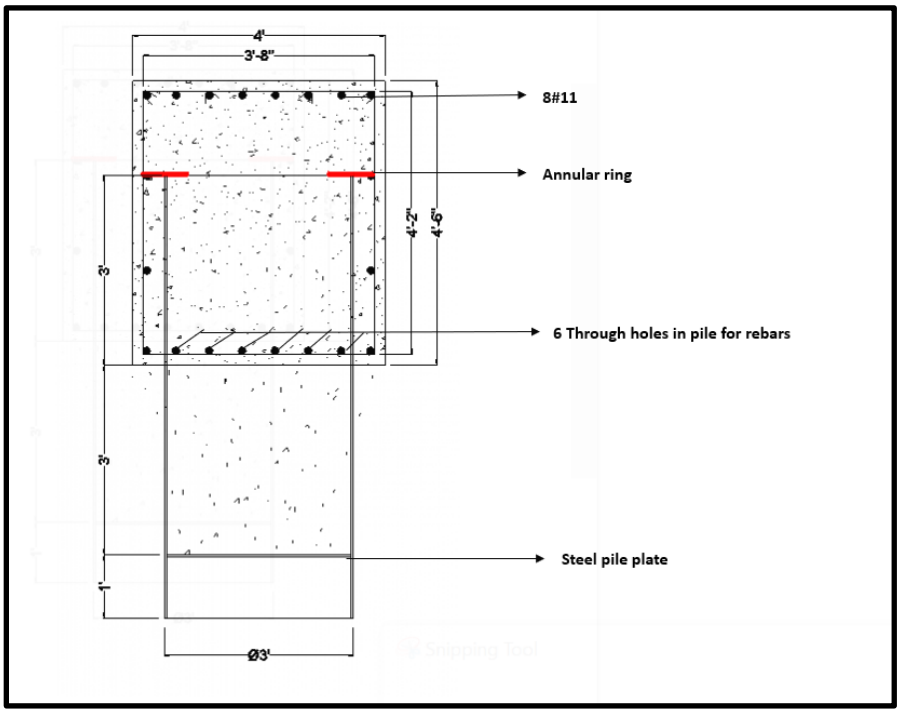

Figure 6.4. O4: Typical Specimen With Annular Ring Connection

6.2.3 Shear Studs

In such connection, shear studs are utilized as mechanical connectors, which are welded to the outside face of the steel pipe to facilitate shear transfer between the steel and concrete, as illustrated in Figure 6.5. Similar to the end plate connection, this type of connection eliminates the requirement for reinforcing rebars that extend into the bent cap. Additionally, the studs can be

installed off-site, streamlining the field erection and assembly process. Connections incorporating shear studs have demonstrated strong pullout and punching shear resistance, effectively transferring the loads from the pipe to the bent cap.

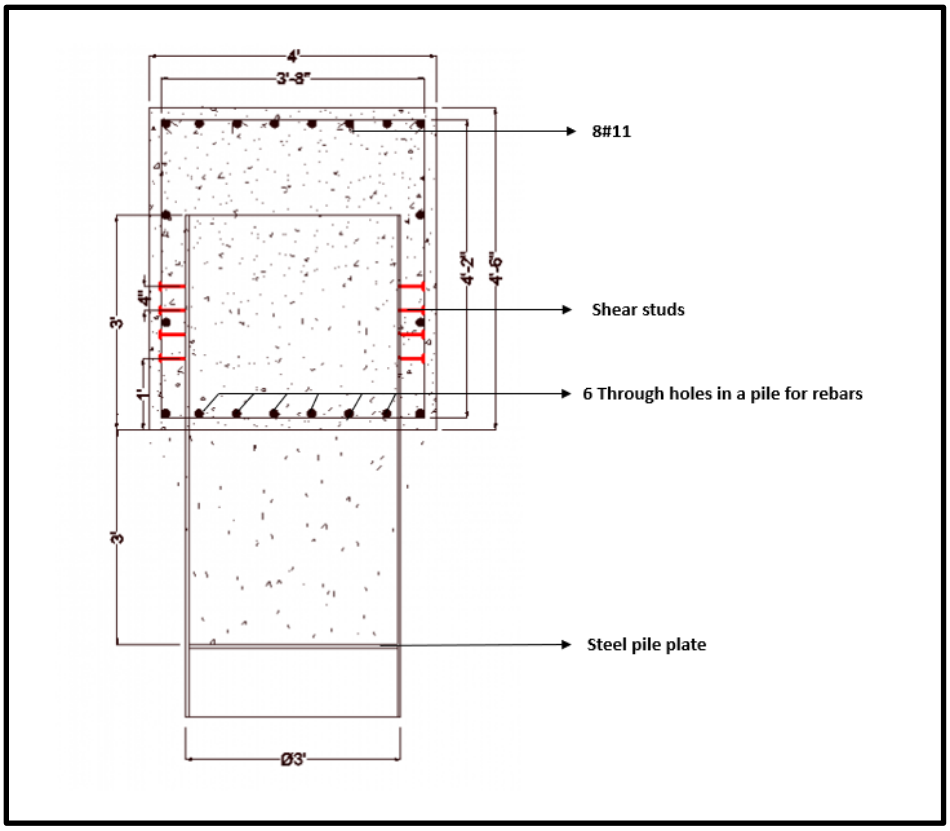

Figure 6.5. O5: Typical Specimen With Shear Studs Connection

6.3 Calculation of strength of proposed connections

6.3.1 Proposed connections

Five different steel pipe pile to RC pile cap connections, referred to as options O1-O5, were proposed. The connection details considered design considerations such as straight rebars (O1), hooked rebars (O2), headed rebars (O3), annular ring (O4), and shear studs (O5). The strength values of the rebars and steel tubes are summarized in Table 6.1. The specifications of the

specimens are presented in Table 6.2. Each specimen consisted of a 3 ft. diameter steel pipe pile with a wall thickness of 0.5 in., embedded within the bent cap. The ultimate tensile strength of the steel pipe pile wall was 60 ksi.

For specimens O1-O3 (Figure 6.1, Figure 6.2, and Figure 6.3, respectively), the connections were treated as concrete piles with reinforcement. In the first step, a minimum reinforcement of 1% (1.2% for symmetry of rebars) was provided in the connection, which consisted of 8#11 rebars with a yield strength of 60 ksi. The spColumn software was used to determine the compressive strength and moment capacity of the connection. The analysis revealed a design axial strength of 1096 kips and a corresponding flexural strength of 1114 kips-ft at a balanced condition. These strengths are both greater than the axial load demand of 530 kips and the corresponding flexural load demand of 292 kips-ft, respectively. Figure 6.6 illustrates the P-M interaction diagram, which indicates that the load demands at the connection lie within the envelope of the design capacity of the connection. Therefore, the 8 #11 rebars were able to meet the demand requirements at the connection point. In this figure, the x-axis represents the flexural strength, while the y-axis represents the axial compressive strength of the connection. P_{max} indicates the maximum compressive strength, while P_{min} represents the minimum strength. Similarly, f_s indicates the stress in rebars, and f_y represents the yield stress of rebars. The figure illustrates the relationship between the flexural strength and axial strength of the connection under different conditions, such as balanced, tension controlled, pure bending, and others.

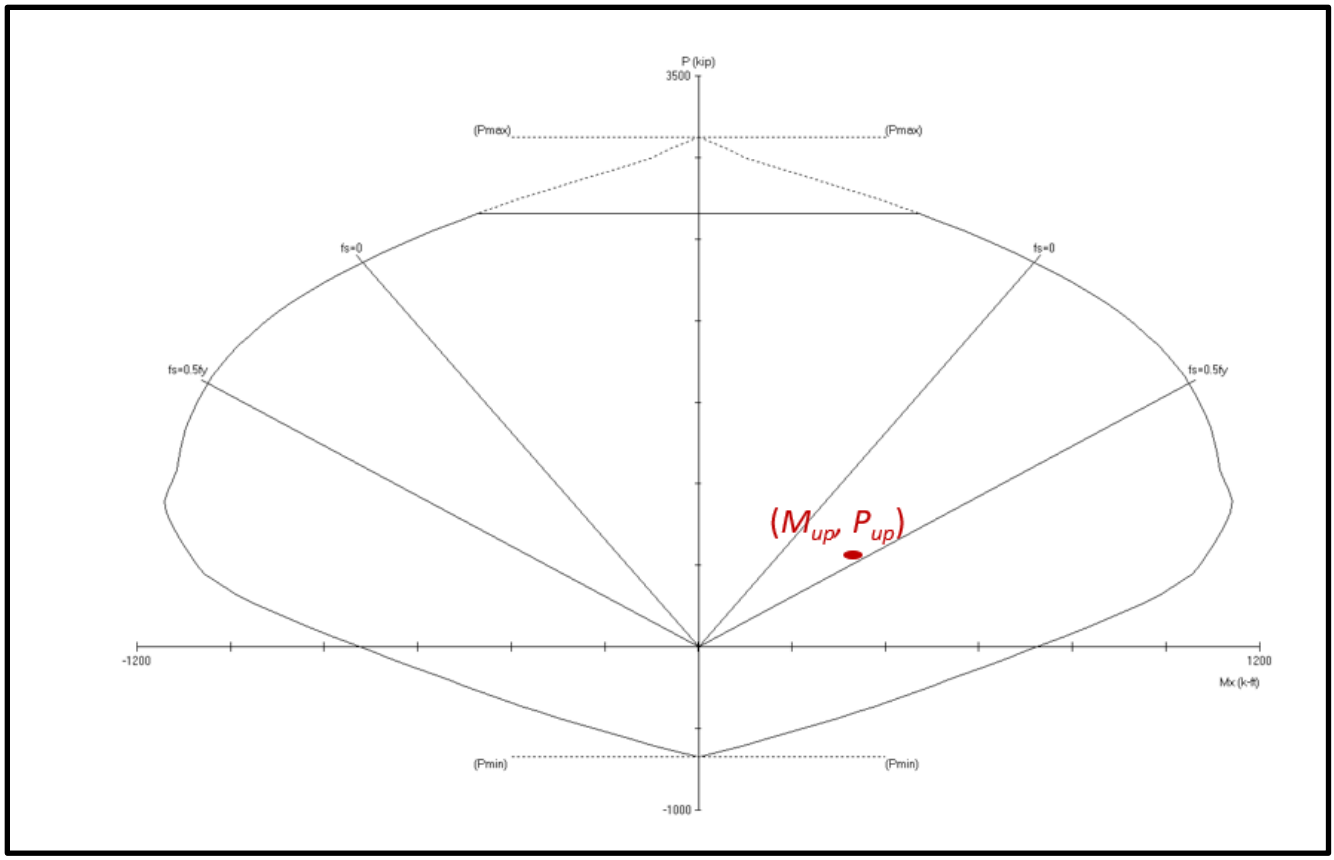

Figure 6.6. P-M interaction diagram

O1 consisted of straight rebars, O2 consisted of hooked rebars, and O3 consisted of headed rebars. In O1, the rebars were extended 3 feet on both the bent cap and the steel pile. These rebars were properly confined with #5 spiral rebars with a pitch of 2.8 inches. A concrete plug with a depth of 5 feet was provided in the steel pile from the top. Similarly, in O2 and O3, the rebars were extended 2 feet and 3 inches and 1 foot and 10 inches, respectively, on both the bent cap and the steel pipe pile. These two connections were provided with a concrete plug of 4 feet on top of the pile. The headed rebars were developed using the nVent Lenton terminator [17] of size D6, with a head diameter of 3¼ inches and a height of $1^{11}/_{16}$ inches. The calculations for the design of the connection are explained in detail in APPENDIX F.

For O4 (Figure 6.4), the design-related calculations are discussed in detail in APPENDIX

G. The annular ring was welded to the tip of the steel tube inside the bent cap, with a size of 0.56 in. The ultimate tensile strength of the annular ring was the same as that of the steel pipe, which is equal to 60 ksi. The outer and inner diameter of the annular ring were 3 ft. and 8 in., and 2 ft. and 4 in., respectively. The steel tube extended 3 ft. inside the bent cap, and no longitudinal reinforcement was provided inside the piles. Furthermore, the strength of the steel piles filled with concrete was compared with the load demands on the pile. The area of the steel pile (56.55 in^2) was conservatively transformed into rebars equivalent to 14#18 (56 in^2). The spColumn software was used to determine the strength of the concrete-filled steel tube. Figure 6.7 illustrates the P-M interaction diagram, which indicates that the load demands at the connection lie within the envelope of the design capacity. The axial and corresponding moment capacity of the concrete-filled steel tube at balanced condition was calculated as 1685 kips and 2340 kips-ft, respectively, which are greater than the axial load demand (530 kips), and corresponding flexural demand (292 kips-ft).

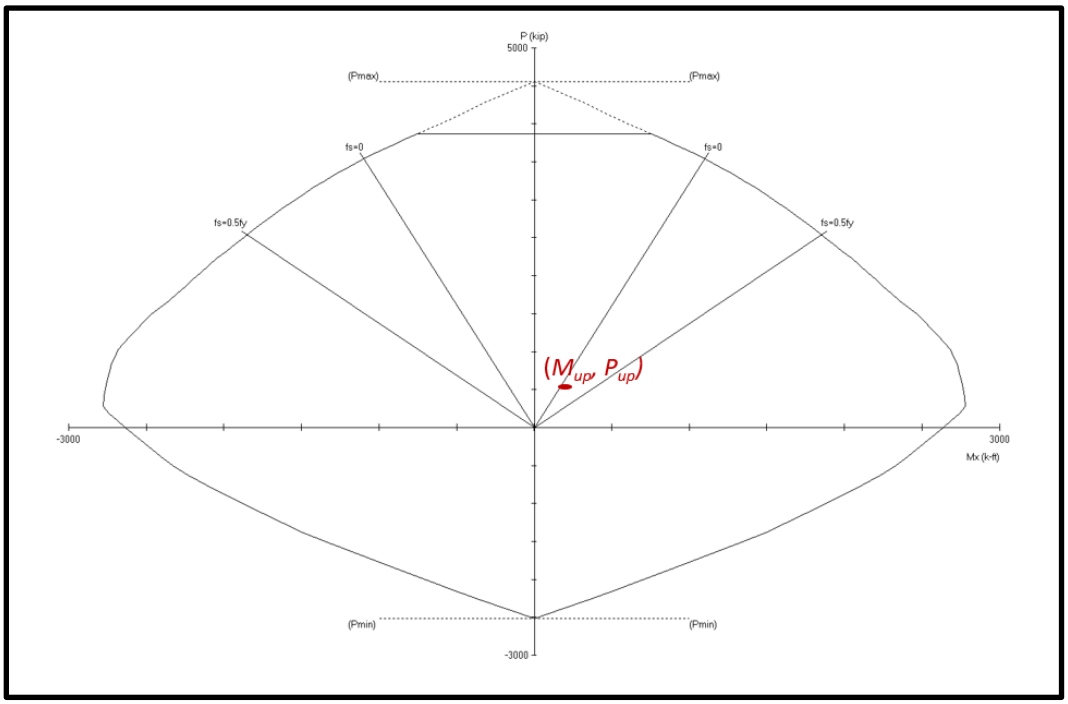

Figure 6.7. P-M interaction diagram

For O5 (Figure 6.5), the design parameters are provided in detail in APPENDIX H. In this connection, 32 shear studs with a diameter of ¾ inch were welded on the outside perimeter of the steel tube in 4 rows, with 8 studs in each row. The diameter of the shear head was 1 ¼ inches, and the height of the stud was 4 inches. The ultimate tensile strength of the shear studs was 65 ksi. Similar to SP4, the pile extended 3 ft. inches inside the bent cap, and no longitudinal reinforcement was provided in the piles.

Table 6.1. Material properties

Specifications	8#11	#5	Steel pile(3 x 0.5)
f_y (ksi)	60	60	50

Table 6.2. Details of Specimens

Specimen	O1	O2	O3	O4	O5
Concrete strength (Ksi)	4	4	4	4	4
Steel Pile (ft x in)	3 x 0.5	3 x 0.5	3 x 0.5	3 x 0.5	3 x 0.5
Anchorage	Straight Rebars	Hooked Rebars	Headed Rebars	Annular Ring	Shear Studs
Connection Details	8#11	8#11	8#11	Φ 3'-8"	32 Φ 0.75"
Bent cap (ft x ft)	4x4.5	4x4.5	4x4.5	4x4.5	4x4.5
Top bars	8#11	8#11	8#11	8#11	8#11
Bottom bars	8#11	8#11	8#11	8#11	8#11
Stirrups	#5 @12 o.c.	#5 @12 o.c.	#5 @12 o.c.	#5 @12 o.c.	#5 @12 o.c.
l_e	1 ft.	1 ft.	1 ft.	3 ft	3 ft
L_{pc}	3 ft. 6 in.	3 ft. 6 in.	3 ft. 6 in.	1 ft. 6 in.	1 ft. 6 in.
Concrete plug (ft)	5	3	3	3	3

6.3.2 Calculation of strength

The connection must possess sufficient strength to withstand compressive forces that could lead to punching failure, as well as forces that could cause pull-out failure. Additionally, it should have strong lateral flexural strength. Therefore, calculations were performed to determine the

punching capacity, pull-out capacity, and flexural strength of the connections, which are presented in the section below.

Punching Capacity

The punching resistance was calculated using the proposed methodology described in Section 4.4.1, considering the resistance provided by concrete (V_c), stirrups (V_s), shear studs (V_{ss}), and the bond between concrete and the steel pile (V_b). The detailed calculation of the punching resistance (V_p) of the connection is summarized in Table 6.3, which also includes a comparison with the punching strength of the original connection. A detailed calculation related to punching resistance of drilled shafts is presented in APPENDIX E.

The specimen with rebars exhibited the highest punching resistance, measuring 1721 kips. In comparison, the punching resistance of the specimen with shear studs was 1267 kips, while the specimen with an annular ring had a punching resistance of 654 kips. The punching resistance provided by each connection was greater than that provided by the drilled shafts, which is 638 kips. It can also be observed that the contribution of concrete was the highest among the different components in providing punching resistance.

Table 6.3. Punching strength of the connection

Specimen	V_c (kips)	V_s (kips)	V_{ss} (kips)	V_b (kips)	V_p (kips)
O1	1449	261	0	11	1721
O2	1449	261	0	11	1721
O3	1449	261	0	11	1721
O4	494	112	0	48	654
O5	430	112	677	48	1267
Drilled shaft	316	322	0	0	638

The results demonstrate that the embedment of the steel tube and the type of anchorage are crucial factors in achieving strong punching resistance against the applied compressive forces.

Pullout capacity

Based on the design methodology discussed in Section 4.4.3, the pullout resistance of the connections was calculated, considering the contribution from concrete (V_c) and stirrups (V_s). The data presented in Table 6.4 summarizes the total resistance offered by different types of connections.

The pullout resistance of specimens with annular ring was the highest, measuring 1320 kips. The resistance for rebars and shear studs were 294 kips and 1210 kips, respectively. Similar to punching resistance, concrete made the highest contribution compared to the others.

Table 6.4. Pull-out strength of the connection

Specimen	V_c (kips)	V_s (kips)	V_{po} (kips)
O1	220	74	294
O2	220	74	294
O3	220	74	294
O4	1099	221	1320
O5	989	221	1210

The results indicate that the embedment of the steel tube and the choice of anchorage type are important considerations to achieve a strong pullout resistance against applied forces.

Flexural capacity

The design moment capacity of each connection was calculated using spColumn software

for every pile, except for the hollow pipe pile. The detailed calculation for the hollow pipe pile can be found in APPENDIX D. The table below, Table 6.5, presents the design flexural capacities corresponding to design axial strength for each connection type. The connection with rebars as anchorage yielded a design moment capacity of 1114 kips-ft, while annular ring and shear studs both provided a moment capacity of 2340 kips-ft for the steel member filled with concrete.

Table 6.5. Flexural strength of the connection

Specimens	Types of pile	ϕM_n (kips-ft)	Remarks
S1	Drilled shafts	2270	Existing pile
S2	Hollow pipe pile	2140	Member strength
O1-O3	Pile with rebars	1114	Same as drilled shaft
O4	Pile with annular ring	2340	Member strength
O5	Pile with shear studs	2340	Member strength

All of the proposed connections demonstrated a high flexural resistance that surpassed the calculated flexural demand on top of the hollow steel pipe pile, ensuring a strong connection.

Chapter 7 Summary, Conclusions, And Future Work

7.1 Summary

The study aimed to compile a comprehensive summary of best practices for connecting steel pipe piles to bent caps, drawing on data from other states and various studies in the field. By analyzing the advantages of steel pipe piles compared to other types of piles, the study sought to establish initial connection details, design methodologies, and calculation procedures that align with the current AASHTO LRFD specifications.

A survey was conducted to assess the prevailing practices among state DOTs regarding the use of steel pipe piles, considering the varying implementations and requirements across different states. Furthermore, research papers were reviewed extensively to gain insights into the strength characteristics of the proposed connections.

The findings from these investigations are detailed in their respective chapters, while the overall observations and conclusions derived from this project are summarized in Section 7.2. Based on these conclusions, recommendations are provided in Section 7.3.

7.2 Observations and Conclusions

7.2.1 Benefits of steel pipe pile

The study outlined the usage and advantages of steel pipe piles, highlighting their benefits and widespread adoption in various states. The current state practices have demonstrated successful utilization and extensive experience of steel pipe piles over a prolonged period.

The evaluation of three different types of piles (drilled shafts, HP-piles, and steel pipe piles) supports the effectiveness of steel pipe piles from a construction perspective. Unlike drilled shafts, which involve tedious processes such as drilling, excessive earth removal, reinforcement casing,

and concrete pouring, and HP-piles, which require pile battering, lateral bracing, and encasing, steel pipe piles offer a more streamlined and efficient construction method. Steel pipe piles are suitable for use in long and heavy bridges, as well as in challenging ground conditions where bearing strata are located deep beneath soft soil.

A quantitative evaluation based on weight demonstrates that steel pipe piles are more cost-effective than drilled shafts. While the initial construction cost of HP-piles may be lower than steel pipe piles, they are not suitable for long-term applications due to observed distressing in the connection between the pile and bent cap. In such cases, steel pipe piles offer a convenient and acceptable substitute for existing piles. Additionally, steel pipe piles enable accelerated bridge construction, making them effective in terms of both construction efficiency and financial considerations.

7.2.2 Conclusions on pipe pile to bent cap connections

Surveying state DOT practices and literature review of research studies provided insights into the connection details between concrete-filled steel pipe piles and bent caps/foundations. The studies indicate that the strength of the connection depends on several factors, including the type of anchorage (e.g., concrete, rebars, shear studs, annular ring), the strength of materials, the embedment depth, and the depth of the bent cap. Based on these elements, design methodologies for the connection between piles and bent caps have been developed. Some of these design methodologies are beyond what is covered in design provisions provided by various design codes such as ACI, AASHTO, and AISC specifications.

The connection between the steel pipe pile and bent cap must possess sufficient strength to withstand various failure modes. Figure 7.1 illustrates the three primary failure modes in an

embedded column base. The connection needs to be robust enough to resist punching failure, pullout failure, and lateral moment. As an overstrength connection is being proposed, it should be designed to ensure adequate resistance against the applied load demands. The design lends itself to overdesigned pile members at the bent cap connection, considering the significant strength of the pile in comparison to the force and moment demands.

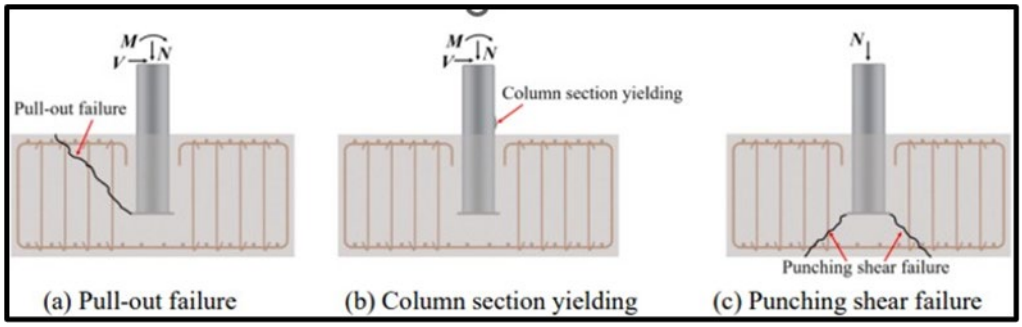

Figure 7.1. Possible failure modes of the embedded column base[14]

Empirical formulas have been proposed to calculate the punching strength and pullout strength. The punching resistance is determined by considering contributions from concrete, stirrups, shear studs, and bond length. The pullout resistance is determined based on contributions from concrete and stirrups alone. It is worth noting that the flexural capacity of the connection exceeds the moment demand for the overstrength connection, ensuring its robustness.

A steel pipe pile with a diameter of 3 ft. and a thickness of 0.5 in. has been selected to have a comparable strength with a typical 3 ft. diameter RC drilled shaft. Due to its large size, hollow steel pipe piles are recommended. However, to ensure stability and prevent buckling and yielding, a concrete plug is recommended to be incorporated near the bent-cap connection. There are three prominent types of anchorage for the connection between the pile and the bent cap: i) non-contact lap splices using rebars (e.g., straight bars, 90-degree and 180-degree hooked rebars), ii) Annular

ring, and iii) shear studs. In terms of the punching strength resistance, the rebar connection has higher strength than the shear studs and annular ring connections. However, when it comes to pull-out resistance, the annular ring connection proves to indicate the greatest strength.

7.3 Recommended future work

Further research programs should be organized to develop refined design methodologies and study the behavior of connections for a wider range of applications. The following are recommended as primary areas of future work:

1. Load testing should be conducted on several candidate pipe pile to bent cap connection types to determine their attachment strength.
2. Finite element analysis should be developed for evaluating the connection and conducting extensive parameter studies on the proposed connections. Parametric analyses can be used to refine and optimize the design and detailing methodology.
3. The development of additional connection details between the pile and bent cap should be explored to enhance the ease of construction for bridge structures.

References

[1] Brown, D. A., Turner, J. P., Castelli, R. J., & Americas, P. B. (2010). *Drilled shafts: Construction procedures and LRFD design methods* (No. FHWA-NHI-10-016). United States. Federal Highway Administration.

[2] Voyiadjis, G. Z., Cai, S., & Alshibli, K. (2016). *Integral Abutment Bridge for Louisiana's Soft and Stiff Soils [Report]* (No. FHWA/LA. 13/517). Louisiana. Dept. of Transportation and Development.

[3] Brown, D. A., & Thompson III, W. R. (2015). *Design and load testing of large diameter open-ended driven piles* (No. Project 20-05, Topic 45-05).

[4] Anderson, J. B., Marshall, J. D., Campbell, J., & Skinner, Z. (2018). Weak axis lateral load testing of a four H pile bent. In *IFCEE 2018* (pp. 419-427).

[5] Marshall, J. D., Anderson, J. B., Campbell, J., Skinner, Z., & Hammett, S. T. (2017). Experimental validation of analysis methods and design procedures for steel pile bridge bents. *Auburn University Highway Research Center, Auburn, Alabama*.

[6] Brown, D. A., Schindler, A. K., Bailey, J. D., Goldberg, A. D., Camp III, W. M., & Holley, D. W. (2007). Evaluation of self-consolidating concrete for drilled shaft applications at lumber River Bridge project, South Carolina. *Transportation research record*, *2020*(1), 67-75.

[7] Nucor Skyline. (n.d.). *Pipe*. Nucor Skyline.

[8] Baig, M. N., Fan, J., & Nie, J. (2006). Strength of concrete filled steel tubular columns. *Tsinghua Science and Technology*, *11*(6), 657-666.

[9] Marcakis, K. (1979). Precast concrete connections with embedded steel members.

[10] Eastman, R. S. (2011). *Experimental investigation of steel pipe pile to concrete cap connections*. Brigham Young University.

[11] Wang, Y., & Yu, J. (2017). 03.27: Punching shear behavior of an innovative connection between steel tubular column to flat concrete slab. *ce/papers*, *1*(2-3), 721-728.

[12] Lehman, D. E., & Roeder, C. W. (2012). Foundation connections for circular concrete-filled tubes. *Journal of Constructional Steel Research*, *78*, 212-225.

[13] Tan, S., Jia, C., Guo, L., Ou, F., & Xu, Y. (2022). Experimental investigation on punching shear behavior of the embedded column base for CFSTs. *Engineering Structures*, *263*, 114371.

[14] Stephens, M. T., Lehman, D. E., & Roeder, C. W. (2015). *Concrete-filled tube bridge pier connections for accelerated bridge construction* (No. CA15-2417).

[15] Li, X., Wu, Y. P., Li, X. Z., Xia, J., & Lv, H. L. (2017). Punching shear strength of CFT bridge column to reinforced concrete four-pile cap connections. *Journal of Bridge Engineering*, *22*(8), 04017036.

[16] American Association of Highway and Transportation Officials. 2020. *AASHTO LRFD Bridge Design Specifications.* 9th. Washington D.C.: American Association of State Highway and Transportation Officials.

[17] nVent Lenton Terminator (nVent.com/LENTON)

[18] American Concrete Institute Committee 318. 2019. *Building Code Requirements for Structural Concrete and Commentary*. Farmington Hills, MI: American Concrete Institute.

[19] *Structures Design Office - Programs Library - Files and links*. FDOT. (n.d.). https://www.fdot.gov/structures/proglib.shtm

[20] Florida Department of Transportation. 2022. *Structural design guidelines*. Florida: Florida DOT

[21] Transportation Officials. (2011). *A Policy on Geometric Design of Highways and Streets, 2011*. AASHTO.

[22] ASCE 7-22 ASCE 7 Hazard Tool, American Society of Civil Engineers, 2017-2018.

[23] AISC 360-16 Specification for Structural Steel Buildings, Chicago, IL: American Institute of Steel Construction, 2016.

[24] ALDOT Structural design manual, Montgomery, AL: Alabama Department of Transportation, 2023.

[25] Autodesk Inc. AutoCAD, Version 2022. San Rafael, CA: Autodesk, 2023.

[26] StructurePoint. spColumn, Version 6.00:Skokie, IL 2017.

APPENDIX A

Table A.0.1: Load parameters for analysis of bent cap

Loads	Abbreviation	Parameters considered
Dead load	DC	Weight of barriers, beams, deck, stay in place forms, and self-weight of bent cap
Dead load	DW	Wearing surfaces and Utilities
Braking load	BR	Horizontal braking force
Centrifugal force	CE	Design speed of vehicle
Wind load	WS	Wind pressure on structure
Wind load on Live load	WL	Wind load experienced by live load on a structure
Water load	WA	Related to flood elevation
Live load	LL	Vehicular load
Temperature load	TU	Omitted

Table A.0.2: Load combination and Load factors for Strength-III limit state analysis

Loads	Υ_s	Remarks
DC	1.25	weight of barriers, beams, deck, stay in place forms, and self-weight of bent cap were considered
DW	1.5	not considered as it is only allowed for short bridges (<100ft)
LL	0	not considered as vehicles become unstable at higher wind velocities
BR	0	not considered due to minimal effect
CE	0	not considered due to minimal effect
WS	1	includes design wind speed of the location
WL	0	not considered due to negligence of live load
WA	1	flood elevation was below the bottom of the bent cap
TU	1.2	not considered due conservative analysis

Table A.0.3 : Summary of load applied on bent cap during analysis

Loads	Type of load	Drilled shafts	HP-piles	Unit
Load parallel to cap	WS	41	41	kips
Load perpendicular to cap	WS	17	17	kips
Self-weight of cap	DC	3.42	0.98	klf
Vertical superstructure load	DC	135.3	135.3	kips/beam line

APPENDIX B DESIGN OF BENT CAP WITH HP-PILES

For the preliminary design, a trapezoidal bent cap with a shorter base of 2 ft. and a larger base of 3 ft., and a height of 2 ft. was assumed. This size is commonly used for bent caps with HP-piles by ALDOT. The bent cap was reinforced with 3#11 compression steel on the top and 3#11 tension steel on the bottom. Additionally, the bent cap was equipped with 2-legged #5 shear stirrups spaced at 12 in. o.c. The effective depth of the bent cap was 22 in. (d), and the average width was 30 in. (b).

Material properties

Compressive strength of concrete (f'_c) = 4 ksi

Yield strength of rebars (f_y) = 60 ksi

Load demands on bent cap

Shear load (V_{ub}) = 98 kips

Flexural load (M_{ub}) = 138 kips-ft

Calculation of moment capacity

In the initial step, the assumption was made that the stress in rebars (f'_s) is less than the yield strength (f_y) for the calculation of nominal moment capacity.

The depth of the neutral axis (c) was calculated using the rectangular stress distribution diagram. The calculation process is summarized below:

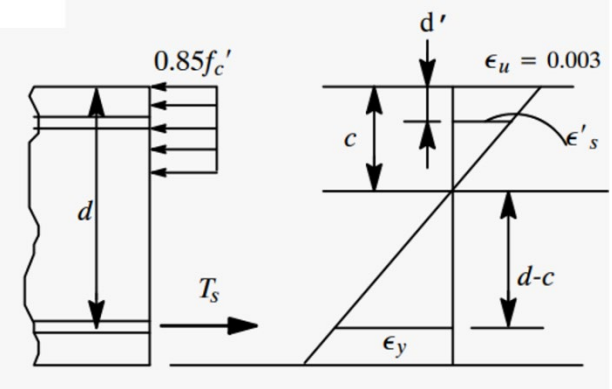

Figure A.1: Plastic stress distribution diagram

Compressive force due to steel (*Cs*):

$$Cs = A'_s f'_s = 1.56 * 3 * 0.003 * \left(\frac{c - d'}{c}\right) * 29000$$

$$Cs = 407.16\left(\frac{c - 2}{c}\right) \text{kips}$$

Compressive force due to concrete (*Cc*):

$$Cc = 0.85\, f'_c \beta_1\, cb = 86.7c \text{ kips}$$

Tensile force due to rebars (*Ts*):

$$Ts = A_s f_y = 1.56 * 3 * 60 = 280.8 \text{ kips}$$

Now for equilibrium: *Cs* + *Cc* = *Ts*

$$407.16\left(\frac{c - 2}{c}\right) + 86.7c = 280.8$$

$$c = 2.42 \text{ in}$$

Now,

$$f'_s = 0.003 * \left(\frac{c-2}{c}\right) * 29000 = 15 < 60\ ksi \text{ (Assumption is OK)}$$

Now, the nominal Moment Capacity(M_n) of the beam is calculated as follows:

$$M_n = C_c\left(d - \frac{\beta_1 c}{2}\right) + C_s(d - d')$$

$$M_n = 86.7 * 2.42\left(22 - \frac{0.85 * 2.42}{2}\right) + 407.16\left(\frac{2.42 - 2}{2.42}\right)(22 - 2)$$

$$M_n = 5813 \text{ kips} - \text{in}(484 \text{ kips} - \text{ft})$$

ϕMn=436 kips-ft> M_{ub} (138 kips-ft)

The design moment capacity of bent cap was calculated to be 436 kips-ft which is greater than moment demand (138 kips-ft).

Calculation of shear strength

According to 5.12.5.3.8c of AASHTO LRFD, the nominal shear resistance due to concrete is given by:

$$V_c = 0.0632\sqrt{f'_c}bd$$

$$V_c = 83.42\ kips$$

The nominal shear resistance due to stirrups is calculated as:

$$V_s = \frac{A_s f_y d}{s}$$

$$V_s = \frac{0.31 * 2 * 60 * 22}{12}$$

$$V_s = 68.2\ kips$$

Total shear resistance (V_n)= V_c+V_s =151.62 kips

According to Section 5.5.4.2, the factor ϕ for shear in a reinforced concrete section is 0.9. The design shear capacity of the bent cap was calculated to be 136 kips, which is greater than V_{ub} (98 kips).

It can be concluded that the assumed size dimensions and detailing of the bent cap were sufficient to withstand the load demands placed on it.

APPENDIX C DESIGN OF HP-PILE

The AASHTO LRFD Bridge Design Manual provides provisions for designing steel HP columns. Based on the load demands at the bottom of the piles, an initial trial of HP-12x63 section was selected. The strength of the HP pile, considering both its compressive strength and moment capacity, was checked against the load demands on the pile, which are summarized below:

Geometric properties of the pile

Width of flange (b_f) =12.125 in.

Thickness of flange (t) = 0.515 in.

Overall depth (d) = 11.94 in.

Thickness of web (t_w) = 0.515 in.

Gross cross-sectional area (A_g) = 18.4 in^2.

Moment of inertia about y-axis (I_y) = 153 in^4.

Section modulus (Z_x) =88.3 in^3.

Section modulus (Z_z) =38.7 in^3.

Radius of gyration (r) =2.88 in.

Length (L) = 5.79 ft.

Effective length (L_c)= 2.9 ft.

Load demands on top of the pile

Axial load (P_{up}) = 179 kips

Flexural load (M_{up}) = 81 kips-ft

Shear demand perpendicular to bent cap (V_{upz}): 3 kips

Shear demand parallel to bent cap (V_{upx}): 7 kips

Load demands on bottom of the pile

Axial load (P_u) = 179 kips

Flexural load in perpendicular direction to bent cap (M_{uz}) = $V_{upz}L$ = 18 kips-ft

Flexural load in parallel direction to bent cap (M_{ux}) = M_{up} +(V_{upx})L =122 kips-ft

Calculation of second-order effects

According to Appendix 8 of AISC specification, the required second order amplified moment, M_r and axial load, P_r is calculated as:

$$M_r = B_1 M_{nt} + B_2 M_{lt}$$

$$P_r = P_{nt} + B_2 P_{lt}$$

where

B_1 = multiplier to account for P-δ effects

B_2 = multiplier to account for P-Δ effects

M_{lt} = first-order moment due to lateral translation of the structure only

M_{nt} = first-order moment with structure restrained against lateral translation

P_{lt} = first-order axial force due to lateral translation of the structure only

P_{nt} = first-order axial force with structure restrained against lateral translation

Multiplier B_1 for P-δ effects

The B_1 multiplier for each member subject to compression and each direction of bending of the member is calculated as:

$$B_1 = \frac{C_m}{1 - \propto {P_u}/{P_{e1}}} \geq 1$$

where, ∝=1 and C_m = equivalent uniform moment factor, assuming no relative translation of the member ends, determined as follows:

$$C_m = 0.6 - 0.4({-M_{up}}/{M_{ux}})$$

$$C_m = 0.86$$

P_{e1} = elastic critical buckling strength of the member in the plane of bending, calculated based on the assumption of no lateral translation at the member ends and is calculated as:

$$P_{e1} = \frac{\pi^2 EI}{(L_c)^2}$$

$$P_{e1} = \frac{\pi^2 \text{ x } 29000 \text{ x } 153}{(2.9 \text{ x } 12)^2}$$

$$P_{e1} = 36160 \text{ kips}$$

By substituting the calculated values, B_1 can be determined as follows:

$$B_1 = \frac{C_m}{1 - \propto P_u / P_{e1}} \geq 1$$

$$B_1 = \frac{0.86}{1 - 1 \text{ x } 179 / 36160} \geq 1$$

$$B_1 = 0.86 \geq 1$$

Therefore, B_1 was calculated as 1.

Multiplier B_2 for P-Δ effects

The B_2 multiplier for each direction of lateral translation is calculated as:

$$B_2 = \frac{1}{1 - \propto P_{story} / P_{estory}} \geq 1$$

where, $\propto$=1 and P_{story} = total vertical load supported by all piles = 837 kips (from analysis), P_{estory} = = elastic critical buckling strength for the story in the direction of translation being considered, determined as follows:

$$P_{estory} = R_M \frac{HL}{\Delta H}$$

where, H/ΔH is member lateral stiffness which is given as:

$$\frac{H}{\Delta H} = \frac{12EI_y}{L^3}$$

$$\frac{H}{\Delta H} = \frac{12 \text{ x } 29000 \text{ x } 153}{(5.79 \text{ x } 12)^3}$$

$$\frac{H}{\Delta H} = 159 \text{ kips/in}$$

And

$$R_M = 1 - 0.15 \left(\frac{P_{mf}}{P_{story}}\right)$$

where, P_{mf} = total vertical load in columns in the story that are part of moment frames, if any, in the direction of translation being considered

R_M can be conservatively taken as 0.85. The final P_{estory} can be determined as follows:

$$P_{estory} = R_M \frac{HL}{\Delta H}$$

$$P_{estory} = 0.85 \text{ x } 159 \text{ x } 5.79 \text{ x } 12$$

$$P_{estory} = 9390 \text{ kips}$$

By substituting the calculated values, B_2 can be determined as follows:

$$B_2 = \frac{1}{1 - {\propto P_{story}}/{P_{estory}}} \geq 1$$

$$B_2 = \frac{1}{1 - {1 \text{ x } 837}/{9390}} \geq 1$$

$$B_2 = 1 \geq 1$$

Therefore, B_2 was conservatively calculated as 1.

The calculated values of B_1 and B_2 indicated that there is no second-order effect. Additionally, the moment load and axial load have been calculated as follows:

$M_{rx} = M_{ux}$ = 122 kips-ft

$M_{rz} = M_{uz}$ = 18 kips-ft

$P_r = P_u$ = 179 kips-ft

Calculation of compressive strength

The nominal compressive strength of steel pile is defined in Section 6.9.4 of the AASHTO LRFD manual. In the first step, the slenderness of the pile is determined as follows:

For flange

$$\frac{b}{t} = 11.75 \leq 0.56\sqrt{\frac{E}{F_y}} = 13.5$$

For web

$$\frac{h}{t_w} = 21.88 \leq 1.49\sqrt{\frac{E}{F_y}} = 36$$

The pile was found to be non-slender based on the calculated width-to-thickness ratio. The compressive strength of a non-slender HP-pile is calculated as:

$$P_n = F_{cr}A_g$$

For zero length, nominal compressive strength is given by:

$$P_n = F_y A_g$$

$$P_n = 920\ kips$$

The calculation procedure for F_{cr} is as follows:

Elastic buckling stress (F_e)

$$F_e = \frac{\pi^2 E}{(\frac{L_c}{r})^2}$$

$$F_e = 1960 \text{ ksi}$$

Since,

$$\frac{F_y}{F_e} = 0.026 \leq 2.25$$

$$\mathrm{F_{cr}} = (0.658^{\frac{F_y}{F_e}})F_y$$

$$\mathrm{F_{cr}} = 49.5 \text{ ksi}$$

$$P_n = 911\ kips$$

$$\phi P_n = 820\ kips$$

The nominal compressive strength was calculated to be 911 kips and the design strength was calculated to be 820 kips which is greater than the axial load demand (179 kips).

Calculation of moment capacity

The nominal moment strength of steel pile is defined in Section 6.12.2 of the AASHTO LRFD manual. For the 1st step, the compactness of the pile is determined by the following steps. For flange:

$$0.38\sqrt{\frac{E}{F_y}} = 9.15 \leq \frac{b}{t} = 11.75 \leq 0.56\sqrt{\frac{E}{F_y}} = 13.5$$

The pile was found to have a non-compact flange based on the diameter-to-thickness ratio. The moment capacity of the HP section was calculated based on provisions provided in Section 6.12.2. The nominal flexural strength, M_n of HP-pile should be obtained according to the limit states of local buckling.

$$M_{nx} = (1 - \left(1 - \frac{0.7F_y}{R_h F_y}\right)\left(\frac{\lambda - \lambda_{pf}}{\lambda_{rf} - \lambda_{pf}}\right))R_h R_b F_y Z_x$$

$$M_{nx} = \left(1 - \left(1 - \frac{0.7 * 50}{1 * 50}\right)\left(\frac{11.75 - 9.15}{13.5 - 9.15}\right)\right)1 * 1 * 50 * 88.3$$

$$M_{nx} = 310 \text{ kips} - \text{ft}$$

$$\phi M_{nx} = 279 \text{ kips} - \text{ft}$$

Similarly,

$$M_{nz} = 136 \text{ kips} - \text{ft}$$

$$\phi M_{nz} = 123 \text{ kips} - \text{ft}$$

The nominal moment capacity of pile was calculated to be 310 kips-ft and the design moment strength was calculated to be 279 kips-ft which is greater than moment demand on bottom of the pile (122 kips-ft) in direction parallel to bent cap. Additionally, the nominal moment capacity of pile was calculated to be 132 kips-ft and the design moment strength was calculated to be 119 kips-ft which is greater than moment demand on bottom of the pile (18 kips-ft) in direction perpendicular to bent cap.

Check of compression member subjected to flexure and compression

According to Section 6.9.2.2.1 of AASHTO LRFD, the following condition must be satisfied for a member to be considered acceptable based on load demands and capacity of pile.

$$\frac{P_r}{\phi P_n} > 0.2, \text{then}$$

$$\frac{P_r}{\phi P_n} + \frac{8}{9}\left(\frac{M_{ux}}{\phi M_{nx}} + \frac{M_{uz}}{\phi M_{nz}}\right) \leq 1$$

$$\frac{179}{820} + \frac{8}{9}\left(\frac{122}{279} + \frac{18}{123}\right) \leq 1$$

$$0.74 \leq 1 \text{ (OK)}$$

Hence, the pile was strong enough to withstand the applied load demand.

APPENDIX D CALCULATION OF STEEL PIPE PILE CAPACITY

AASHTO LRFD Bridge Design Manual has the provision for the calculation of the strength of hollow steel pipe. The strength consists of compressive strength and moment capacity of the proposed steel pipe pile.

Geometric properties of the pile

Diameter (D) = 3 ft.

Thickness of wall (t) = 0.5 in.

Gross cross-sectional area (A_g) = 56.55 in^2.

Moment of inertia about y-axis (I_y) = 8786 in^4.

Plastic sectional modulus (Z) = 630 in^3

Elastic sectional modulus (S) = 488 in^3

Radius of gyration (r) =12.55 in.

Length (L) = 5.79 ft.

Effective length (L_c)= 2.9 ft.

Load demands on top of the pile

Axial load (P_{up}) = 530 kips

Flexural load (M_{up}) = 292 kips-ft

Shear demand perpendicular to bent cap (V_{upz}): 9 kips

Shear demand parallel to bent cap (V_{upx}): 21 kips

Load demands on bottom of the pile

Axial load (P_u) = 530 kips

Flexural load in perpendicular direction to bent cap (M_{uz}) = $V_{upz}L$ = 52 kips-ft.

Flexural load in parallel direction to bent cap (M_{ux}) = M_{up} +(V_{upx})L =414 kips-ft.

Calculation of second-order effects

According to Appendix 8 of AISC specification, the required second order amplified moment, M_r and axial load, P_r is calculated as:

$$M_r = B_1 M_{nt} + B_2 M_{lt}$$

$$P_r = P_{nt} + B_2 P_{lt}$$

Multiplier B_1 for P-δ effects

The B_1 multiplier for each member subject to compression and each direction of bending of the member is calculated as:

$$B_1 = \frac{C_m}{1 - \propto {P_u}/{P_{e1}}} \geq 1$$

where, ∝=1 and C_m is determined as follows:

$$C_m = 0.6 - 0.4({-M_{up}}/{M_{ux}})$$

$$C_m = 0.88$$

P_{e1} is calculated as:

$$P_{e1} = \frac{\pi^2 EI}{(L_c)^2}$$

$$P_{e1} = \frac{\pi^2 \text{ x } 29000 \text{ x } 8786}{(2.9 \text{ x } 12)^2}$$

$$P_{e1} = 2076493 \text{ kips}$$

By substituting the calculated values, B_1 can be determined as follows:

$$B_1 = \frac{C_m}{1 - \propto {P_u}/{P_{e1}}} \geq 1$$

$$B_1 = \frac{0.88}{1 - {1 \text{ x } 530}/{2076493}} \geq 1$$

$$B_1 = 0.88 \geq 1$$

Therefore, B_1 was calculated as 1.

Multiplier B_2 for P-Δ effects

The B_2 multiplier for each direction of lateral translation is calculated as:

$$B_2 = \frac{1}{1 - {\propto P_{story}}/{P_{estory}}} \geq 1$$

where, $\propto$=1 and P_{story} = 936 kips (From analysis), P_{estory} is determined as follows:

$$P_{estory} = R_M \frac{HL}{\Delta H}$$

where, H/ΔH is story lateral stiffness which is given as:

$$\frac{H}{\Delta H} = \frac{12EI_y}{L^3}$$

$$\frac{H}{\Delta H} = \frac{12 \text{ x } 29000 \text{ x } 8786}{(5.79 \text{ x } 12)^3}$$

$$\frac{H}{\Delta H} = 9116 \text{ kips/in}$$

And

$$R_M = 1 - 0.15 \left(\frac{P_{mf}}{P_{story}}\right)$$

R_M can be conservatively taken as 0.85. The final P_{estory} can be determined as follows:

$$P_{estory} = R_M \frac{HL}{\Delta H}$$

$$P_{estory} = 0.85 \text{ x } 9116 \text{ x } 5.79 \text{ x } 12$$

$$P_{estory} = 538373 \text{ kips}$$

By substituting the calculated values, B_2 can be determined as follows:

$$B_2 = \frac{1}{1 - {\propto P_{story}}/{P_{estory}}} \geq 1$$

$$B_2 = \frac{1}{1 - {1 \text{ x } 936}/{538373}} \geq 1$$

$$B_2 = 1 \geq 1$$

Therefore, B_2 was calculated as 1.

The calculated values of B_1 and B_2 indicated that there is no second-order effect. Additionally, the moment load and axial load have been calculated as follows:

$M_{rx} = M_{ux} = 414$ kips-ft

$M_{rz} = M_{uz} = 52$ kips-ft

$P_r = P_u = 530$ kips-ft

Calculation of compressive strength

The nominal compressive strength of a steel pipe pile is defined in Chapter 6 of the manual. In the first step of the calculation, the slenderness of the pile is determined as follows :

$$\frac{D}{t} = 72 \geq 0.11\frac{E}{F_y} = 63.8$$

The pile was found to be slender based on the calculated diameter-to-thickness ratio. The compressive strength of slender Round HSS was calculated based on provisions provided in Section 6.9.4.

$$P_n = F_{cr}A_e$$

For zero length, compressive strength is given by:

$$P_n = F_y A_g$$

$$P_n = 50 * 56.55\ kips$$

$$P_n = 50 * 56.55\ kips$$

$$P_n = 2828\ kips$$

Since,

$$0.11\frac{E}{F_y} < \frac{D}{t} < 0.45\frac{E}{F_y}$$

$$A_e = [\frac{0.038E}{F_y\left(\frac{D}{t}\right)} + \frac{2}{3}]A_g$$

$$A_e = \left[\frac{0.038 * 29000}{50 * (72)} + \frac{2}{3}\right] 56.55$$

$$A_e = 55\ in^2$$

The calculation procedure for F_{cr} is as follows:

Elastic buckling stress (F_e)

$$F_e = \frac{\pi^2 E}{(\frac{L_c}{r})^2}$$

$$F_e = 37224 \text{ ksi}$$

Since,

$$\frac{F_y}{F_e} = 0.0013 \leq 2.25$$

$$\mathrm{F_{cr}} = (0.658^{\frac{F_y}{F_e}})F_y$$

$$\mathrm{F_{cr}} = 49.97 \text{ ksi}$$

$$P_n = 2748\ kips$$

$$\phi P_n = 2473\ kips$$

The nominal compressive strength was calculated to be 2748 kips and the design strength was calculated to be 2473 kips which is greater than the axial load demand (530 kips).

Calculation of moment capacity

The nominal moment strength of steel pipe pile is defined in Section 6.12.2.2.3 of the manual. In the first step, the limit of the pile is determined as :

$$\frac{D}{t} = 72 \leq 0.45\frac{E}{F_y} = 261$$

The nominal flexural strength, M_n should be a lower value obtained according to the limit states of yielding and local buckling.

1. Yielding

$$M_{n1} = M_p = F_y Z$$

$$M_{n1} = 2625\ kips - ft$$

2. Local Buckling

$$\text{If } \frac{D}{t} = 72 \leq 0.31\frac{E}{F_y} = 180$$

$$M_{n2} = \left[\frac{0.021E}{\frac{D}{t}} + F_y\right]S$$

$$M_{n2} = 2377\ kips - ft$$

$$M_n = 2377\ \text{kips} - \text{ft}$$

$$\phi M_n = 2140\ kips - ft$$

The nominal moment capacity of pile was calculated to be 2377 kips-ft and the design moment strength was calculated to be 2140 kips-ft which is greater than moment demand on bottom of the pile (M_{ux}= 414 kips-ft and M_{uz}=56 kips-ft).

Check of member subjected to flexure and compression

According to Section 6.9.2.2.1 of AASHTO LRFD, the following condition must be satisfied for a member to be considered acceptable based on load demands and capacity of pile.

$$\frac{P_r}{\phi P_n} > 0.2, \text{then}$$

$$\frac{P_r}{\phi P_n} + \frac{8}{9}\left(\frac{M_{ux} + M_{uz}}{\phi M_n}\right) \leq 1$$

$$\frac{530}{2473} + \frac{8}{9}\left(\frac{466}{2140}\right) \leq 1$$

$$0.41 \leq 1 \text{ (OK)}$$

Hence, the pile was strong enough to withstand the applied load demand.

APPENDIX E CALCULATION OF ORIGINAL BENT CAP CAPACITY

The bent cap used as a reference for the design of the connection is included in APPENDIX B. The bent cap consisted of 4- legged #5 shear stirrups @ 12 in. o.c. (*s*), the effective depth of 52 in. (*d*), and width of 48 in. (*b*). The bent cap consisted of 8#11 compression steel on top and 8#11 tension steel on the bottom of the bent cap.

Material properties

f'_c= 4 ksi

f_y of rebars = 60 ksi

Load demands on bent cap

V_{ub}= 345 kips

M_{ub}= 1266 kips-ft

Calculation of moment capacity

In the initial step, the assumption was made that the stress in rebars (f'_s) is less than the yield strength (f_y) for the calculation of nominal moment capacity.

The depth of the neutral axis (*c*) was calculated using the rectangular stress distribution diagram. The calculation process is summarized below:

Compressive force due to steel (*Cs*):

$$Cs = A'_s f'_s = 1.56 * 8 * 0.003 * \left(\frac{c - d'}{c}\right) * 29000$$

$$Cs = 1086\left(\frac{c - 2}{c}\right) \text{kips}$$

Compressive force due to concrete (*Cc*):

$$Cc = 0.85\, f'_c \beta_1\, cb = 138.72c \text{ kips}$$

Tensile force due to rebars (Ts)

$$Ts = A_s f_y = 1.56 * 8 * 60 = 748.8 \text{ kips}$$

For equilibrium: *Cs* + *Cc* = *Ts*

$$1086\left(\frac{c-2}{c}\right) + 138.72 = 748.8$$

$$c = 4.6 \text{ in}$$

Now,

$$f'_s = 0.003 * \left(\tfrac{c-2}{c}\right) * 29000 = 49.17 < 60\ ksi \text{ (Assumption is OK)}$$

Now, the nominal Moment Capacity (M_n) of the beam is calculated as:

$$M_n = C_c\left(d - \frac{\beta_1 c}{2}\right) + C_s(d - d')$$

$$M_n = 138.72 * 4.6\left(52 - \frac{0.85 * 4.6}{2}\right) + 1086\left(\frac{4.6-2}{4.6}\right)(52-2)$$

$$M_n = 62625 \text{ kips} - \text{in}(5219 \text{ kips} - \text{ft})$$

ϕM_n=4700 kips-ft> M_{ub} (1266 kips-ft)

The design moment capacity of bent cap was calculated to be 4700 kips-ft which is greater than moment demand (1266 kips-ft).

Calculation of shear strength

According to 5.12.5.3.8c of AASHTO LRFD, the nominal shear resistance due to concrete is given as:

$$V_c = 0.0632\sqrt{f'_c}bd$$

$$V_c = 316\ kips$$

The nominal shear resistance due to stirrups is calculated as:

$$V_s = \frac{A_s f_y d}{s}$$

$$V_s = \frac{0.31 * 4 * 60 * 52}{12}$$

$$V_s = 322\ kips$$

Total shear resistance (V_n)= V_c+V_s =638 kips

According to Section 5.5.4.2, ϕ for shear in the reinforced concrete section is 0.9, and the design shear capacity of the bent cap was calculated to be 574 kips which is greater than V_{ub} (345 kips).

It can be concluded that the assumed size dimensions and detailing of the bent cap were sufficient to withstand the load demands placed on it

Calculation of punching strength

The width of the bent cap i.e., 4 ft. is very narrow for achieving two-way shear action, so the punching strength was calculated based on one-way action. According to Section 5.7.3.3 of AASHTO LRFD, the shear contribution of concrete is given as:

$$V_c = 0.0316n\sqrt{f'_c}b_w d_v$$

Here, b_w was taken as 4 ft. and d_v was 52 in., and n was 2 for two planes.

$$V_c = 316\ kips$$

The shear resistance due to stirrups was similar to the shear strength due to stirrups which was calculated to be 322 kips. Moreover, the final punching shear strength of the connection was calculated to be 638 kips.

APPENDIX F CONNECTION WITH REBARS

Based on the AASHTO LRFD specifications, #11 rebars were used, and the development length of the rebars was calculated.

Material properties

f'_c= 4 ksi

f_y = 60 ksi

Load demands on top of the pile

P_{ub}= 530 kips

M_{ub}= 292 kips-ft

Geometrical properties of rebars

Diameter of rebar (d_b) = 1.41 in.

Calculation of development length for straight rebars

The development length was calculated using Eq. (4.1) and Eq. (4.2) for straight rebars. The basic development length is calculated as:

$$L = 2.4 d_b * \frac{f_y}{\sqrt{f'_c}}$$

$$L = 101.5\ in.$$

By providing a specific amount of confinement with spiral reinforcement, the development length is modified as follows:

$$L_d = L \frac{\lambda_{rl} \lambda_{cf} \lambda_{rc} \lambda_{er}}{\lambda}$$

λ_{rl}, λ_{cf}, λ_{er}, and λ were assumed 1 and the confinement factor, λ_{rc} plays a vital role in the reduction of development length as described in Eq. (4.3).

$$0.4 \leq \lambda_{rc} \leq 1.0$$

in which

$$\lambda_{rc} = \frac{d_b}{c_b + k_{tr}}$$

Where, c_b is the smaller of the distance from the center of the bar or wire being developed to the nearest concrete surface (4 in.) and one-half the center-to-center spacing of the bars or wires being developed (8.77 in.) which was calculated to be 4 in., k_{tr} is transverse reinforcement ratio which was assumed as 0 because AASHTO has a provision to assume A_{tr} as 0 in^2.

Thus,

$$\lambda_{rc} = 0.35$$

$$L_d = 0.35 * 101.5$$

$$L_d = 3\ ft.$$

Similarly, for a specific amount of confinement, the spiral reinforcement should satisfy Eq. (4.4).

$$\rho_s = \frac{4A_{sp}}{d_c s} \geq 0.45(\frac{A_g}{A_c} - 1)\frac{f'_c}{f_y}$$

$$\frac{4 * 0.31}{29.25 * s} \geq 0.45(\frac{1018}{672} - 1)\frac{4}{60}$$

$$\frac{0.042}{s} \geq 0.015$$

$$2.9 \geq s$$

The bars were developed 3 ft. inside bent cap and steel pipe pile too for strong connection and spiral reinforcement of #5 bar was provided with the pitch of 2.8 in.

Calculation of development length for hooked rebars

For the hooked rebars, the development length is calculated using Eq. (4.5) as follows:

$$(a) L = \frac{38.0 * d_b * f_y}{60.0\sqrt{f'_c}} = 2\ ft.\ 3\ in.$$

(b) $8d_b$= 9 in.

(c) 6in

Thus, 2 ft. 3 in. of development length was provided for hooked rebars either 180° or 90°.

Calculation of development length for headed rebars

For the headed rebars, the development length is calculated using Eq. (4.6).

$$\text{(a) } L = \left(\frac{f_y \Psi_e \Psi_p \Psi_o \Psi_c}{75\sqrt{f'_c}}\right) d_b^{1.5} = 1\ \text{ft.}\ 10\ \text{in.}$$

(b) $8d_b$=11.28 in

(c) 6in

Thus, 1 ft. 10 in. of development length was provided for headed rebars.

APPENDIX G CONNECTION WITH ANNULAR RING

The annular ring was designed based on research carried out at Washington University.

Material properties

f'_c = 4 ksi

Ultimate tensile strength of steel tube (f_u) = 60 ksi

Weld metal strength (F_{exx}) = 70 ksi

Geometrical properties of the annular ring

Diameter of rebar (d_b) = 1.41 in.

Thickness of annular ring=Thickness of steel pipe (t) =0.5 in.

Outer diameter of the annular ring(D_o)= D+16t= 3 ft. 8 in.

Inner diameter of annular ring=D-16t= 2 ft. 4 in.

Calculation of size of weld

The size of the weld of the annular ring to the steel pipe pile is calculated using Eq. (4.8).

$$w \geq \frac{1.31tF_u}{F_{exx}} = \frac{1.31*0.5*60}{70} = 0.56 \text{ in.}$$

The size of the weld was measured to be 0.56 in.

Calculation of the Required Tube Embedment Depth into the Cap Beam

The embedment depth is calculated to resist the tensile capacity of the steel pipe pile using Eq. (4.9).

$$L_e = \sqrt{\frac{{D_o}^2}{4} + \frac{DtF_u}{6\sqrt{f'_c}}} - \frac{D_o}{2} \ (psi)$$

$$L_e = \sqrt{\frac{44^2}{4} + \frac{36 * 0.5 * 60000}{6\sqrt{4000}}} - \frac{44}{2}$$

$$L_e = 3 \text{ ft}$$

The steel pipe pile should be embedded 3 ft. inside the bent cap for stronger attachment.

Calculation of the Required Depth Above the Embedded Tube

The depth of the foundation should be enough to resist the punching failure in the bent cap. The depth of the bent cap above the embedded steel pipe pile is calculated using Eq. (4.10).

$$L_{pc} = \sqrt{\frac{D^2}{4} + \frac{C_c + C_s}{6\sqrt{f'_c}}} - \frac{D}{2} - L_e(psi)$$

$$d_f > \sqrt{\frac{D^2}{4} + \frac{C_c + C_s}{6\sqrt{f'_c}}} - \frac{D}{2}$$

Maximum compressive strength (P_o):4550 kips (Using spColumn software)

$$P_u/P_o = 530/4550 = 0.12$$

To calculate the depth of foundation based on demand, the condition of $0.1 < P_u/P_o < 0.2$ should be satisfied for a full range of loading, so $C_c + C_s = 0.2 \times P_o = 910$ kips for maximum strength.

$$d_f > \sqrt{\frac{36^2}{4} + \frac{910000}{6\sqrt{4000}}} - \frac{36}{2}$$

$$52 > \sqrt{\frac{36^2}{4} + \frac{910000}{6\sqrt{4000}}} - \frac{36}{2}$$

$$52 \text{ in.} > 35 \text{ in. (OK)}$$

$$L_{pc} = 1 \text{ ft. } 6 \text{ in.}$$

APPENDIX H CONNECTION WITH SHEAR STUDS

The shear studs are provided based on the axial and moment demand at the bent cap on top of the pile. The number of shear studs was calculated using Eq. (4.7).

Material properties

f'_c= 4 ksi

Elastic modulus of concrete (E_c)= 3600 ksi

Ultimate tensile strength (F_u) = 65 ksi

Load demands on top of the pile

P_{ub}= 530 kips

M_{ub}= 292 kips-ft

Geometrical properties of studs

Adopting standard headed stud anchors according to ASTM,

Diameter of studs (d_s) = ¾ in.

Diameter of the head (d_h) = 1 ¼ in.

The height of shear studs was given as 4 in. based on the relation of h/d_{sc}>=4 and spacing of 4 in. based on relation of s>=4d_{sc}.

Calculation of number of shear studs for axial resistance

For axial demand on top of pile (P_{ub}) the number of shear studs is calculated as follows:

$$P_{up} \geq (0.5 \text{ x } A_{sc} \text{ x } n \text{ x} \sqrt{f'c \text{ x } E_c} \leq A_{sc} \text{ x } n \text{ x } F_u)$$

$$530 \geq (0.5 \text{ x } 0.44 \text{ x } n \text{ x } \sqrt{4 \text{ x } 3600} \leq 0.44 \text{ x } n \text{ x } 65)$$

$$530 \geq (26.4\text{n} \leq 28.8n)$$

$$n = 20$$

Calculation of number of shear studs for moment resistance

For the moment resistance, a force couple (P_M) was assumed to form on either side of the pile to resist the moment demand at the connection, as illustrated in Figure A.2. The nominal moment capacity was calculated by obtaining the flexural resistance generated by the force couple, P_M x D= M_{up}, where D is diameter of pile (36 in.), and M_{up} is moment demand on top of pile (292 kips-ft). The force couple, P_M was calculated to be 98 kips. Accordingly, the number of shear studs (n) to achieve this force was calculated as 4, as presented below:

$$P_M \geq (0.5 \text{ x } A_{sc} \text{ x } n \text{ x } \sqrt{f'_c \text{x } E_c} \leq A_{sc} \text{ x } n \text{ x } F_u)$$

$$98 \geq 0.5 \text{ x } 0.44 \text{ x } n \text{ x } \sqrt{4 \text{ x } 3600} \leq 0.44 \text{ x } n \text{ x } 65$$

$$98 \geq 26.4n \leq 28.6n$$

$$n = 4$$

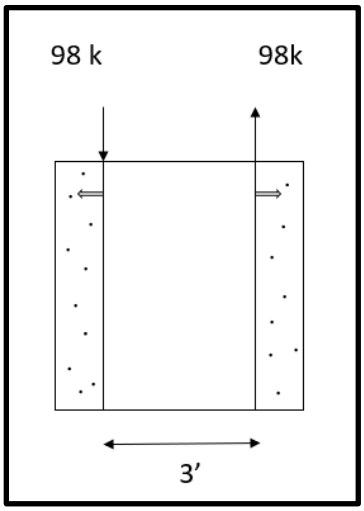

Figure A.1: Moment demand coupled

Assuming a symmetric studs layout around the pipe to generate on each side if the pipe to resist 98 kips required a total number of shear studs was 8 for moment resistance. Figure A.3 shows the shear studs generating the force couples and participating in the moment resistance. To satisfy

the required number of studs, four rows of shear studs are provided with 8 shear studs in each row, such that a total of 32 shear studs resist both the moment and axial demands.

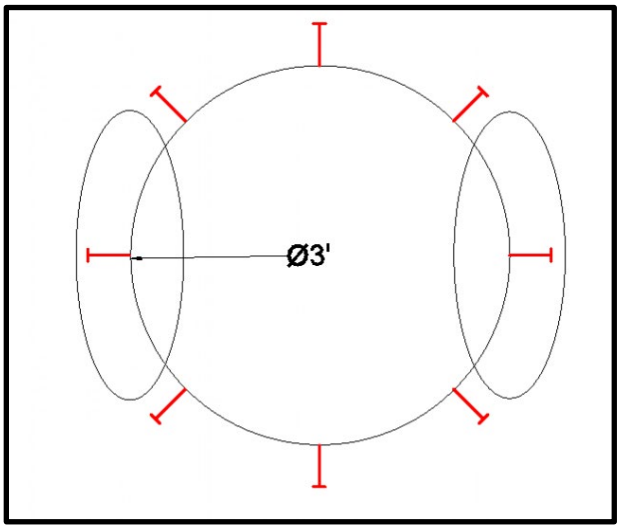

Figure A.2: Shear studs participating in resistance

APPENDIX I

This appendix consists of drawings related to the bridge structure on SR-3 over Cedar Creek Station in Morgan County which were used as reference for the design of the connection between steel pipe piles and reinforced concrete bent cap.

DRAWINGS RELATED TO BRIDGE SR-3 OVER CEDAR CREEK STATION IN MORGAN COUNTY

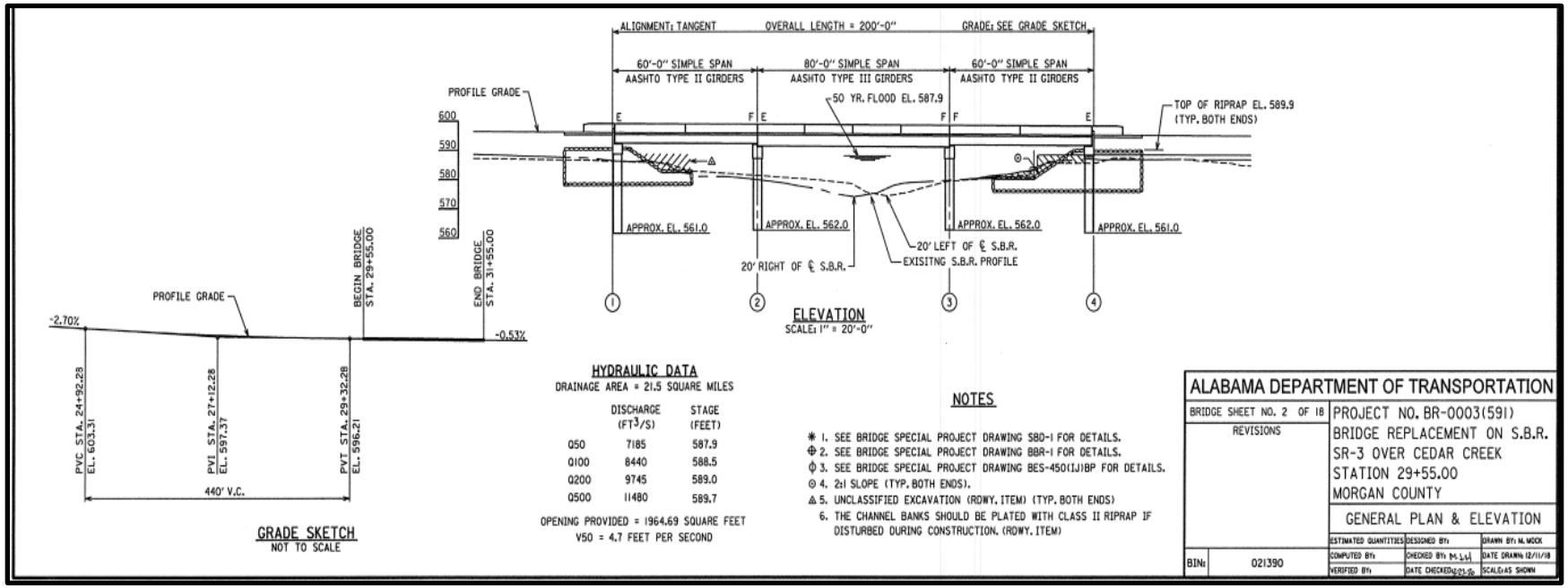

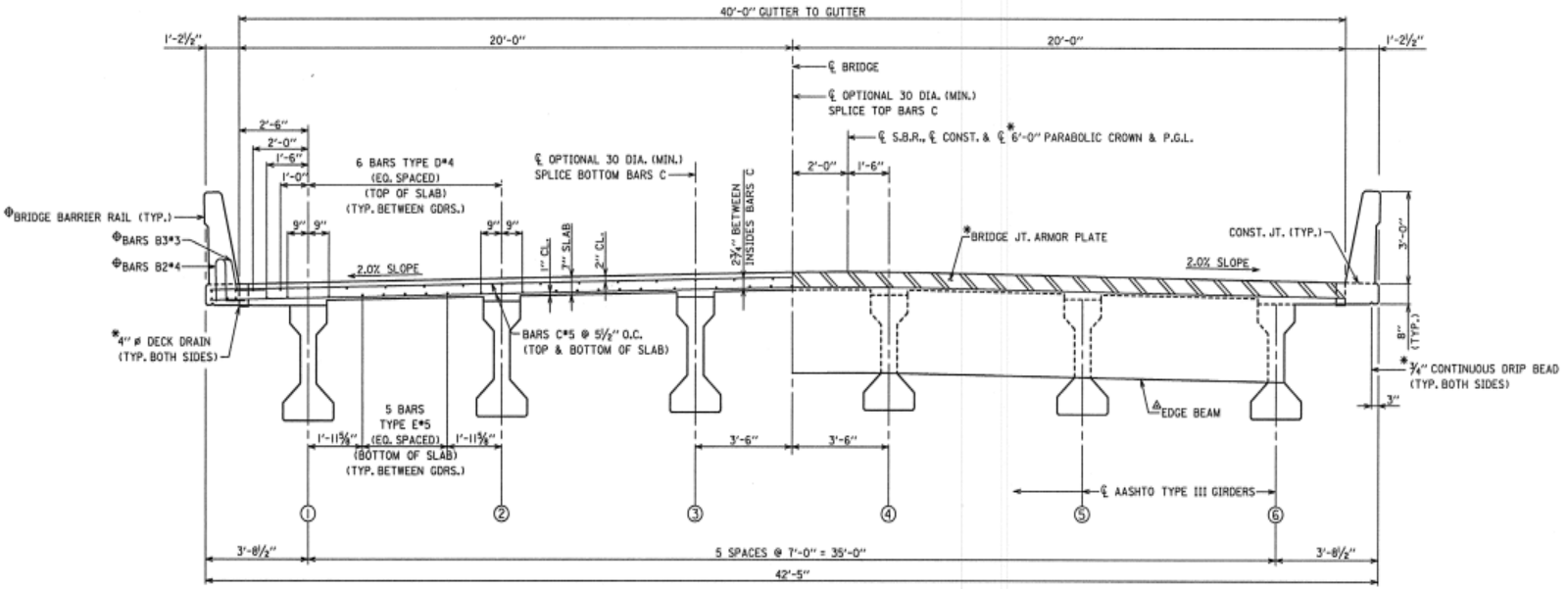

HALF TYPICAL SECTION
SCALE: ½" = 1'-0"

HALF END VIEW
SCALE: ½" = 1'-0"

NOTES

*1. SEE BRIDGE SPECIAL PROJECT DRAWING SBD-1 FOR DETAILS.

Φ2. SEE BRIDGE SPECIAL PROJECT DRAWING BBR-1 FOR DETAILS.

△3. SEE BRIDGE SPECIAL PROJECT DRAWING EBEW3 FOR DETAILS.

4. SEE BRIDGE SHEET 7 FOR PLAN VIEW OF SPAN.
SEE BRIDGE SHEET 9 FOR GIRDER DETAILS.

5. AT THE CONTRACTOR'S OPTION, BARS C MAY BE SPLICED 30 DIA. (MIN.). SPLICE TOP BARS CENTERED AT MID-POINT BETWEEN GIRDERS AND BOTTOM BARS CENTERED OVER CENTERLINE OF GIRDER OR AS SHOWN, EXCEPT THAT NO SPLICE SHALL BE CENTERED OVER THE EXTERIOR GIRDER.

ALABAMA DEPARTMENT OF TRANSPORTATION			
BRIDGE SHEET NO. 8 OF 18	PROJECT NO. BR-0003(591)		
REVISIONS	BRIDGE REPLACEMENT ON S.B.R. SR-3 OVER CEDAR CREEK STATION 29+55.00 MORGAN COUNTY		
	SPAN 2 DETAILS		
	ESTIMATED QUANTITIES	DESIGNED BY: AJS	DRAWN BY: M. WOOK
BIN: 021390	COMPUTED BY:	CHECKED BY: MAH	DATE DRAWN: 8/7/18
	VERIFIED BY:	DATE CHECKED: 8-23-18	SCALE: AS SHOWN

PROJECT NUMBER	YEAR	NUMBER
BR-0003(591)	2020	1106

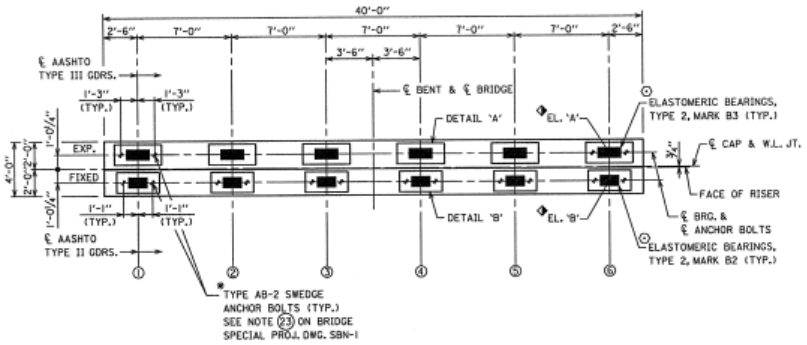

PLAN
SCALE: 1/4" = 1'-0"

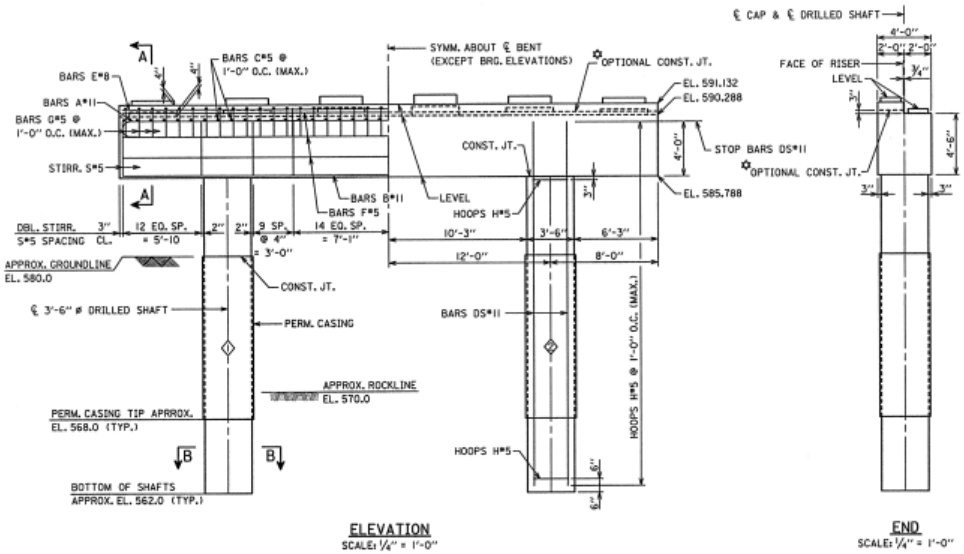

ELEVATION
SCALE: 1/4" = 1'-0"

END
SCALE: 1/4" = 1'-0"

BEARING ELEVATIONS						
	GIRDER 1	GIRDER 2	GIRDER 3	GIRDER 4	GIRDER 5	GIRDER 6
EL. 'B'	591.465	591.605	591.745	591.817	591.685	591.545
EL. 'A'	590.621	590.761	590.901	590.973	590.841	590.701

BILL OF REINFORCEMENT					
MARK	SIZE	NUMBER	LENGTH	LOCATION	BENDING
A	11	8	42'-8"	CAP	SEE DIAG.
B	11	8	39'-6"	CAP	STRAIGHT
C	5	40	4'-7"	CAP	SEE DIAG.
F	5	6	39'-6"	CAP/RISER	STRAIGHT
S	5	148	11'-11"	CAP	SEE DIAG.
E	8	4	39'-6"	RISER	STRAIGHT
G	5	40	5'-9 1/4"	RISER	SEE DIAG.
U1	3	24	5'-4 1/2"	PEDESTALS	SEE DIAG.
U2	3	90	3'-8 1/2"	PEDESTALS	SEE DIAG.
U3	3	24	5'-8 1/2"	PEDESTALS	SEE DIAG.
DS	11	24	26'-9 1/2"	D.S.	STRAIGHT
H	5	46	9'-8 1/4"	D.S.	SEE DIAG.

NOTES

* 1. SEE BRIDGE SPECIAL PROJECT DRAWING SBD-1 FOR DETAILS.
⊙ 2. SEE BRIDGE SPECIAL PROJECT DRAWING SPGD-1 FOR DETAILS.
◆ 3. BEARING ELEVATIONS ARE ON TOP OF PEDESTALS AT ℄ GIRDER AND ℄ BEARING.
✡ 4. COAT OPTIONAL CONSTRUCTION JOINT WITH AN APPROVED EPOXY ADHESIVE PRIOR TO POURING REMAINDER OF RISER.
5. FOR SECTIONS A-A, B-B, PEDESTAL & REINFORCEMENT DETAILS, SEE BRIDGE SHEET 14.
6. PAYMENT FOR DRILLED SHAFT CONCRETE TO BE INCLUDED IN PAY ITEM 506C, "LIN. FT., DRILLED SHAFT CONSTRUCTION, 3'-6" DIA., CLASS DSI CONCRETE." (APPROX. 0.36 CU. YDS./LIN. FT. OF SHAFT.)
7. STEEL REINFORCEMENT FOR DRILLED SHAFTS IS INCLUDED IN PAY ITEM 502A "LBS., STEEL REINFORCEMENT".
8. TOP OF SHAFT ELEVATIONS ARE APPROXIMATE ONLY AND MAY REQUIRE ADJUSTMENT DEPENDING ON THE ACTUAL GROUNDLINE ELEVATION AT THE LOCATION OF EACH SHAFT.
9. BOTTOM OF SHAFT ELEVATIONS ARE APPROXIMATE ONLY AND MAY REQUIRE ADJUSTMENT TO INSURE A MINIMUM OF 2 DIA. INTO MATERIAL CLASSIFIED AS "HARD GRAY LIMESTONE" ON THE TEST BORING RECORD SHEET.
10. IT SHALL BE THE RESPONSIBILITY OF THE CONTRACTOR TO INSURE THE STABILITY OF THE PERMANENT CASING DURING CONSTRUCTION OF THE DRILLED SHAFT.
11. MINIMUM DESIGN DIAMETER OF SHAFT AND PERMANENT CASING SHOWN. CASING MAY BE OVERSIZED TO FACILITATE EXCAVATION OF THE SHAFT. PAYMENT FOR OVERSIZE CASING SHALL BE AT THE UNIT PRICE BID FOR THE MINIMUM DIAMETER SHOWN.

GRADE 60 ⌀ MIN. 28 DAY STRENGTH 4000 PSI

ESTIMATED QUANTITIES			
	UNITS	ITEM NO.	DESCRIPTION
10,500	POUND	502A	STEEL REINFORCEMENT
34.4	CUBIC YARD	510A	SUBSTRUCTURE CONCRETE

ALABAMA DEPARTMENT OF TRANSPORTATION

BRIDGE SHEET NO. 12 OF 18

REVISIONS

PROJECT NO. BR-0003(591)
BRIDGE REPLACEMENT ON S.B.R. SR-3 OVER CEDAR CREEK
STATION 29+55.00
MORGAN COUNTY

BENT 2

ESTIMATED QUANTITIES BY: APG — DESIGNED BY: APG — DRAWN BY: M. MOCK
COMPUTED BY: MM — CHECKED BY: MM — DATE DRAWN: 12/5/18
VERIFIED BY: CW — DATE CHECKED: 12/13/18 — SCALE: AS SHOWN

BIN: 021390

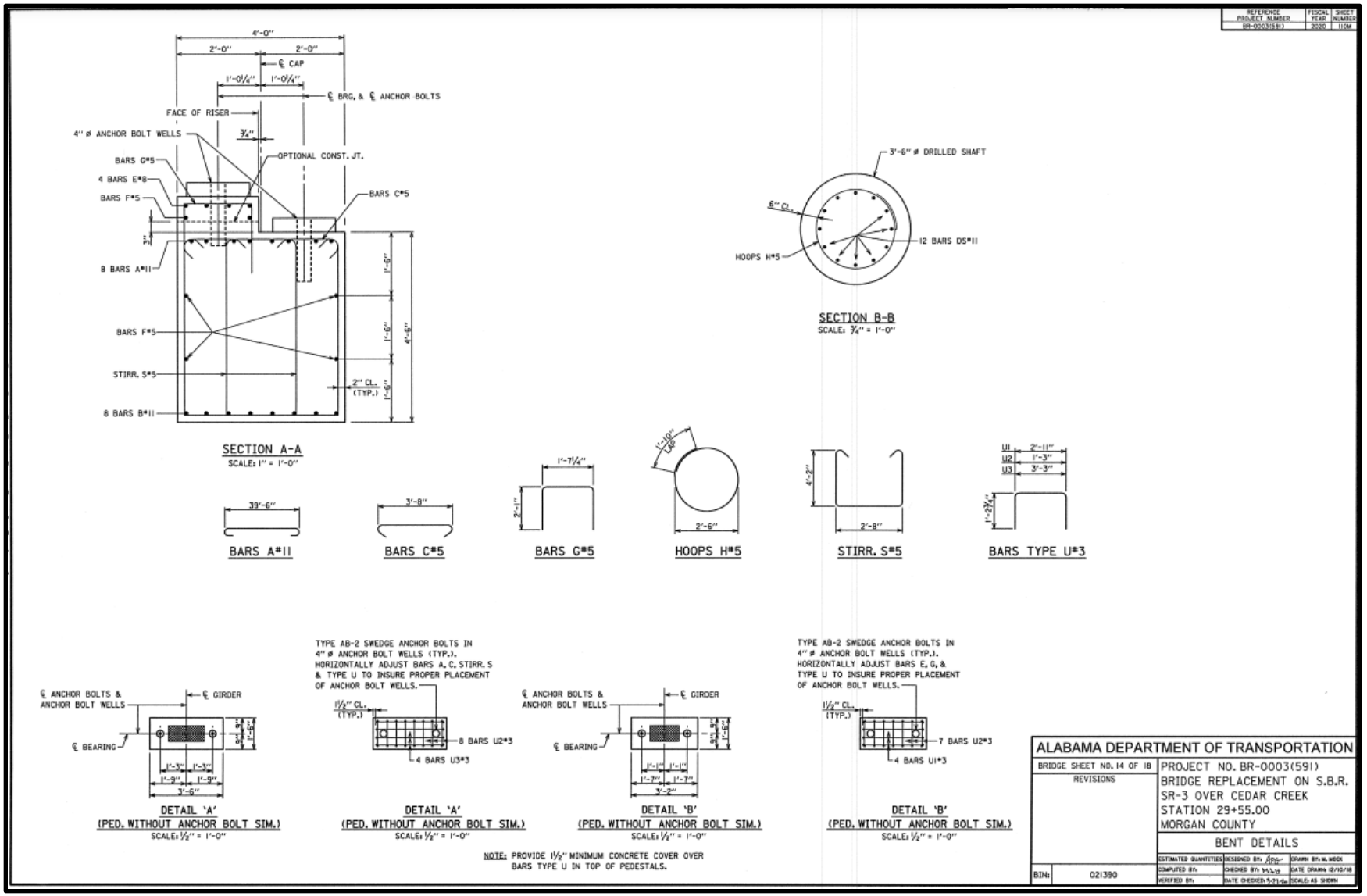
REFERENCE PROJECT NUMBER
FISCAL YEAR
SHEET NUMBER
4'-0"
2'-0"
2'-0"
℄ CAP
1'-0 1/4"
1'-0 1/4"
℄ BRG. & ℄ ANCHOR BOLTS
FACE OF RISER
4" ø ANCHOR BOLT WELLS
3/4"
OPTIONAL CONST. JT.
BARS G*5
4 BARS E*8
BARS F*5
BARS C*5
3"
8 BARS A*11
1'-6"
1'-6"
4'-6"
BARS F*5
STIRR. S*5
2" CL. (TYP.)
1'-6"
8 BARS B*11
SECTION A-A
SCALE: 1" = 1'-0"
3'-6" ø DRILLED SHAFT
6" CL.
HOOPS H*5
12 BARS D5*11
SECTION B-B
SCALE: 3/4" = 1'-0"
39'-6"
BARS A*11
3'-8"
BARS C*5
1'-7 1/4"
2'-1"
BARS G*5
1'-10" LAP
2'-6"
HOOPS H*5
4'-2"
2'-8"
STIRR. S*5
U1
U2
U3
2'-11"
1'-3"
3'-3"
1'-2 3/4"
BARS TYPE U*3
℄ ANCHOR BOLTS & ANCHOR BOLT WELLS
℄ GIRDER
℄ BEARING
9 3/4"
1'-5"
1'-3"
1'-3"
1'-9"
1'-9"
3'-6"
DETAIL 'A'
(PED. WITHOUT ANCHOR BOLT SIM.)
SCALE: 1/2" = 1'-0"
TYPE AB-2 SWEDGE ANCHOR BOLTS IN 4" ø ANCHOR BOLT WELLS (TYP.). HORIZONTALLY ADJUST BARS A, C, STIRR. S & TYPE U TO INSURE PROPER PLACEMENT OF ANCHOR BOLT WELLS.
1 1/2" CL. (TYP.)
8 BARS U2*3
4 BARS U3*3
DETAIL 'A'
(PED. WITHOUT ANCHOR BOLT SIM.)
SCALE: 1/2" = 1'-0"
℄ ANCHOR BOLTS & ANCHOR BOLT WELLS
℄ GIRDER
℄ BEARING
9 3/4"
1'-5"
1'-1"
1'-1"
1'-7"
1'-7"
3'-2"
DETAIL 'B'
(PED. WITHOUT ANCHOR BOLT SIM.)
SCALE: 1/2" = 1'-0"
TYPE AB-2 SWEDGE ANCHOR BOLTS IN 4" ø ANCHOR BOLT WELLS (TYP.). HORIZONTALLY ADJUST BARS E, G, & TYPE U TO INSURE PROPER PLACEMENT OF ANCHOR BOLT WELLS.
1 1/2" CL. (TYP.)
7 BARS U2*3
4 BARS U1*3
DETAIL 'B'
(PED. WITHOUT ANCHOR BOLT SIM.)
SCALE: 1/2" = 1'-0"
NOTE: PROVIDE 1 1/2" MINIMUM CONCRETE COVER OVER BARS TYPE U IN TOP OF PEDESTALS.
ALABAMA DEPARTMENT OF TRANSPORTATION
BRIDGE SHEET NO. 14 OF 18
REVISIONS
PROJECT NO. BR-0003(591)
BRIDGE REPLACEMENT ON S.B.R.
SR-3 OVER CEDAR CREEK
STATION 29+55.00
MORGAN COUNTY
BENT DETAILS
BIN: 021390
ESTIMATED QUANTITIES
DESIGNED BY:
DRAWN BY:
COMPUTED BY:
CHECKED BY:
DATE DRAWN:
VERIFIED BY:
DATE CHECKED:
SCALE: AS SHOWN